MODELLING
OF
WASTEWATER SYSTEMS

Henrik Bechmann

Lyngby 1999
ATV Erhvervsforskerprojekt EF 623
IMM-PHD-1999-69

Krüger

IMM

ISSN 0909-3192
ISBN 87-88306-01-1

Printed by jespersen offset
Bound by Hans Meyer, Technical University of Denmark

The work documented in this thesis is also published in the following papers:

Paper A: Bechmann, H., Nielsen, M. K., Madsen, H., and Poulsen, N. K. (1998). Control of sewer systems and wastewater treatment plants using pollutant concentration profiles. *Water Science and Technology*, **37**(12), 87–93.

Paper B: Bechmann, H., Madsen, H., Poulsen, N. K., and Nielsen, M. K. (1999). Grey box modelling of first flush and incoming wastewater at a wastewater treatment plant. *Environmetrics*, **11**(1), 1–12.

Paper C: Bechmann, H., Nielsen, M. K., Madsen, H., and Poulsen, N. K. (1999). Grey-box modelling of pollutant loads from a sewer system. *UrbanWater*, **1**(1), 71–78.

Paper D: Nielsen, M. K., Bechmann, H., and Henze, M. (1999). Modelling and test of aeration tank settling ATS. In *8th IAWQ Conference on Design, Operation and Economics of Large Wastewater Treatment plants*, pages 199–206. International Association on Water Quality, IAWQ, Budapest University of Technology, Department of Sanitary and Environmental Engineering.

Paper E: Bechmann, H., Nielsen, M. K., Poulsen, N. K., and Madsen, H. (1999). Grey-box modelling of aeration tank settling. Submitted.

Paper F: Bechmann, H., Nielsen, M. K., Poulsen, N. K., and Madsen, H. (1999). Effects and control of aeration tank settling operation. Submitted.

Preface

This thesis has been prepared at the Department of Mathematical Modelling (IMM), The Technical University of Denmark, and Krüger A/S, in partial fulfilment of the requirements for the degree of Ph.D. in engineering.

The thesis is concerned with the modelling of wastewater processes with the objective of using the models for control of sewer systems and wastewater treatment plants. The main contribution to this field includes both linear and nonlinear dynamic stochastic modelling of the influents to wastewater treatment plants as well as modelling of processes in the wastewater treatment plant.

Ramløse, 12th November 1999.

Henrik Bechmann

Henrik Bechmann

Acknowledgements

I wish to express my gratitude to all who have contributed to this research.

First of all, I wish to thank my supervisors, Professor Henrik Madsen, IMM, DTU, Associate Professor Niels Kjølstad Poulsen, IMM, DTU, and Senior Engineer Marinus K. Nielsen, Krüger A/S, for guidance, encouragement and constructive criticism during this work.

I wish to thank my colleagues at Krüger, especially past and present members of the STAR/S&P group: Tine B. Önnerth, Jacob Carstensen, Steven Isaacs, Kenneth F. Janning, Kenneth Kisbye, Peter Lindstrøm, Thomas Munk-Nielsen, Niels B. Rasmussen, Henrik A. Thomsen, and Dines Thornberg. Thanks are also due to my colleagues of the Krüger R&D Department: Kjær H. Andreasen, Claus P. Dahl, René Dupont and Flemming Norsk, as well as to our manager Rune Strube. Furthermore, I am very grateful to Lærke Christensen for proofreading this thesis and making suggestions regarding my use of the English language.

At IMM, I wish to thank past and present members of the Time Series Analysis group, the Control group and the Statistics group: Helle Andersen, Judith L. Jacobsen, Harpa Jonsdottir, Trine Kvist, Karina Stender, Sabine Vaillant, Jens Strodl Andersen, Klaus Kaae Andersen, Mikkel Baadsgaard, Alfred K. Joensen, Henrik Aalborg Nielsen, Jan Nygaard Nielsen, Torben Skov Nielsen, Magnus Nørgaard, Payman Sadegh, Uffe Høgsbro Thygesen, and Peter Thyregod.

Special thanks to Henrik Öjelund for reading a draft of this thesis and good suggestions concerning improvements.

Also, I am very grateful to Associate Professor Peter Steen Mikkelsen, Department of Environmental Science and Engineering (IMT), DTU, for having shared his knowledge about urban runoff and urban runoff systems with me.

Thanks are also due to the staff at the wastewater treatment plants of Skive, Aalborg East and Aalborg West, especially Pernille Iversen, for their support during data collection, for carrying out laboratory analyses and for running the on-line sensors.

I also thank my former colleague at UNI•C, Peter Busk Laursen, for sharing his profound knowledge and experience with LaTeX and friends, and valuable advice about preparing the thesis.

This research was funded by the Danish Academy for Technical Sciences and Krüger A/S, to whom I would like to express my gratitude.

Finally, I am grateful to my family, my wife Iben and our three children, Louise, Daniel and Mathilde as well as my parents and parents in law for their support and great patience during the preparation of this thesis.

Summary

In this thesis, models of pollution fluxes in the inlet to 2 Danish wastewater treatment plants (WWTPs) as well as of suspended solids (SS) concentrations in the aeration tanks of an alternating WWTP and in the effluent from the aeration tanks are developed. The latter model is furthermore used to analyze and quantify the effect of the Aeration Tank Settling (ATS) operating mode, which is used during rain events. Furthermore, the model is used to propose a control algorithm for the phase lengths during ATS operation.

The models are mainly formulated as state space model in continuous time with discrete-time observation equations. The state equations are thus expressed in stochastic differential equations. Hereby it is possible to use the maximum likelihood estimation method to estimate the parameters of the models. A Kalman filter is used to estimate the one-step ahead predictions that are used in the evaluation of the likelihood function. The proposed models are of the grey-box type, where the most important physical relations are combined with stochastic terms to describe the deviations between model and reality as well as measurement errors.

The pollution flux models are models of the COD (Chemical Oxygen Demand) flux and SS flux in the inlet to the WWTP. COD is measured by means of a UV absorption sensor while SS is measured by a turbidity sensor. These models include a description of the deposit of COD and SS amounts, respectively, in the sewer system, and the models can thus be used to quantify these amounts as well as to describe possible first flush effects. The buildup and flush out of the deposits are modelled by differential equations, thus the models are dynamic

models. The dynamic models are furthermore compared to simpler static models and it is found that the dynamic models are better at modelling the fluxes in terms of the multiple correlation coefficient R^2.

The model of the SS concentrations in the aeration tanks of an alternating WWTP as well as in the effluent from the aeration tanks is a mass balance model based on measurements of SS in one aeration tank and in the common outlet of all the aeration tanks, respectively. This model is a state space model with the SS concentrations and the sludge blanket depths in the aeration tanks as state variables and with the SS concentrations in one aeration tank and in the common outlet as observations.

The SS concentration model is used to quantify the benefits of ATS operation in terms of increased hydraulic capacity. The model is furthermore used to propose a control algorithm for the phase lengths during ATS operation. The quantification of the benefits of ATS operation as well as the proposal for a control algorithm is based on the assumption that if the SS concentration in the secondary clarifier increases beyond a plant and situation specific amount above the normal dry weather level, the SS concentration in the effluent increases to an unacceptable level. It was found that ATS increases the hydraulic capacity of the WWTP considered by more than 167%, while the proposed control algorithm is yet to be implemented in full scale.

Resumé (in Danish)

I denne afhandling er der udviklet modeller for henholdsvis forureningsflux i indløbet til 2 danske renseanlæg og for koncentrationer af suspenderet stof (SS) i luftningstankene på et alternerende renseanlæg såvel som i udløbet fra luftningstankene. Sidstnævnte model er desuden anvendt til at analysere og kvantificere effekten af Aeration Tank Settling (ATS) driftsformen, der anvendes under regn. Desuden er modellen anvendt til at foreslå en styringsalgoritme for faselængderne under ATS drift.

Modellerne er hovedsagligt formuleret som tilstandsmodeller i kontinuert tid med diskret tids observationsligninger. Tilstandsligningerne er derfor formuleret i stokastiske differentialligninger. Herved er det muligt at anvende maximum likelihood estimationsmetoden til at estimere modellernes parametre, idet et Kalmanfilter anvendes til at estimere et-trins prædiktionerne der bruges til evaluering af likelihood-funktionen. De foreslåede modeller er af grey-box typen hvor de væsentligste fysiske sammenhænge benyttes i modelformuleringen kombineret med stokastiske termer til at beskrive afvigelserne mellem model og virkelighed samt målefejl.

Forureningsfluxmodellerne er modeller for COD (Chemical Oxygen Demand) flux og SS flux, i indløbet til renseanlægget. COD er målt vha. en UV absorptionssensor mens SS er målt vha. en turbiditetssensor. Disse modeller inkluderer en beskrivelse af aflejringerne af henholdsvis COD og SS mængder i afløbssystemet, hvorved modellerne kan anvendes til at kvantificere disse mængder, samt til at beskrive eventuelle first flush effekter. Opbygningen og udskylningen af aflejringerne er modelleret vha. differentialligninger, så

modellerne er dynamiske modeller. De dynamiske modeller er desuden sammenlignet med simplere statiske modeller og det er fundet at de dynamiske modeller er bedre til at modellere fluxene målt vha. den multiple korrelations koefficient R^2.

Modellen for SS koncentrationerne i luftningstankene i et alternerende renseanlæg såvel som i udløbet fra luftningstankene er en massebalancemodel baseret på målinger af henholdsvis SS i én luftningstank og i det fælles udløb fra alle luftningstankene. Denne model er en tilstandsmodel med SS koncentrationerne samt slamspejlsdybderne i luftningstankene som tilstande, og med SS koncentrationerne i den ene luftningstank samt i det fælles udløb som observationer.

SS koncentrationsmodellen er anvendt til at kvantificere fordelene ved ATS drift målt i øget hydraulisk kapacitet ved at kvantificere SS mængderne i luftningstankene under ATS drift. Modellen er desuden anvendt til at foreslå en styringsalgoritme for faselængderne under ATS drift. Kvantificeringen af fordelene ved ATS drift samt den foreslåede styringsalgoritme er baseret på en antagelse om at stiger SS koncentrationen i efterklaringstanken mere end en anlægs- og situationsspecifik størrelse over normal tørvejrsniveau, stiger SS koncentrationerne i udløbet til et uacceptabelt niveau. Det er fundet at ATS øger den hydrauliske kapacitet for det betragtede renseanlæg med mere end 167 %, mens den foreslåede styringsalgoritme endnu ikke er implementeret i fuldskala.

Contents

I

Part I

Background and discussion

Chapter 1

Introduction

Urban drainage was introduced to improve sanitary conditions. It involves the diversion of wastewater and storm water out of the cities as efficiently as possible and away from the surface of the streets. However, the discharge of wastewater has a major impact on the receiving waters. Potentially insufficient or no wastewater treatment could devastate the ecological balance of nature, e.g. by lowered oxygen levels and possibly death of fish in the receiving waters. Hence, wastewater treatment plants has in this century been established and upgraded to remove pollutants in form of organic matter and nutrients from the wastewater.

As a consequence of the cholera epidemics in Europe in the middle of the 19th century, sewer systems were established, to divert the wastewater out of the cities. Then the wastewater could be removed from the cities, but the pollution was just transported to the surrounding environment. The organic pollution in the wastewater resulted in loss of oxygen in the recipients, which lead to the development of wastewater treatment plants that remove organic matter. Nutrients in form of ammonia, nitrate and phosphate stimulate the growth of algae which in the receiving waters and result in excessive loss of oxygen and undesirable changes in the aquatic life. Hence, nutrient removal was introduced on the wastewater treatment plants. In Denmark, the introduction of nutrient removal was mainly caused by the water pollution act enacted in 1987. Today, the wastewater treatment is so effective that the critical situations arise during rain storms, during which the upper limits of the sewers and wastewater treatment plants are reached. This result in untreated wastewater being lead to the receiving waters. Hence, the focus is today on extension of the sewer systems with detention basins to store the excessive water from a rain storm until the rain stops. Another possibility is to use modern on-line measurement equipment combined with on-line controllers to control the sewers and wastewater treatment plants so that more water can be handled.

To be able to design the optimal control laws the dynamics of the sewers and wastewater treatment plants has to be understood.

The understanding of the dynamic behavior of sewer systems and wastewater treatment plants is today often formulated as dynamic models. As the models can be formulated in many ways, it is important that the model formulation and complexity is in agreement with the modelling objective, i.e. some models are developed to yield a very detailed description of the involved processes while other models are developed to be operational for prediction and control purposes.

1.1 Modelling approaches

Deterministic (white-box) models are developed from the idea that a full understanding of nature can be obtained by identifying and describing all the physical, chemical and biological laws that govern the system concerned. The IAWQ[1] Activated Sludge Models for the processes in an activated sludge wastewater treatment plant (Henze et al., 1987, 1995, 1999; Gujer et al., 1999) and the commercially available urban drainage modelling tools based on the St. Vernant equations (Chow et al., 1988) such as Mouse (Lindberg et al., 1989; Crabtree et al., 1995; Mark et al., 1995, 1998b), are examples of deterministic models. The deterministic models are often formulated in continuous time, i.e. the dynamics are described by differential equations. Due to the large number of parameters it is often impossible to estimate the parameters uniquely from available measurements.

[1] IAWQ is an abbreviation for International Association on Water Quality, formerly International Association for Water Pollution Research and Control abbreviated IAWPRC. In 1999 International Water Association, IWA, was formed by the merger of IAWQ and International Water Services Association, IWSA.

Black-box models (Ljung, 1995, 1999; Sjöberg et al., 1995) are developed following a data based approach. The objective is to describe the input-output relations by equations that do not reflect physical, chemical, biological etc. considerations. Time series models: Auto Regressive (AR) models, Auto Regressive Moving Average (ARMA), AR with eXternal input (ARX), ARMA with eXternal input (ARMAX), Box-Jenkins (transfer function) models etc. (Box and Jenkins, 1976; Box et al., 1994; Ljung, 1995, 1999; Madsen, 1995; Poulsen, 1995) are examples of black-box models. These models are formulated in discrete time, i.e. the dynamics of the phenomenon concerned are described by difference equations. The time series models include stochastic terms to account for uncertainties in model formulation and measurements. As the models do not incorporate any prior knowledge, the parameters have to be estimated. Neural networks are another type of black-box models. The parameters of neural networks are also found by an estimation method, but the terminology is that neural networks *learn* by *training* (see e.g. Sjöberg et al. (1995)).

Grey-box models are based on the most important physical, chemical and biological relations and with stochastic terms to count in uncertainties in model formulation as well as in observations. The objective is to have physically interpretable parameters that are possible to estimate by means of statistical methods. Grey-box models are often formulated as a combination of continuous time and discrete time relations. The physical relations are formulated in continuous time, with differential equations to describe the dynamics, and the observation equations are expressed as discrete time relations, as measurements are taken at discrete time events. By including stochastic terms in both the continuous time description of the system and the discrete time description of the observations, it is possible to distinguish between modelling uncertainties and measurement uncertainties, and to quantify the uncertainties.

Physical insight can also be used to establish models formulated in discrete time only (Young and Wallis, 1985; Young et al., 1997). However, the estimated parameters are not directly the parameters of the underlying continuous time model, even though there are unique relations between the discrete time and continuous time parameters.

1.1.1 Sewer system modelling

Sewer systems are often modelled by means of commercially available software like the Storm Water Management Model, SWMM (Meinholz et al., 1974), Hydroworks (Heip et al., 1997) and Mouse (Lindberg et al., 1989; Crabtree et al., 1995; Mark et al., 1995, 1998b). Modelling with such packages has been used as a planning tool for introducing real time control of sewer systems (Entem et al., 1998; Hernebring et al., 1998; Mark et al., 1998a), where the modelling software is used to simulate the sewers.

The time series modelling approach has been used by Capodaglio (1994) to make one day ahead predictions of the water flow in a sewer system based on measurements of rainfall. Delleur and Gyasi-Agyei (1994) use transfer function models to predict suspended solids concentrations in sewers from observations of temperature and flow rate. Modelling of flow rate from rainfall observations has been carried out by Ruan and Wiggers (1997).

Liong and Chan (1993) use neural networks to predict storm runoff volumes from a catchment. The predicted volumes from the neural networks are compared with output from the SWMM model. Nouh (1996) applies neural networks to model the peak concentrations of total suspended solids, nitrates and total phosphorus in sewer flows, and compares the results with those of SWMM.

The grey-box method is applied by Grum (1998) to model suspended organic matter (suspended COD concentration) and the water level at an overflow structure in a Dutch combined sewer system.

1.1.2 Sedimentation and first flush

Sedimentation in combined sewers (sewers that handle both municipal wastewater and runoff water) and the first flush phenomenon are closely related to the different flow conditions during dry weather and wet weather. If sedimentation of pollutants in the sewer (and on impervious areas of the catchment) can occur during dry weather periods, the sediments can be flushed out of the sewer during wet weather situations, due to the increased flow. In the first part of the rain event the concentrations will be increased, thus the term first flush.

If the rain continues after the sewer is cleaned, the rain water is assumed to dilute the municipal wastewater, with lower concentrations as a result.

Ashley and Crabtree (1992) analyse the sources of sediments in sewers, how the sediments can be classified and how they are deposited in combined sewers. The flushing effects are treated by Geiger (1987); Deletic (1998); Saget et al. (1996); Bertrand-Krajewski et al. (1998); Gupta and Saul (1996), who classify the effects by plotting the cumulative load of pollutants (suspended solids, COD etc.) normalized with the total amount of pollutants against the cumulative flow normalized with the total amount of water for a storm event, see Fig. 1.1. If the observed curve is above the equilibrium line $y = x$, flushing

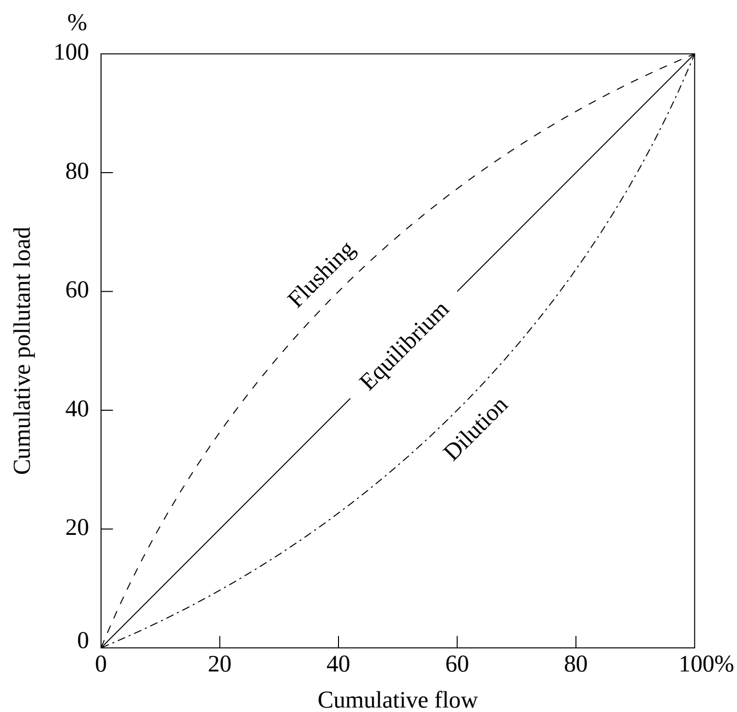

Figure 1.1. Cumulative pollution curves.

is taking place and if the observed curve is below the equilibrium line dilution has occurred. It should be noted that this method treats all storm events equal, and it is not possible from an observed curve to see if the origin was a light rain event or a heavy thunder storm.

Gupta and Saul (1996) perform regression analyses on the cumulative load of pollutants and find that peak rainfall intensity, the storm duration and the antecedent dry weather period are most informative among the analysed variables.

1.1.3 Control of sewer systems

The introduction of automatic control of sewer systems is a cost effective way to improve the effluent quality, compared e.g. to building new overflow structures, as automatic control is expected to enable better utilization of the existing facilities.

By means of appropriate models, predictive control algorithms can be established. These algorithms utilize predictions from the models to select the best control action at a given time.

Entem et al. (1998), Hernebring et al. (1998), and Mark et al. (1998b) prepare for the application of the Mouse model for on-line control purposes, i.e. a complicated deterministic model, suitable for simulation studies, is expected to produce predictions applicable for on-line control, even though Carstensen et al. (1996) stress that no single model exists that is suitable for both planning, detailed analysis and on-line control. Carstensen and Harremoës (1997) compared the flow predictions from a Mouse model used on-line with a much simpler transfer-function model based on measurements of rainfall intensity and time of day only and estimated on observations from the catchment considered, and finds that the transfer-function model is much better in predicting the flow. It is thus not expected that white-box models like Mouse is usable for on-line purposes.

1.1.4 Wastewater treatment plant modelling

Activated sludge wastewater treatment plants are often modelled by the IAWQ Activated Sludge Models (Henze et al., 1987, 1995, 1999; Gujer et al., 1999). Commercial software that implements the models is available, see e.g. EFOR Version 3.0 (1998). Computer models based on the IAWQ models are used to simulate different control strategies and the possible benefits (Dupont and

Sinkjær, 1994; Rangla et al., 1998).

Novotny et al. (1991); Capodaglio et al. (1992); Berthouex and Box (1996) apply the traditional time series analysis models to wastewater treatment plants. Novotny et al. (1991) and Capodaglio et al. (1992) use physical insight in form of mass balances combined with Euler approximation to establish corresponding discrete time models.

Ward et al. (1996) combine the Activated Sludge Model No. 1 (Henze et al., 1987) with time series models to establish a hybrid model of the activated sludge process and to enable prediction of suspended solids in the effluent.

Zhao et al. (1999) compare the Activated Sludge Model No. 2 (Henze et al., 1995) with a simplified model and a neural net model, while Pu and Hung (1995) establish a neural network model for a trickling filter plant.

Modelling of secondary clarifiers is treated in Ekama et al. (1997), which include a description of the Vesilind model (Vesilind, 1968, 1979) for hindered sludge settling velocity. Härtel and Pöpel (1992) have re-parameterized the original Vesilind mode, to include the dependency of sludge volume index, SVI, on the settling velocity. Dupont and Dahl (1995) suggest a model that is adequate for both free and hindered settling.

Comparison of different one-dimensional sedimentation models is carried out by Grijspeerdt et al. (1995) and Koehne et al. (1995). In Grijspeerdt et al. (1995) both steady state and dynamic properties of the examined models are compared. It is found that the Takács model (Takács et al., 1991) is the most reliable. Koehne et al. (1995) conclude that the models considered all model storm water flow situations well, but lack sufficient accuracy in simulating dry weather situations.

1.1.5 Control of wastewater treatment plants

Concepts of control of wastewater treatment plants are treated by Olsson et al. (1989) and Olsson (1992), who also treat the instrumentation problem as well as the subject of building models suitable for control purposes. Note that the model structures suggested are of the time series analysis type, and not of the detailed deterministic IAWQ activated sludge model type.

Results from the introduction of on-line instrumentation combined with advanced control strategies in wastewater treatment plants are reported by Nielsen and Önnerth (1995) and Önnerth and Bechmann (1995), where both more cost effective operation and better treatment results are obtained.

1.1.6 Purpose

The purpose of this research project is to establish on-line operational models for the wastewater coming to a wastewater treatment plant and for selected processes in the plant, and to suggest control algorithms that utilize the existing facilities in the sewer and treatment plant in an optimal way. The project is a contribution towards the total integrated control of sewer systems and wastewater treatment plants.

1.2 Outline of the thesis

This thesis is based on 6 papers written during the project and is divided into two parts. The first part contains a summary of the theory behind the modelling carried out in preparation of the papers as well as a compilation of the results of the papers, which are are included in Part II.

In Chapter 2 the background for stochastic modelling of dynamic systems is given. The aim is to give the background for establishing models comprised of continuous time descriptions of the system dynamics and discrete time descriptions of the measurement process. Hence, the chapter begins with a description of stochastic systems. Then a maximum likelihood method for estimation of the parameters in the models is presented. This estimation method requires use of the extended Kalman filter, which is introduced next. A method for treating uncertain and missing observations is presented before the validation of the estimated models is treated. Finally in this chapter, the grey-box modelling concept is explained and the advantages of this concept is explained.

Chapter 3 summarizes the results presented in the papers and discusses aspects of the work behind the papers not treated in them. The papers should be read in connection with Chapter 3, as the results in the papers are not repeated in this chapter. Furthermore, suggestions concerning future work in the areas treated is given.

Finally, the conclusions is presented in Chapter 4, after which the papers are included.

Chapter 2

Stochastic modelling of dynamic systems

In this chapter some of the mathematical and statistical background for stochastic modelling of dynamic systems is given. The objective is to establish the basis for building continuous time stochastic state space models with discrete time observations, to estimate the parameters of the models, and finally to validate the models.

2.1 The Wiener process

The Scottish botanist Robert Brown observed the irregular motion of pollen grains suspended in water in 1828. The motion, called Brownian motion, was later explained by the random collisions between the pollen grains and the water molecules. The Wiener process is a fundamental stochastic process providing a mathematical description of the Brownian motion. The application of the Wiener process goes far beyond the study of microscopic suspended particles, and includes modelling of noise and random perturbations in physical systems, e.g. thermal noise in electrical circuits.

The properties that define the n-dimensional Wiener process $\{\boldsymbol{w}_t, t \geq 0\}$ are:

1. $\boldsymbol{w}_0 = 0$ with probability 1
2. The increments $\boldsymbol{w}_{t_1} - \boldsymbol{w}_{t_0}, \boldsymbol{w}_{t_2} - \boldsymbol{w}_{t_1}, \ldots, \boldsymbol{w}_{t_k} - \boldsymbol{w}_{t_{k-1}}$, of the process are mutually independent for any partitioning of the time interval $0 \leq t_0 < t_1 < \cdots < t_k < \infty$
3. The increment $\boldsymbol{w}_t - \boldsymbol{w}_s$ for any $0 \leq s < t$ is Gaussian with mean and covariance:

$$\mathrm{E}[\boldsymbol{w}_t - \boldsymbol{w}_s] = 0 \tag{2.1}$$

$$\mathrm{V}[\boldsymbol{w}_t - \boldsymbol{w}_s] = \boldsymbol{\Sigma}_{\boldsymbol{w}}(t-s) \tag{2.2}$$

   where $\boldsymbol{\Sigma}_{\boldsymbol{w}}$ is a positive semi definite matrix.

When $\boldsymbol{\Sigma}_{\boldsymbol{w}}$ is the identity matrix, a standard Wiener process is obtained.

Among other important properties of the Wiener process, it should be noted that the sample paths are continuous with probability one, but nowhere differentiable with probability one.

Even though the Wiener process is not differentiable, the formal time derivative of $\boldsymbol{w}_t$ is called Gaussian white noise. This derivative only makes sense as a generalized function. The process has a uniform spectral density function for all real frequencies, which is a characteristic of white light, hence, the term *white noise*.

See e.g. Melgaard (1994); Madsen and Holst (1996); Øksendal (1995); Jazwinski (1970) for more details about the Wiener process.

2.2 Stochastic differential equations

In order to be able to handle stochastic terms in differential equations it is necessary to introduce stochastic integrals.

Consider the one-dimensional stochastic differential equation:

$$dX_t = f(X_t, t)dt + G(X_t, t)dw_t \tag{2.3}$$

where $f(X_t, t)$ is the drift coefficient, $G(X_t, t)$ is the diffusion coefficient and w_t is a standard one-dimensional Wiener process.

A formal integration of (2.3) yields:

$$X_t = X_0 + \int_0^t f(X_s, s)ds + \int_0^t G(X_s, s)dw_s \tag{2.4}$$

The first of the integrals can be interpreted as a standard Riemann integral, but the second integral is more difficult to handle, as the sample paths of the Wiener process have unbound variation (Madsen and Holst, 1996). One solution is to apply the Itô stochastic integral, defined as the mean-square limit of the left hand rectangular approximation:

$$\sum_{i=0}^{N-1} G(X_{t_i}, t_i)(w_{t_{i+1}} - w_{t_i}) \tag{2.5}$$

for all partitions $0 = t_0 < t_1 < \cdots < t_N = t$ as the maximum step size $\max_i(t_{i+1} - t_i) \to 0$.

More details can be found in e.g. Øksendal (1995); Kloeden and Platen (1995); Madsen et al. (1998); Madsen and Holst (1996).

2.3 Stochastic state space models

State space models are often used to describe dynamic systems. With the introduction of stochastic differential equations it is possible to establish continuous time stochastic state space models with discrete time observations. This is reasonable because physical systems are of a continuous time nature, and measurements are taken at discrete time instances. In a stochastic state space model, stochastic terms are used both in the differential equations and in the observation equations. Hereby, it is possible to distinguish between modelling uncertainty in the differential equations and measurement uncertainty in the observation equations.

The dynamics of a general non-linear stochastic state space model are described by:

$$d\boldsymbol{X}_t = \boldsymbol{f}(\boldsymbol{X}_t, \boldsymbol{U}_t, \boldsymbol{\theta}, t)dt + \boldsymbol{G}(\boldsymbol{U}_t, \boldsymbol{\theta}, t)d\boldsymbol{w}_t, \quad t \geq 0 \tag{2.6}$$

Here, $\boldsymbol{X}_t$ is the state vector, $\boldsymbol{f}$ is a vector function that describes the evolution of the system as a function of the current state, the input vector $\boldsymbol{U}_t$, the parameters of the model represented by the parameter vector $\boldsymbol{\theta}$, and the time t. The vector function $\boldsymbol{G}$ describes how the noise enters the system. The noise is represented by the stochastic process $\boldsymbol{w}(t)$, which is an n-th order standard Wiener process.

The measurements are taken at discrete time intervals and are thus expressed in the observation equation:

$$\boldsymbol{Y}_k = \boldsymbol{h}(\boldsymbol{X}_k, \boldsymbol{U}_k, \boldsymbol{\theta}, t_k) + \boldsymbol{e}_k, \quad t_k \in \{t_0, t_1, \dots, t_N\} \tag{2.7}$$

where $\boldsymbol{h}$ is a function that expresses how the measurements are related to the states and the input, and finally N is the number of observations. The observation noise $\boldsymbol{e}$ is assumed to be a Gaussian white noise sequence independent of $\boldsymbol{w}$. Here, the subscript k is introduced as a shorthand notation for t_k.

2.4 Maximum likelihood estimation

When a stochastic state space model of a given system is formulated and measurements from the system are obtained, the parameters are to be estimated. Even though different approaches to the estimation problem are described in the literature (see e.g. Ljung (1999)), only the maximum likelihood method will be described here.

The observations are considered as realizations of stochastic variables. The objective of the method is to maximize the probability of the observations, i.e. when a maximum likelihood estimate of the parameters $\boldsymbol{\theta}$ is found, no other parameters will result in a higher probability of the observed data.

In the following it is assumed that the system is observed at regular time intervals (i.e. with a constant sampling time). To simplify the notation the time is normalized with the sampling time, and thus the time index belongs to the set $0, 1, 2, \dots, N$, where N is the number of observations. In general every observation is a vector.

Let $\mathcal{Y}(t)$ denote the matrix of all observed outputs until and including time t:

$$\mathcal{Y}(t) = [\boldsymbol{Y}_t, \boldsymbol{Y}_{t-1}, \dots, \boldsymbol{Y}_1, \boldsymbol{Y}_0]' \tag{2.8}$$

The unconditional likelihood function $L'(\boldsymbol{\theta}; \mathcal{Y}(N))$ is the joint probability of all the observations assuming that the parameters are known, i.e.:

$$L'(\boldsymbol{\theta}; \mathcal{Y}(N)) = p(\mathcal{Y}(N)|\boldsymbol{\theta}) \tag{2.9}$$

In order to express the likelihood function as a product of conditional densities, successive applications of the rule $P(A \cap B) = P(A|B)P(B)$ are used:

$$\begin{aligned} L'(\boldsymbol{\theta}; \mathcal{Y}(N)) &= p(\mathcal{Y}(N)|\boldsymbol{\theta}) \\ &= p(\boldsymbol{Y}_N|\mathcal{Y}(N-1), \boldsymbol{\theta})p(\mathcal{Y}(N-1)|\boldsymbol{\theta}) \\ &= \left(\prod_{t=1}^{N} p(\boldsymbol{Y}_t|\mathcal{Y}(t-1), \boldsymbol{\theta})\right)p(\boldsymbol{Y}_0|\boldsymbol{\theta}) \end{aligned} \tag{2.10}$$

The conditional likelihood function (conditioned on $\boldsymbol{Y}_0$) is then:

$$L(\boldsymbol{\theta}; \mathcal{Y}(N)) = \prod_{t=1}^{N} p(\boldsymbol{Y}_t|\mathcal{Y}(t-1), \boldsymbol{\theta}) \tag{2.11}$$

As the increments of $\boldsymbol{w}$ and the observation noise $\boldsymbol{e}$ are Gaussian, the conditional densities for a linear system are also Gaussian. For a non-linear system like (2.6) we shall assume that the conditional densities are approximately Gaussian. The Gaussian assumption enables an evaluation of the likelihood function. The normal distribution is completely characterized by the mean and the covariance. Hence, in order to parameterize the conditional distributions, the conditional mean and conditional covariance are introduced as:

$$\hat{\boldsymbol{Y}}_{t|t-1} = \mathrm{E}[\boldsymbol{Y}_t|\mathcal{Y}(t-1), \boldsymbol{\theta}] \quad \text{and} \tag{2.12}$$

$$\boldsymbol{R}_{t|t-1} = \mathrm{V}[\boldsymbol{Y}_t|\mathcal{Y}(t-1), \boldsymbol{\theta}] \tag{2.13}$$

respectively. Notice that (2.12) is the one-step prediction and (2.13) the associated covariance.

The innovations or one-step prediction errors are:

$$\boldsymbol{\epsilon}_t = \boldsymbol{Y}_t - \hat{\boldsymbol{Y}}_{t|t-1} \tag{2.14}$$

Then the conditional likelihood function (2.11) becomes:

$$\begin{aligned} & L(\boldsymbol{\theta}; \mathcal{Y}(N)) \\ & = \prod_{t=1}^{N} \Big((2\pi)^{-m/2} \det \boldsymbol{R}_{t|t-1}^{-1/2} \exp(-\tfrac{1}{2} \boldsymbol{\epsilon}_t' \boldsymbol{R}_{t|t-1}^{-1} \boldsymbol{\epsilon}_t) \Big) \end{aligned} \tag{2.15}$$

where m is the dimension of the $\boldsymbol{Y}$ vector. Traditionally the logarithm of the conditional likelihood function is considered, i.e.

$$\begin{aligned} & \log L(\boldsymbol{\theta}; \mathcal{Y}(N)) \\ & = -\tfrac{1}{2} \sum_{t=1}^{N} \Big(\log \ \det \boldsymbol{R}_{t|t-1} + \boldsymbol{\epsilon}_t' \boldsymbol{R}_{t|t-1}^{-1} \boldsymbol{\epsilon}_t \Big) + \text{const} \end{aligned} \tag{2.16}$$

The maximum likelihood estimate of $\boldsymbol{\theta}$ is found as the value that maximizes the conditional likelihood function $L(\boldsymbol{\theta}; \mathcal{Y}(N))$, which is the same value that maximizes $\log L(\boldsymbol{\theta}; \mathcal{Y}(N))$ and minimizes $-\log L(\boldsymbol{\theta}; \mathcal{Y}(N))$. Thus, the maximum likelihood estimate of $\boldsymbol{\theta}$ is found as:

$$\hat{\boldsymbol{\theta}} = \arg \min_{D_{\mathcal{M}}} \sum_{t=1}^{N} \Big(\log \ \det \boldsymbol{R}_{t|t-1} + \boldsymbol{\epsilon}_t' \boldsymbol{R}_{t|t-1}^{-1} \boldsymbol{\epsilon}_t \Big) \tag{2.17}$$

where $D_{\mathcal{M}}$ is the set of allowed values of $\boldsymbol{\theta}$

As it is not possible to optimize the likelihood function analytically, a numerical method has to be used. The quasi Newton method is a reasonable choice.

The maximum likelihood estimator is asymptotically normally distributed with mean $\boldsymbol{\theta}$ and variance

$$\boldsymbol{D} = \boldsymbol{H}^{-1} \tag{2.18}$$

where $\boldsymbol{H}$ is the Hessian given by

$$\{h_{lk}\} = -\mathrm{E}\Big[\frac{\partial^2}{\partial \theta_l \partial \theta_k} \log L(\boldsymbol{\theta}; \mathcal{Y}(N)) \Big] \tag{2.19}$$

where $\{h_{lk}\}$ denotes the element in row l and column k of $\boldsymbol{H}$ and θ_j denotes element j of $\boldsymbol{\theta}$ (Conradsen, 1984a).

An estimate of $\boldsymbol{D}$ is obtained by equating the observed value with its expectation and applying

$$\{h_{lk}\} \approx -\Big(\frac{\partial^2}{\partial \theta_l \partial \theta_k} \log L(\boldsymbol{\theta}; \mathcal{Y}(N)) \Big) \Big|_{\boldsymbol{\theta} = \hat{\boldsymbol{\theta}}} \tag{2.20}$$

Equation (2.20) is used to estimate the variance of the parameter estimates. The variance estimate of each of the parameter estimates serves as basis for calculating t-test values for test under the hypothesis that the parameter is equal to zero. Furthermore, the correlation between the parameter estimates is found based on the estimate of $\boldsymbol{D}$.

2.5 The extended Kalman filter

The Kalman filter provides estimates of the states in a state space model based on measurements from the real system. In the maximum likelihood estimation method described above, the one step predictions and associated covariances are needed for calculating the likelihood function, and this is what the Kalman filter provides. The Kalman filter is derived for linear systems, and is thus not directly applicable to non-linear systems. However, the extended Kalman filter, based on linearizations of the system equation (2.6) around the current state estimate, can then be applied.

Consider now the model described by:

$$d\boldsymbol{X}_t = \boldsymbol{f}(\boldsymbol{X}_t, \boldsymbol{U}_t, \boldsymbol{\theta}, t)dt + \boldsymbol{G}(\boldsymbol{\theta}, t)d\boldsymbol{w}_t, \tag{2.21}$$

with $\boldsymbol{w}_t$ being a standard Wiener process. Note that $\boldsymbol{G}$ is now limited to be a function of the parameters and time only. The observations are taken at discrete time instants t_k and described by:

$$\boldsymbol{Y}_k = \boldsymbol{h}(\boldsymbol{X}_k, \boldsymbol{U}_k, \boldsymbol{\theta}, t_k) + \boldsymbol{e}_k, \quad t_k \in \{t_0, t_1, \dots, t_N\} \tag{2.22}$$

where $\boldsymbol{e}$ is a Gaussian white noise process independent of $\boldsymbol{w}$, and with

$$\boldsymbol{e}_k \in N(\boldsymbol{0}, \boldsymbol{S}(\boldsymbol{\theta}, t_k)) \tag{2.23}$$

For the continuous-discrete time extended Kalman filter for the state space model (2.21)–(2.22) the prediction equations are:

$$\frac{d\hat{\boldsymbol{X}}_{t|k}}{dt} = \boldsymbol{f}(\hat{\boldsymbol{X}}_{t|k}, \boldsymbol{U}_t, \boldsymbol{\theta}, t), \quad t \in [t_k, t_{k+1}[\tag{2.24}$$

$$\begin{aligned}\frac{d\boldsymbol{P}_{t|k}}{dt} &= \boldsymbol{A}(\hat{\boldsymbol{X}}_{t|k}, \boldsymbol{U}_t, \boldsymbol{\theta}, t)\boldsymbol{P}_{t|k} \\ &\quad + \boldsymbol{P}_{t|k}\boldsymbol{A}'(\hat{\boldsymbol{X}}_{t|k}, \boldsymbol{U}_t, \boldsymbol{\theta}, t) \\ &\quad + \boldsymbol{G}(\boldsymbol{\theta}, t)\boldsymbol{G}'(\boldsymbol{\theta}, t), \quad t \in [t_k, t_{k+1}[\end{aligned} \tag{2.25}$$

where $\boldsymbol{A}$ is obtained by a linearization of the system equation (2.21):

$$\boldsymbol{A}(\hat{\boldsymbol{X}}_{t|k}, \boldsymbol{U}_t, \boldsymbol{\theta}, t) = \frac{\partial \boldsymbol{f}}{\partial \boldsymbol{X}}\Big|_{\boldsymbol{X}=\hat{\boldsymbol{X}}_{t|k}} \tag{2.26}$$

At the observation times t_k the updates are:

$$\boldsymbol{K}_k = \boldsymbol{P}_{k|k-1}\boldsymbol{C}'_k[\boldsymbol{C}_k\boldsymbol{P}_{k|k-1}\boldsymbol{C}'_k + \boldsymbol{S}(\boldsymbol{\theta}, t_k)]^{-1} \tag{2.27}$$

$$\hat{\boldsymbol{X}}_{k|k} = \hat{\boldsymbol{X}}_{k|k-1} + \boldsymbol{K}_k(\boldsymbol{Y}_k - \boldsymbol{h}(\hat{\boldsymbol{X}}_{k|k-1}, \boldsymbol{U}_k, \boldsymbol{\theta}, t_k)) \tag{2.28}$$

$$\boldsymbol{P}_{k|k} = \boldsymbol{P}_{k|k-1} - \boldsymbol{K}_k\boldsymbol{C}_k\boldsymbol{P}_{k|k-1} \tag{2.29}$$

where $\boldsymbol{C}$ is the linearization of the observation equation (2.22):

$$\boldsymbol{C}_k = \boldsymbol{C}(\hat{\boldsymbol{X}}_{k|k-1}, \boldsymbol{U}_k, \boldsymbol{\theta}, t_k) = \frac{\partial \boldsymbol{h}}{\partial \boldsymbol{X}}\Big|_{\boldsymbol{X}=\hat{\boldsymbol{X}}_{k|k-1}} \tag{2.30}$$

To make the integration of (2.24) and (2.25) computationally feasible and numerically stable for stiff systems, the time interval $[t_k, t_{k+1}[$ between to subsequent observations is divided into n_s subintervals (sub-sampled) and the equations (2.24) and (2.25) are linearized around the state estimate at each subsampling time. The state propagation equation for the subinterval $[t_j, t_{j+1}[$ becomes:

$$\begin{aligned}\frac{d\hat{\boldsymbol{X}}_t}{dt} &= \boldsymbol{f}(\hat{\boldsymbol{X}}_j, \boldsymbol{U}_j, \boldsymbol{\theta}, t_j) + \boldsymbol{A}(\hat{\boldsymbol{X}}_j, \boldsymbol{U}_j, \boldsymbol{\theta}, t_j)(\hat{\boldsymbol{X}}_t - \hat{\boldsymbol{X}}_j) \\ &= \boldsymbol{A}(\hat{\boldsymbol{X}}_j, \boldsymbol{U}_j, \boldsymbol{\theta}, t_j)\hat{\boldsymbol{X}}_t \\ &\quad + (\boldsymbol{f}(\hat{\boldsymbol{X}}_j, \boldsymbol{U}_j, \boldsymbol{\theta}, t_j) - \boldsymbol{A}(\hat{\boldsymbol{X}}_j, \boldsymbol{U}_j, \boldsymbol{\theta}, t_j)\hat{\boldsymbol{X}}_j) \quad t \in [t_j, t_{j+1}[\end{aligned} \tag{2.31}$$

Equation (2.31) has the solution:

$$\hat{\boldsymbol{X}}_{j+1} = \hat{\boldsymbol{X}}_j + (\boldsymbol{\Phi}_s(j) - \boldsymbol{I})(\boldsymbol{A}(\hat{\boldsymbol{X}}_j, \boldsymbol{U}_j, \boldsymbol{\theta}, t_j)^{-1}\boldsymbol{f}(\hat{\boldsymbol{X}}_j, \boldsymbol{U}_j, \boldsymbol{\theta}, t_j)) \tag{2.32}$$

where

$$\mathbf{\Phi}_s(j) = e^{\boldsymbol{A}(\hat{\boldsymbol{X}}_j, \boldsymbol{U}_j, \boldsymbol{\theta}, t_j)\tau_s} \tag{2.33}$$

and $\tau_s = t_{j+1} - t_j = T/n_s$ where T is the sampling time. The matrix exponential can be calculated by e.g. Padé approximation (cf. Madsen et al. (1998)). The state covariance equation becomes:

$$\boldsymbol{P}_{j+1} = \mathbf{\Phi}_s(j)\boldsymbol{P}_j\mathbf{\Phi}_s(j)' + \mathbf{\Lambda}_s(j) \tag{2.34}$$

where

$$\mathbf{\Lambda}_s(j) = \int_0^{\tau_s} \mathbf{\Phi}_s(j)\boldsymbol{G}(\boldsymbol{\theta}, t)\boldsymbol{G}(\boldsymbol{\theta}, t)'\mathbf{\Phi}_s(j)'ds \tag{2.35}$$

The extended Kalman filter and the iterated extended Kalman filter are treated in more detail in e.g. Madsen et al. (1998) and Jazwinski (1970).

2.6 Uncertain and missing observations

When working with real systems in an imperfect real world, measurements are sometimes missing. Sometimes all measurements are available, but the modeller has a priori information that some measurements are less valid than others. This is easily handled by adjusting the covariance $\boldsymbol{S}(\boldsymbol{\theta}, t)$ of the observation noise process according to the validity of the measurements. If a measurement is considered uncertain, the corresponding parameter in $\boldsymbol{S}(\boldsymbol{\theta}, t)$ is increased. How much, depends on how uncertain the measurement is. If a measurement is completely missing, the corresponding variance is ideally set at ∞. When increasing $\boldsymbol{S}(\boldsymbol{\theta}, t)$ the Kalman gain $\boldsymbol{K}_k$ is reduced and the data update (2.28) of the state estimates that depend on the given measurement is reduced correspondingly.

Missing observations in the input data should be handled otherwise. If a single or at least few observations in a row are missing, these can be substituted by interpolated values, but in case of long periods with missing observations interpolation is often not an option. In this case a change in the model should be considered. Sometimes it is possible to change an input variable to an output variable, by a slight modification of the model. When this is done, the missing observations can be handled by means of the method proposed above.

2.7 Model validation

When an estimation of the parameters of a model has been carried out, it is important to check if the resulting model is satisfactory. This is done by model validation. This is often carried out by applying several methods simultaneously, of which some will be mentioned in the following.

2.7.1 Tests in the model

The maximum likelihood estimation method provides estimates of the variance of the parameters, cf. Section 2.4, and enables test for the significance of the parameters, i.e. to test whether the parameters are significantly different from zero. The hypothesis to test is:

$$H_0 : \theta_j = 0 \quad \text{against} \quad H_1 : \theta_j \neq 0 \tag{2.36}$$

The test value is $\frac{\hat{\theta}_j}{\hat{\sigma}_{jj}}$, where $\hat{\theta}_j$ denotes the j-th parameter estimate and $\hat{\sigma}^2_{jj}$ the associated variance estimate. As the parameter estimates are asymptotically normally distributed, the test value is t distributed, and then a t-test of the hypothesis in (2.36) can be performed (Conradsen, 1984b).

Based on the estimate of the parameter covariance (2.18), the corresponding correlation matrix can be computed. Over-parameterization of the model is indicated by closely correlated parameters, i.e. by correlation coefficients between two parameters close to 1 or -1. Hence if correlation coefficients close to 1 or -1 are observed, a reformulation of the model should be considered.

2.7.2 Graphical methods

An obvious method for model validation is a graphical comparison of the model output and the observations, which is simply carried out by plotting the observed and modelled data. The question is if the outputs of the model seem to match the observations. Note that it is possible to obtain both one-step (or k-step) predictions and simulations from a state space model. The one-step predictions use the observations at time t and the model equations to predict the observations at the next sample time, while the k-step predictions use the observations at time t and the model equations to predict the observations k sample times ahead. Simulations are characterized by only using the initial conditions, the inputs and the model to simulate the outputs.

The model output can also be compared with the observations by plotting the residuals, i.e. the difference between the observations and modelled data. Naturally, this can be done for both the one-step (or k-step) predictions and the simulations.

The states of the model are often interpretable in a physical sense. Hence, the state estimates should be plotted so that it can be checked if they are realistic. This is particularly important, when unmeasured states are included in the model.

Often the graphical methods reveal possibilities for model enhancements, e.g. inclusion of bounds on states etc.

2.7.3 Residual analysis

The residuals are that part of the observations that the model does not count in. Hence, an analysis of the residuals can provide useful information on how to improve the model, or to improve the confidence in the model. If the model describes the true system well, the residuals are white noise, and it is thus obvious to test if the residuals can in fact be considered as white noise. Furthermore, the maximum likelihood method is based on a white noise assumption. If this assumption is not fulfilled, the appealing properties of the method are lost. If the residuals are not white noise, the properties of the residuals can give an indication of how to improve the model. For instance, if the autocorrelation function of the residuals show first order autoregressive behaviour, then an extra state is needed in the model.

Auto- and cross-correlations

If the residuals ϵ_t of a scalar process are white noise, the estimated autocorrelation function is

$$\hat{\rho}_\epsilon(k) \in_{approx} N(0, \frac{1}{N}) \tag{2.37}$$

Approximative 95% and 99% confidence limits are $\pm 2\sigma = \pm 2/\sqrt{N}$ and $\pm 3\sigma = \pm 3/\sqrt{N}$. Plots of both the estimated autocorrelations for the residuals and the confidence limits provide a graphical way to test whether the white noise assumption should be rejected.

The cross-correlations between input u and residuals can be used to check whether the input contains more information that has to be included in the model. Provided that the residuals (or the inputs) are white noise, the estimated cross-correlation function is

$$\hat{\rho}_{u\epsilon}(k) \in_{approx} N(0, \frac{1}{N}) \tag{2.38}$$

Hence, a significance test equivalent to the one described above for the autocorrelation function can be carried out. Note, however, that autocorrelations in u or ϵ can generate large cross-correlations between the two, even though they are not mutually correlated (Madsen, 1995).

Estimators for the auto- and cross-correlations are given in Madsen (1995).

Cumulative periodogram

The periodogram for the residuals for the frequencies

$$\nu_i = \frac{i}{N}, \qquad i = 0, 1, \ldots, N/2$$

is for N even:

$$\hat{I}(\nu_i) = \frac{1}{N}\left[\Big(\sum_{t=1}^{N} \epsilon_t \cos 2\pi\nu_i t\Big)^2 + \Big(\sum_{t=1}^{N} \epsilon_t \sin 2\pi\nu_i t\Big)^2\right] \tag{2.39}$$

The periodogram is a frequency domain description of the variation of the residuals, as $I(\nu_i)$ indicates how much of the variation of the residuals is present at the frequency ν_i.

The normalized cumulative periodogram is

$$\hat{C}(\nu_j) = \frac{\sum_{i=1}^{j} \hat{I}(\nu_i)}{\sum_{i=1}^{N/2} \hat{I}(\nu_i)} \tag{2.40}$$

which is a non-decreasing function, defined for the frequencies ν_i. For white noise the variation is uniformly distributed over the frequencies. The total variation for N observations is $N\sigma_\epsilon^2$ and hence the theoretical periodogram for white noise is

$$I(\nu_i) = 2\sigma_\epsilon^2 \tag{2.41}$$

The theoretical cumulative periodogram is thus a straight line from origo to (0.5, 1). If the residuals are white noise, it is expected that $\hat{C}(\nu_i)$ is close to this line. Confidence intervals around the straight line can be calculated using a Kolmogorov-Smirnov test, cf. Melgaard (1994).

Note that ν_i are normalized frequencies, normalized by the sampling frequency $1/T$, i.e.. $f_i = \nu_i/T$.

2.7.4 Cross validation

Cross validation is a method that requires two data sets: 1) an estimation data set, and 2) a validation data set. The estimation data set is used for the parameter estimation. The validation data set is then used to test if the estimated model describes this data set equally well as the estimation data set. It is important to carry out this type of test, as a pitfall a modeller might fall into is to model the data and not the system. When testing the model on a new data set from the same system, it will be evident if the estimation data or the system was modelled.

2.8 Grey-box modelling

Traditionally modelling of dynamic systems has been carried out following one of two approaches. The *black-box* concept is a data based concept, where prior knowledge of the system is not included in the model. Examples of black-box models are the traditional time series models: autoregressive (AR) models, moving average (MA) models, and combinations of these (ARMA). To these models external input can be included to build e.g. ARX or ARMAX models. Another type of black-box models is neural networks. A deterministic model purely based on known relations for a system is characterized as a *white-box* model. White-box models of complex systems as sewer systems and wastewater treatment plants are often comprised of numerous detailed equations for the subsystems of the system. White-box models are subject to uncertainties, but a description of these is usually not included in the models, and hence not quantified.

In the environmental sciences, the IAWQ Activated Sludge Models (Henze et al., 1987, 1995, 1999; Gujer et al., 1999) for the processes in activated sludge wastewater treatment plants, and the Mouse models (Lindberg et al., 1989; Crabtree et al., 1995; Mark et al., 1995, 1998b), based on the St. Vernant equations (Chow et al., 1988) for sewer systems, are examples of deterministic or white-box models.

Often the deterministic models are very detailed and have many parameters, which makes it difficult or impossible to estimate the parameters by ordinary statistical methods.

The grey-box method is supposed to be the best mix of the two methods. A grey-box model combines the available knowledge of the most important physical relations with statistical modelling tools. Hereby it is possible to establish models with few parameters compared to the white-box models, and with parameters that have physical meaning as opposed to the black-box models. Furthermore, the uncertainties are included in the grey-box model, and the parameters of the noise processes are also estimated. Hence, the model uncertainties are quantified.

2.9 Summary

In this chapter an overview of stochastic modelling is given. The Wiener process is introduced in order to describe continuous time white noise. Itô stochastic integrals and differential equations serve as basis for establishing continuous time stochastic state space models. The parameters in such models are suggested estimated by the maximum likelihood method. The extended Kalman filter is described, as it calculates the one-step predictions that are needed by the estimation method. When a model is established and the parameters are estimated, it should be validated. Therefore a set of validation tools is presented. Finally, the grey-box modelling approach is presented and compared with other modelling approaches.

Chapter 3

Results and discussion

The results of the work carried out in the present Ph.D. project are documented in the papers included in Part II of this thesis. The purpose of this chapter is to discuss aspects of the work that are not treated in the papers, to look at the results in a broader perspective and to compile the results of the papers, as well as to suggest areas for future research.

The work presented here is divided into two parts:

The first part focuses on the wastewater coming into the wastewater treatment plant. The emphasis has been on developing dynamic grey-box models capable of describing the first flush phenomenon by modelling the incoming fluxes, but the results presented also cover the on-line measurements of pollutants and comparison with static models. This work is presented in Papers A–C.

In the second part, focus is on the biological part of the wastewater treatment plant, especially during wet weather conditions, where Aeration Tank Settling (ATS) operation is activated. In Paper D a model for ATS is presented and the result of implementing the model on-line is documented. The model of Paper D forms the basis for further modelling as carried out in preparation of Paper E.

In Paper E ATS operation is described in more detail, and a dynamic grey-box model of the suspended solids concentrations in the aeration tanks as well as in the effluent from these is established. This model is used in Paper F to quantify the advantages of ATS operation in terms of increased hydraulic capacity of the biological part of the plant and the results are compared with the hydraulic capacity during ordinary dry weather operation. A control algorithm for enabling ATS and for selecting the optimal combination of phase lengths during ATS is also proposed in Paper F.

3.1 Sewer models

The influent pollutant fluxes at two wastewater treatment plants, and hence two catchments, have been modelled. Skive wastewater treatment plant delivered data used in the preparation of Paper A and Paper B, and data from Aalborg East wastewater treatment plant was used in Paper C.

The models estimated in Paper A and Paper B are based on the same model structure: A diurnal profile of the incoming flux combined with a first order linear differential equation for the deposits in the sewer and on impervious areas of the catchment.

The estimations in Paper A were carried out using the Matlab System Identification Toolbox (Ljung, 1995) with the `bj` (Box-Jenkins) function in discrete time, and the results were translated to continuous time (with the `d2cm` function). In this paper the model structure is applied directly to the UV absorption flux and the turbidity flux. If COD and UV absorption as well as SS and turbidity are proportional, this approach is equivalent to modelling COD and SS fluxes, but as the relationships are affine, the models of UV absorption and turbidity fluxes are not equivalent to the models of COD and SS fluxes. However in this paper UV absorption and turbidity are thought of as measures of COD and SS concentrations, respectively.

The estimated models are cross validated, i.e. one data set is used for the estimation and another data set is used for the validation of the model. Furthermore, the estimated diurnal profiles for UV absorption and turbidity fluxes are shown. The modelled amounts of UV absorption and turbidity deposited in the sewers are also shown. As it is not possible to estimate the actual levels of the deposits in the sewer with the model structure used, only deviations from the initial level can be found.

In Paper B the COD and SS fluxes are modelled. The estimations were made with the CTLSM software (Madsen and Melgaard, 1991; Melgaard and Madsen, 1991), hence, the parameters are estimated by a maximum likelihood method directly in continuous time. In this paper the standard deviations of the parameter estimates are also included.

The modelling carried out in Paper B is based on the same data as used in Paper A and the estimated models are cross validated like in Paper A. However, the models of Paper B are models of the COD and SS fluxes (as opposed to the models of Paper A). In Paper B the estimated amounts of deposits in the sewer are shown as deviations from the unknown average for the time period concerned. Due to the fact that the models are of COD and SS fluxes, respectively, the deposits are amounts COD and SS.

In Paper C four different model structures are estimated and compared. The data used in this paper are from Aalborg East wastewater treatment plant. The contribution from this paper is twofold: 1) The dynamic model structure used in the previous papers is compared with simpler static models, and 2) The dynamic model structure is applied to a different sewer system.

Cross validations of the estimated models was not carried out in Paper C. This would, however, be relevant to do so that the different models could be compared on a validation data set also.

3.1.1 Cumulated flux vs. cumulated flow

When dealing with sewer systems and rain storms, it is of interest whether first flushes are present or not. As the proposed models do not directly describe whether and when a first flush is present, this issue will be discussed here. The graph of the normalized cumulated flux vs. cumulated flow is used in the characterization whether a first flush was present, i.e. a graph with the parametric description:

$$(x,y) = \left(\frac{\int_{t_0}^{t} Q dt}{\int_{t_0}^{t_1} Q dt}, \frac{\int_{t_0}^{t} QX dt}{\int_{t_0}^{t_1} QX dt}\right) \quad t_0 \leq t \leq t_1 \tag{3.1}$$

where X is the concentration of the pollutant concerned, Q is the flow, and t_0 and t_1 denote the start and end times of the rain incident.

When using this method, it is not possible from a given graph to distinguish between different types of rain incidents, e.g. between a short intensive thunderstorm and a long rain with lower intensity.

It is easier to distinguish different rain incidents from the non-normalized graph:

$$(x, y) = (\int_{t_0}^{t} Q dt, \int_{t_0}^{t} QX dt) \quad t_0 \leq t \leq t_1 \tag{3.2}$$

Model 1 of Paper C consists only of a diurnal profile (a harmonic function with a 24-hour period), and is therefore not applicable to storm situations. Model 2 models the pollutant fluxes as affine with the flow $QX = c_0 + c_1 Q$, i.e. the pollutant flux is modelled as a constant level with addition of a term proportional to the flow. Hence, the deviation from the constant pollutant flux level is modelled as a flux with constant concentration. Models 1 and 2 are thus not capable of describing first flush phenomena. Hence, it is only meaningful to apply the cumulated flow – cumulated flux methodology to models 3 and 4 of Paper C.

The cumulated flow – cumulated flux methodology is applied to a rain incident in the data series from Aalborg East wastewater treatment plant. The flow to the plant during the period in question is shown in Figure 3.1

In Figures 3.2 and 3.3 the normalized cumulated SS flux vs. normalized cumulated flow of models 3 and 4 are shown, and in Figures 3.4 and 3.5, the corresponding non-normalized graphs are shown. Note that the observed fluxes are compared to simulations from the models, and not one (or k) step ahead predictions. From Figures 3.2 and 3.3 it can be seen that both models can predict increased pollutant concentrations during the rain incident, but also that the simulated fluxes are too low in the first approx. 70 – 80 % of the incident. When inspecting the non-normalized graphs in Figures 3.4 and 3.5, it becomes clear that the modelled fluxes are too low as the graphs for the measurements and the simulations does not end in the same point.

The normalized cumulated COD flux vs. the normalized cumulated flow is shown in Figures 3.6 and 3.7 with the corresponding non-normalized graphs

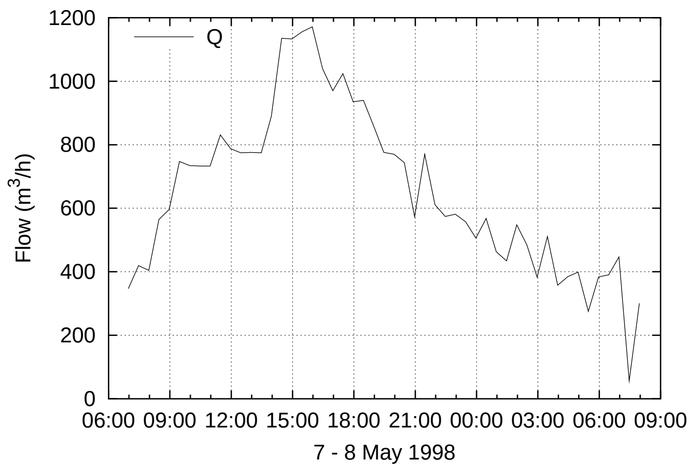

Figure 3.1. Influent flow to Aalborg East wastewater treatment plant.

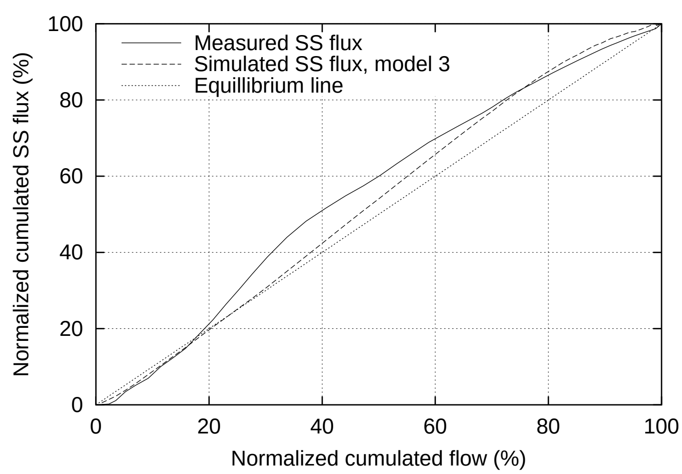

Figure 3.2. Normalized cumulated SS flux vs. normalized cumulated flow, model 3.

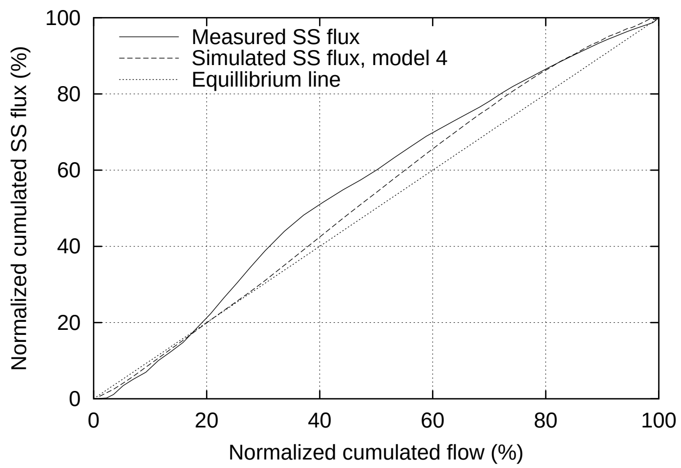

Figure 3.3. Normalized cumulated SS flux vs. normalized cumulated flow, model 4.

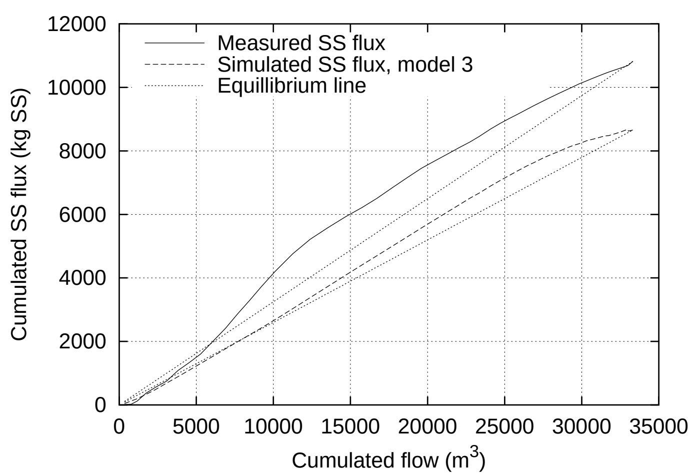

Figure 3.4. Cumulated SS flux vs. cumulated flow, model 3.

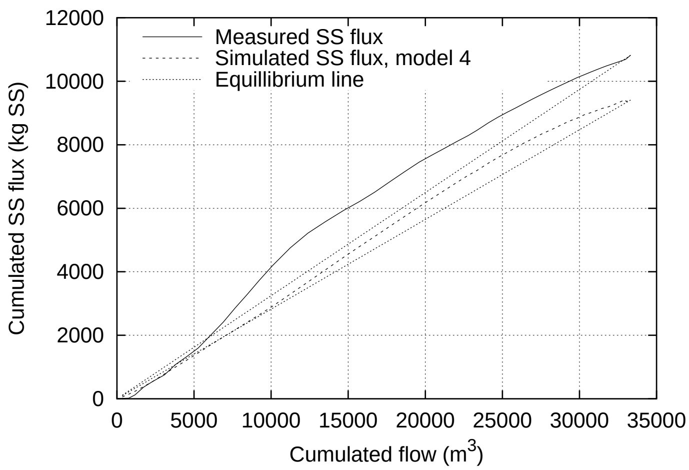

Figure 3.5. Cumulated SS flux vs. cumulated flow, model 4.

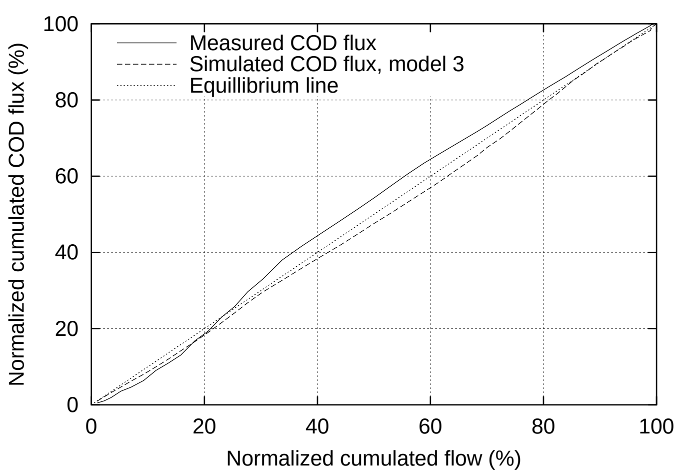

Figure 3.6. Normalized cumulated COD flux vs. normalized cumulated flow, model 3.

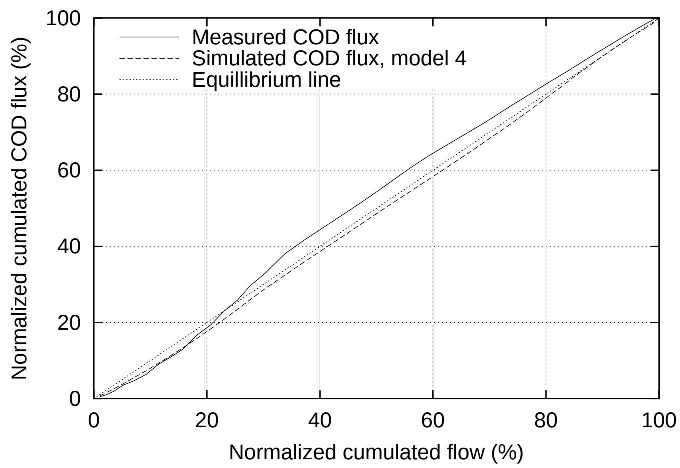

Figure 3.7. Normalized cumulated COD flux vs. normalized cumulated flow, model 4.

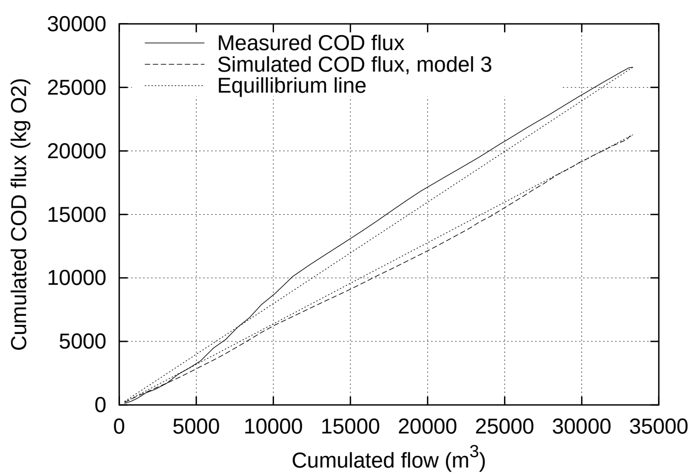

Figure 3.8. Cumulated COD flux vs. cumulated flow, model 3.

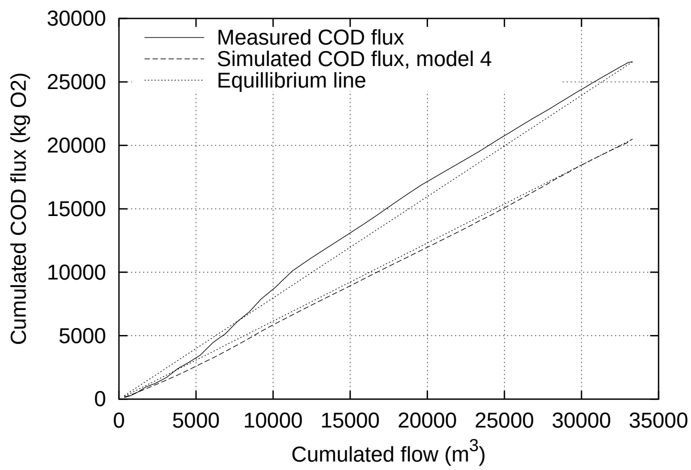

Figure 3.9. Cumulated COD flux vs. cumulated flow, model 4.

in Figures 3.8 and 3.9.

The increase of COD concentrations during the rain incident are not as clear as the increase of SS concentrations, and the COD flux models simulate the fluxes lower than the observed data. From Figures 3.8 and 3.9 it can be seen that the models predict a small degree of dilution, even though a (small) flush effect is present.

From the non-normalized graphs in Figures 3.8 and 3.8 it is also clear that the modelled COD fluxes are lower than the observed fluxes as the measurement graphs does not end in the same point as the corresponding simulation graphs.

When comparing the SS and COD flux graphs it is seen that first flush is more apparent for SS than for COD. When COD is stabilized in the sewer and SS is not, this difference is expected.

In general the models of SS and COD fluxes under estimate the concentration increases during the rain incident in question.

3.1.2 Suggestions concerning future research – sewer models

As the proposed models are quite simple linear models, it is not surprising that they do not describe the observed data perfectly, and that the models should be reformulated, for example by increasing the order of the differential equation describing the pollution deposits and/or including non-linear terms. Furthermore, the sub-model for buildup and flush-out of pollutants in the sewer can be split up into two: 1) A sub-model describing the buildup of pollutants in dry weather periods, and 2) A sub-model for flush-out during wet weather periods. These two sub-models need not be of the same order – the buildup model could for example be made up of a first order differential equation, whereas the flush-out model could be of a higher order. The switch between the two sub-models should be controlled by the flow, and implemented by application of smooth threshold functions (see Paper E for an application of smooth threshold functions).

As first flushes and dilutions are expected to be a result of limited amounts of pollutants deposited in the sewer, introduction of limitations on the deposits in the sewer system could be an important extension to the dynamic model 4. However, to be able to estimate the limits of the deposits, the data must include periods where the limits are reached, i.e. intensive rain events where the sewer system is cleaned and long dry weather periods where the deposited pollutants reach the upper limits. Such data series with a sufficient number of observations of the extreme events might be difficult to obtain.

3.2 ATS operation

Aeration Tank Settling (ATS) is introduced to enable the biological treatment facilities to handle larger wastewater flows than possible with ordinary dry weather operation. The traditional way to handle storm situations is to store the excess water that the biological part of the plant cannot handle in storm tanks, if available. If the plant is not equipped with storm tanks or if they are already full, the excess water has to bypass the aeration tanks and secondary clarifiers. Hence, bypass wastewater, which has not been biologically treated, is being lead to the receiving waters. The details of ATS operation are described in

Papers D–F.

When ATS is activated, the biological tanks of the plant are capable of handling a significantly larger flow, and thus to remove nutrients from considerably more wastewater during a rain event.

Paper D documents the first preliminary modelling of ATS operation. The model is formulated in discrete time, and forms the basis for the work of the following papers.

In Paper E the modelling of suspended solids in the aeration tanks of an alternating BioDenipho plant as well as in the effluent from the aeration tanks during ATS is documented. In this paper the model is formulated in continuous time with discrete-time observations. The modelling is based on measurements of flow to the biological part Q_{i}, the recirculation flow Q_{r}, the concentrations of suspended solids in one aeration tank X_{ssm6}, in the recirculation flow X_{ssr} and in the effluent from the aeration tanks X_{ssoutat}. The flow path through each of the aeration tank pairs as well as the mixing signals ($f_{\mathrm{p}kl}$, m_k and m_l for the aeration tank pair consisting of aeration tanks k and l, $(k,l) \in \{(1,2),(3,4),(5,6)\}$, are also used as inputs to the model. The incoming flow Q_{i} is actually measured in the effluent from the secondary clarifier, but when the water dynamics of the aeration tanks and clarifier are insignificant, these flows are equal.

In Figure 3.10 the data set used for the parameter estimation in Paper E is shown. The flow path and mixing signals are only shown for aeration tanks 5 and 6, as the signals for the other two tank pairs are delayed versions of these data. The data set covers two ATS operation events with a dry weather period in between. The first ATS event covers the period from 25 October 1:30 to October 26 15:50. Then the plant is in dry weather operation until October 27 12:30. The second ATS period continues to the end of the data set on October 29 0:00.

Note that the average SS concentration in the influent to the aeration tanks (assuming that the SS concentration in Q_{in} is zero) calculated as

$$X_{\mathrm{ssinat}}(t) = \frac{Q_{\mathrm{r}}}{Q_{\mathrm{i}} + Q_{\mathrm{r}}} X_{\mathrm{ssr}} \tag{3.3}$$

is included in the graphs. It is reasonable to assume that the SS concentration in Q_{in} is zero as the estimations carried out in preparation of Paper E showed

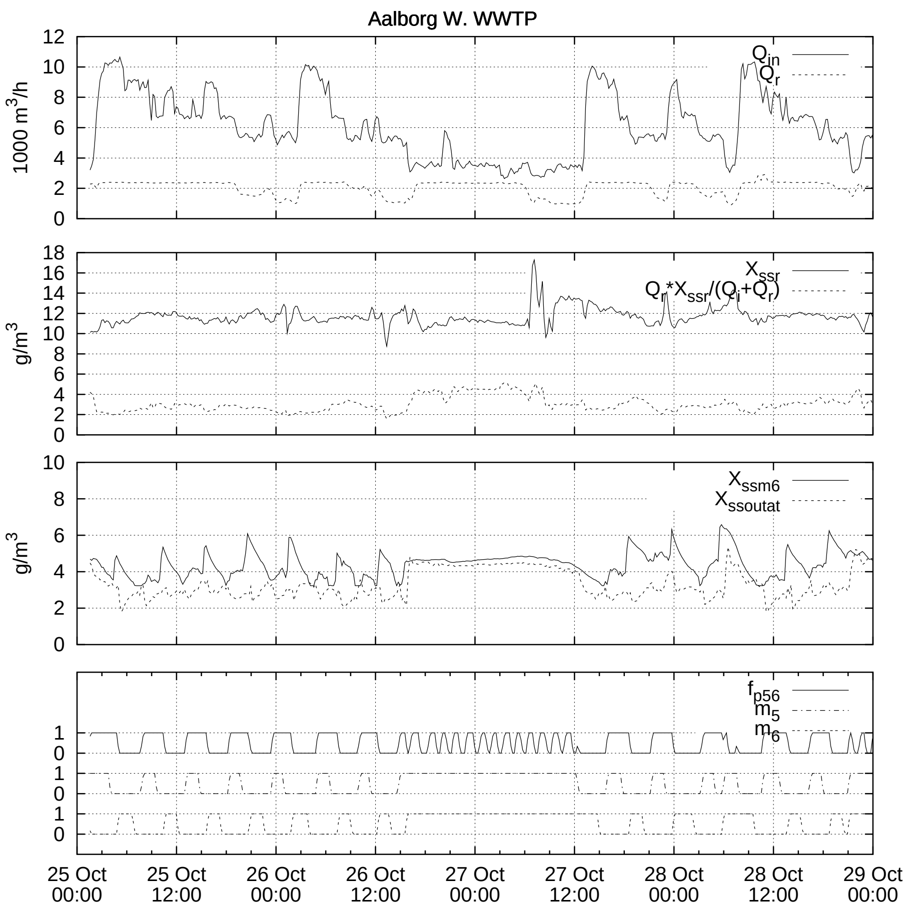

Figure 3.10. The data set used for the parameter estimation.

that this concentration was insignificant.

In Figures 3.11 and 3.12 estimated and simulated SS concentrations and sludge blanket depths for a part of the estimation data set used in Paper E are shown. Both the estimated and the simulated variables are output from the extended Kalman filter. The estimated values are the data updated state estimates, where the measurements have been used to compute the results. The simulated data are the results of a simulation of the model, i.e. only the input data to the model (flow path through the aeration tanks, mixing signals, return sludge concentrations, inflow and return sludge flow) and initial values of the SS concentrations and sludge blanket depths in the aeration tanks are used. The flow path f_{p56} through the considered aeration tank pair is also included. When $f_{\mathrm{p56}} = 1$ the incoming wastewater as well as the return sludge flow is directed to aeration tank 5 and the clarifier is fed from aeration tank 6 and vice versa when $f_{\mathrm{p56}} = 0$.

From Figure 3.11 it can be seen that the sludge concentration is increasing in the aeration tank with discharge to the clarifier and decreasing in the influent tank. When comparing the SS concentrations in the aeration tanks in Figure 3.11 with the average SS concentration in the wastewater entering the aeration tanks in Figure 3.10, it is noted that the average SS concentration in the influent is about 3 g SS/m^3 and that the SS concentrations in the aeration tanks fluctuate around 4.5 g SS/m^3. Hence, the SS concentration in the wastewater entering the influent aeration tank is lower than in the wastewater already in the tank. As the amount of water in the tanks is almost constant, the fluctuations in the sludge concentrations in the aeration tanks are caused by the fact that the incoming water pushes the sludge over to the effluent tank, and when the flow path is changed the sludge is pushed back again. The result of the sludge moving between the aeration tanks is seen in the SS concentrations in the effluent from the tanks. When the flow path is switched, the effluent is taken from a tank with a lower concentration. The concentration in the effluent tank then increases until the next change of flow path, but as sludge settling occurs in the tank, the SS concentration in the effluent is not increasing at the same rate as in the aeration tank.

The estimated and simulated sludge blanket depths in aeration tanks 5 and 6 are shown in Figure 3.12. It can be seen that the sludge blanket depth is limited to about 0.8 m. Unfortunately, the aeration tanks at the Aalborg West plant are not equipped with sludge blanket sensors, so it is not possible to

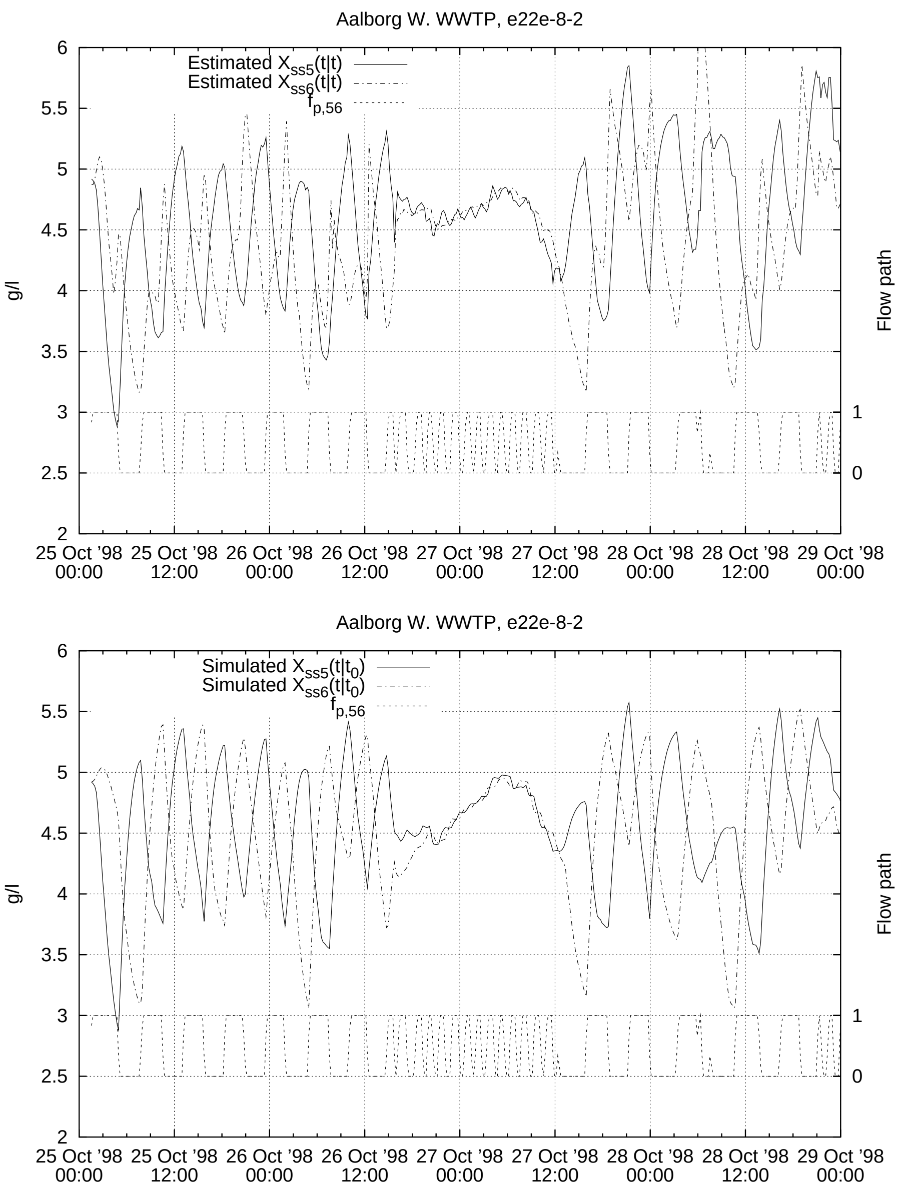

Figure 3.11. Estimated and simulated SS concentrations in aeration tanks 5 and 6.

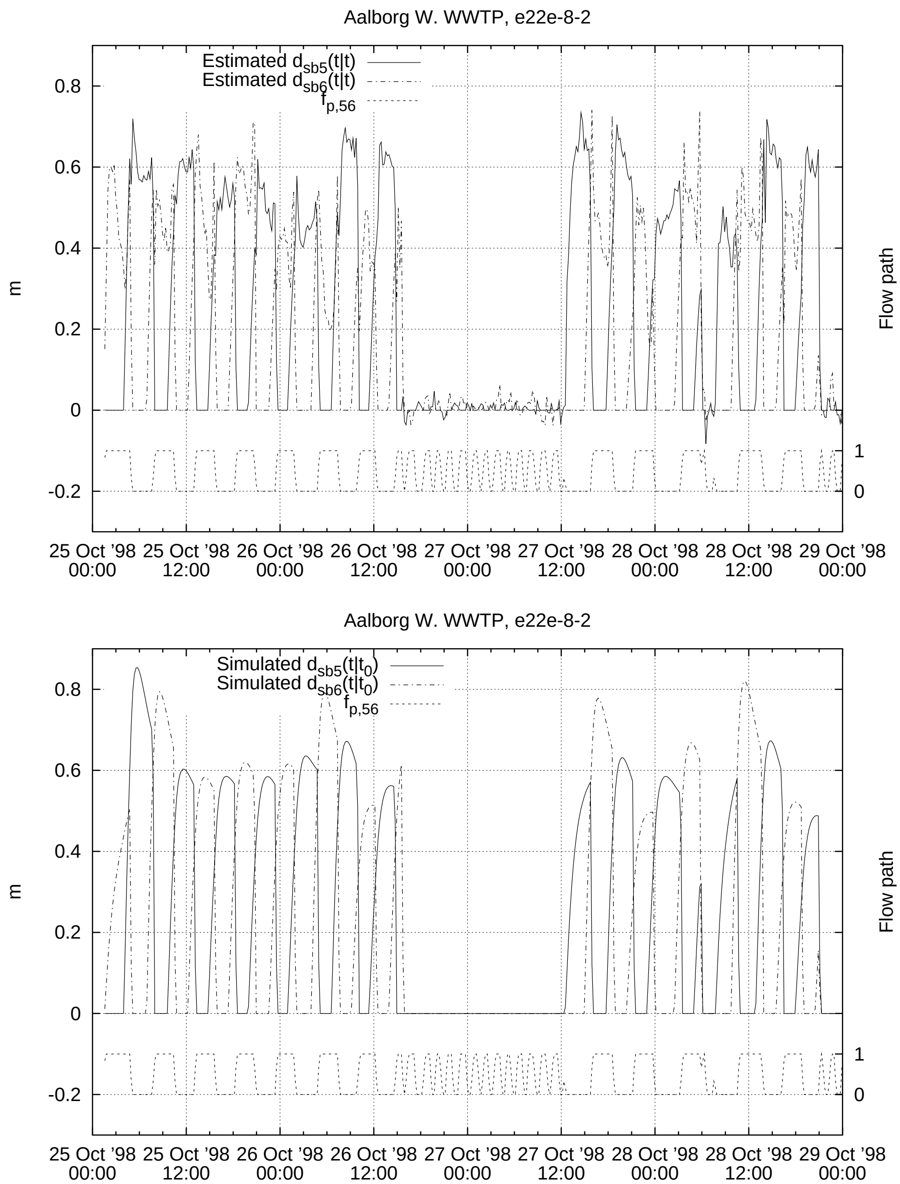

Figure 3.12. Estimated and simulated sludge blanket depths in aeration tanks 5 and 6.

compare the estimated and simulated values with measurements. However, it is straight forward to include sludge blanket measurements in the model, if sludge blanket sensors are installed. From the estimated sludge blanket depths it is seen that they become negative, especially in dry weather periods. This is of course not feasible, but this physical limitation was not included in the model. However, the negative values occurring are small, and thus not considered a major problem.

The estimated model is used in Paper F to simulate different operating modes of the plant, i.e. dry weather operation and 5 different ATS strategies, which result in different flow capacity increases at the plant. The simulations are used to quantify how much ATS operation can increase the flow capacity, as well as to propose a control algorithm for selecting the optimal ATS operating mode. Examples of both dry weather and ATS operation situations at Aalborg West wastewater plant are included in Paper F to illustrate a real ATS operation situation and to compare with a dry weather situation. It should be noted that the ATS event illustrated is controlled by another control algorithm than the one proposed in the paper. In order to make the comparison fair and because the load of the plant varies over the week, both situations include a Saturday and a Sunday. The selection of the days was carried out by first looking for a storm situation and then selecting a similar period with dry weather.

3.2.1 Suggestions concerning future research – aeration tank SS model

In the model for SS in the aeration tanks as well as in the effluent from these established in Paper F, parameters for errors in the measurements of X_{ssr} and X_{ssoutat} are estimated simultaneously with the other model parameters. Of course there can also be systematic errors in the flow measurements, but parameters for errors in the flow observations were not estimated. Error parameters for the flow observations should be included in the model to make it possible to test whether there are significant errors in the measurements of the flows.

The model includes all 6 aeration tanks of Aalborg West wastewater treatment plant, which are operated in an identical way except for time delays between each of the tank pairs. The time delay is equal to the re-sampling interval (12 minutes). The benefits of using a full 6-tank model compared to a simplified

2-tank model are expected to be of minor significance, as the 6-tank model is made up of 3 identical 2-tank models, with a time delay of 1 re-sampling interval between each of the tank pairs. A simplified model should therefore be tried and the results compared with the full 6-tank model. The advantage of a simplified model is that it will only contain 4 states (2 SS concentrations and 2 sludge blanket depths) instead of the 12 states (6 SS concentrations and sludge blanket depths) of the full model, and hence the computations required for estimation and simulation are reduced significantly. Furthermore will the application of the model on other plants with a different number of aeration tanks be simpler.

As can be seen from the estimated sludge blanket depths in Figure 3.12, the depths sometimes become negative. As this is not physically possible, the sludge blanket sub-model could therefore be reformulated to prevent negative sludge blanket depths values, e.g. by means of a logarithm transformation of the sludge blanket depth equations.

The sludge blanket depths are unobserved states of the model. It is thus not possible to compare the modelled sludge blanket depths with measurements. Therefore addition of sludge blanket depth sensors in at least on of the aeration tanks could be used to gain more confidence in the model. Furthermore will addition of sludge blanket sensors enable estimation of the sludge settling parameters.

The possibilities for developing a better model of X_{ssoutat} should be investigated as the current model does not perform as well as desired. It is expected that a good X_{ssoutat} model is required for modelling the SS conditions in the secondary clarifier and in the effluent from here. Better modelling of X_{ssoutat} could be achieved by refining the sludge settling model, e.g. by introducing more layers in the sludge settling model than the two used here.

Control of ATS operation

The content of suspended solids in the secondary clarifier has not been modelled in the present work. Inclusion of a clarifier model is another extension option, which should enable predictions of the SS concentrations in the effluent to the receiving waters, and thus make it possible to design control algorithms that can control the effluent SS concentrations to the recipient closer to the allowed limits and thus further optimize ATS operation.

Finally, a combined ATS control strategy based on both information from the influent to the wastewater treatment plant and from the current state in the aeration tanks and secondary clarifier should be established. The control strategy should control both the ATS operation and the bypass flow. Hereby, it should be possible to decide whether it is advantageous to use the ATS capabilities to handle the incoming flow or some of the flow should bypass the biological part of the plant. The use of available detention basins at the treatment plant should be included in the strategy as well. The control of ATS, bypass flow and detention basins at the wastewater treatment plant should be integrated with the control of the overflow structures, storage basins, pumping stations etc., of the sewer system to enable optimal operation of the total system.

Chapter 4

Conclusions

In this thesis, stochastic models for the incoming wastewater to two different wastewater treatment plants as well as for the SS concentrations in the aeration tanks of an alternating wastewater treatment plant and in the effluent from the aeration tanks are presented. The latter model is furthermore used to quantify the effects of the Aeration Tank Settling (ATS) operating mode as well as to propose a control algorithm for controlling the phase lengths during ATS.

The objective of modelling the incoming wastewater to a wastewater treatment plant was to model possible first flush effects. In Papers A and B dynamic models of the COD flux and SS flux in the influent to two Danish wastewater treatment plants are developed. The models include the buildup and flush out of pollutants in the form of COD and SS in the sewer and on impervious areas of the catchment. The results show that the models can be used to describe some of the first flush effect, but also that the models in some situations predict a dilution even though this is not the case. It is furthermore found that the models make it possible to estimate the deviations in COD and SS deposits in the sewer and on impervious areas of the catchment from an initial level but not the actual amounts in the sewer.

In Paper C the dynamic models are compared to simpler static models to quantify the improvements of including the dynamics of the deposits. The quality of the models is measured by the multiple correlation coefficient (R^2) of the model simulations. This comparison shows that inclusion of the deposits results in significant improvements of the simulation abilities of the model. However, an analysis of the model predictions shows that the proposed models could and should be improved. Hence, suggestions concerning future research within modelling of incoming wastewater are given. It is thus suggested that the models could be improved by increasing the order of the differential equations that describe the pollution deposits and by separating the model into a dry weather part and a wet weather part. Furthermore is it suggested that non-linear terms are included to describe the physical limitations of the deposits.

The second part of the work is about ATS operation in an alternating wastewater treatment plant. ATS is an operating mode that increases the hydraulic capacity of the wastewater treatment plant and thus enables the plant to treat considerably increased wastewater amounts. In Papers D and E a mass balance model of the SS concentrations in the aeration tanks as well as in the effluent from these is established. In Paper E the model is estimated. The resulting model performs very well in simulating the SS concentrations in the aeration tanks. The simulations of the SS concentrations in the effluent from the aeration tanks are not as good as the simulations of the concentrations in the aeration tanks but are however still good. In order to improve the model, it is therefore suggested that the sub-model for the SS concentrations in the effluent from the aeration tanks be refined, e.g. by introducing more layers in the sludge settling model. The work with the mass balance model proved that there were systematic errors in the SS concentration measurements, and therefore error models on the SS observations were included in the model. It is, however, not yet clear whether the flow measurements are also subject to systematic errors. It is therefore suggested that error models for the flow measurements are included so that it could be investigated if they are also subject to errors.

The Aalborg West wastewater treatment plant, which was the subject of the model estimation, has 3 aeration tank pairs. All 6 aeration tanks are included in the model. As the tank pairs are operated in an identical way except for a short time delay, it might be a good idea to simplify the model to only one logical tank pair. The benefits of this simplification are reduced computation time and easier generalization to other plants with a different number of aeration tank pairs.

The model is used to quantify ATS operation as well as to propose a control algorithm for choosing the optimal phase lengths during ATS. It is found that ATS increases the hydraulic capacity of the considered plant by more than 167% (from the dry weather capacity of 6000 m^3/h to more than 16000 m^3/h). A comparison between ATS and the construction of detention basins capable of handling some of the excess water reveals that the financial advantages of ATS are extremely good.

II

Part II

Included papers

List of Included papers

Paper A: Bechmann, H., Nielsen, M. K., Madsen, H., and Poulsen, N. K. (1998). Control of sewer systems and wastewater treatment plants using pollutant concentration profiles. *Water Science and Technology*, **37**(12), 87–93.

Paper B: Bechmann, H., Madsen, H., Poulsen, N. K., and Nielsen, M. K. (1999). Grey box modelling of first flush and incoming wastewater at a wastewater treatment plant. *Environmetrics*, **11**(1), 1–12.

Paper C: Bechmann, H., Nielsen, M. K., Madsen, H., and Poulsen, N. K. (1999). Grey-box modelling of pollutant loads from a sewer system. *UrbanWater*, **1**(1), 71–78.

Paper D: Nielsen, M. K., Bechmann, H., and Henze, M. (1999). Modelling and test of aeration tank settling ATS. In *8th IAWQ Conference on Design, Operation and Economics of Large Wastewater Treatment plants*, pages 199–206. International Association on Water Quality, IAWQ, Budapest University of Technology, Department of Sanitary and Environmental Engineering.

Paper E: Bechmann, H., Nielsen, M. K., Poulsen, N. K., and Madsen, H. (1999). Grey-box modelling of aeration tank settling. Submitted.

Paper F: Bechmann, H., Nielsen, M. K., Poulsen, N. K., and Madsen, H. (1999). Effects and control of aeration tank settling operation. Submitted.

A

Paper A

Control of sewer systems and wastewater treatment plants using pollutant concentration profiles.

Published in *Water Science and Technology*, ***37****(12), pp. 87–93, 1998*

Abstract

On-line measurements of pollutants in the wastewater combined with grey-box modelling are used to estimate the amount of deposits in the sewer system. The pollutant mass flow at the wastewater treatment plant is found to consist of a diurnal profile minus the deposited amount of pollutants. The diurnal profile is found to be a second order harmonic function and the pollutants deposited in the sewer is identified using first order ordinary differential equations.

Key words: Sewer system, wastewater treatment plant, grey-box models, statistical identification, first flush.

Introduction

When designing control systems for sewer systems and wastewater treatment plants, only the hydraulic load of the sewer system and the hydraulic capacity of the wastewater treatment plant are normally considered. This means that first flush effects are not taken into account, and that a maximum amount of wastewater is sent through the equalisation basins or primary clarifiers of the treatment plants. This practice often multiplies the pollutant discharge with the combined sewer overflows.

The wastewater composition is often described by two components - a contribution from the dry weather wastewater and a contribution from the run-off water assumed to have constant concentrations. The pollutant concentrations of the dry weather flow are described by a diurnal mean and the run-off water is considered as having constant pollutant concentrations - typically 1/10 to 1/5 of the dry weather concentration level. This approach does not yield a realistic description when pollutants are depositing in the sewer system.

On-line measurements of UV absorption and turbidity in the sewer system can be used to estimate the actual level of chemical oxygen demand (COD) and suspended solids (SS) in the wastewater (Kanaya et al., 1985; Ruban et al., 1993; Nowack and Ueberbach, 1995; Matsché and Stumwöhrer, 1996), and hence to identify diurnal concentration variations and the amount of deposits settled in the sewer system in dry weather, and the washing out of this during rain.

In the present work a grey-box model for the deposition of pollutants in the sewer system is suggested. A grey-box model is a stochastic model which describes only the most important relationships of the deterministic theory, and such a model is very useful when the objective is control of the wastewater system (Carstensen et al., 1996). The parameters of the model are estimated and using the estimated model it is shown how the deposits in the sewer system grow in dry weather and are washed out during rain.

Data catchment

In Skive in central Jutland, Denmark, the a measuring box developed by Krüger has been operating during the early spring of 1997. The Krüger measuring box is a compact and portable unit, and consists of a datalogger, a UV absorbance sensor and a turbidity sensor. Furthermore the measuring box is collecting flow measurements through a connection to the supervisory control and data acquisition (SCADA) system of the WWTP. The SCADA system computes estimates of the inlet flow based on measurements from the inlet pumping station. The inlet flow consists of a flow to the biological part of the WWTP and a flow to an equalisation basin. The measuring box is equipped such that it is possible to remote control the box and to transfer data to the Krüger office. Off-line measurements of the rain fall are also available, as is laboratory analyses of COD and SS.

Two sets of data are used in this paper. The first set covers the two week period from 13th to 26th of March, and it is used for the estimation. The second set which covers 9 days from 28th of March to 5th of April, is used for validation. The data sets are shown in Figures 1 and 2. Unfortunately there is only some relatively small rain incidents available, and the available incidents are mutual alike.

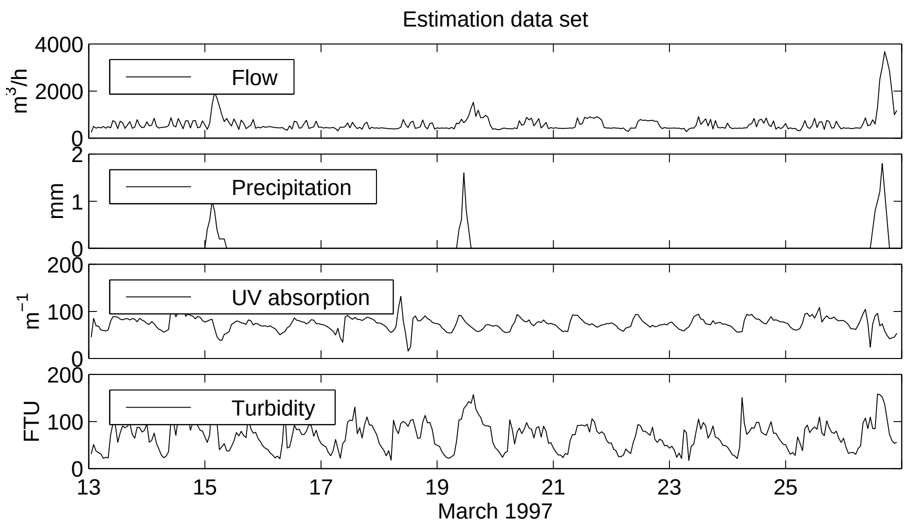

Figure 1. The estimation data set.

Theory

It has been found previously that the relationships between COD and UV absorption (UV), and between SS and turbidity (Turb) are linear (Kanaya et al., 1985; Ruban et al., 1993; Nowack and Ueberbach, 1995; Matsché and Stumwöhrer, 1996), i.e.

$$\mathrm{COD} = \alpha_{\mathrm{U}}\mathrm{UV} + \beta_{\mathrm{U}} \tag{1}$$

$$\mathrm{SS} = \alpha_{\mathrm{T}}\mathrm{Turb} + \beta_{\mathrm{T}} \tag{2}$$

where α_{U}, β_{U}, α_{T} and β_{T} are constants. This means that the UV absorption and turbidity measurements can be thought of as concentrations of COD and SS, respectively. Therefore $\mathrm{Q_U} = \mathrm{Q} \times \mathrm{UV}$ and $\mathrm{Q_T} = \mathrm{Q} \times \mathrm{Turb}$ describe the pollutant mass flow in terms of UV absorption and turbidity "masses", respectively. The quantity of pollutant deposits in the sewer system can also be modelled in terms of UV absorption and turbidity masses.

It is assumed that pollutants gradually deposits in the sewer (and on impervious areas) during dry weather (low wastewater flow) and that the deposists are flushed out during storm situations. The amounts of COD deposits modelled in UV absorbance terms, and SS deposits modelled in turbidity terms are x_{U}

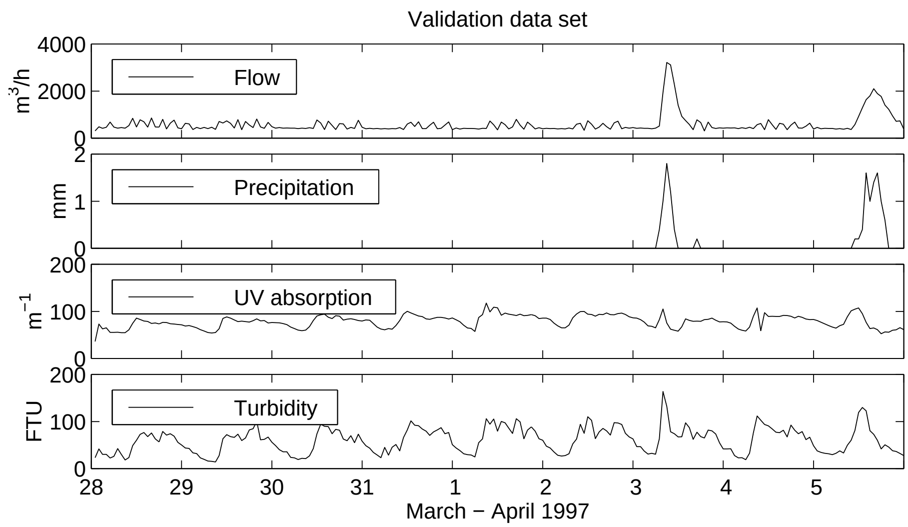

Figure 2. The validation data set.

and x_{T}. The time derivatives of these, dx_{U}/dt and dx_{T}/dt are the flows of UV absorbance and turbidity masses into the sewer depots.

The flow of COD and SS measured as UV absorption and turbidity masses to the WWTP, is assumed to consist of a fixed diurnal profile (the pollutants that enter the sewer system) minus a contribution to the depots in the sewer system. The diurnal profile is assumed to be a periodic function with a 24 hour period, which can be described by a n-th order harmonic. Letting t denote is the time of the 24 hour period given in (decimal) hours, the flows are then described by:

$$\mathrm{Q_U} = a_0 + \sum_{k=1}^{n} \left(a_k \sin(2\pi k \frac{t}{24\mathrm{h}}) + b_k \cos(2\pi k \frac{t}{24\mathrm{h}}) \right) - \frac{dx_{\mathrm{U}}}{dt} \qquad (3)$$

$$\mathrm{Q_T} = c_0 + \sum_{k=1}^{n} \left(c_k \sin(2\pi k \frac{t}{24\mathrm{h}}) + d_k \cos(2\pi k \frac{t}{24\mathrm{h}}) \right) - \frac{dx_{\mathrm{T}}}{dt} \qquad (4)$$

respectively, where a_0 and c_0 are assumed to be the global mean values of $\mathrm{Q_U}$ and $\mathrm{Q_T}$ over the entire data set.

With t_0 as the initial time point of the measuring period, and y_{U} and y_{T} defined as:

$$y_{\mathrm{U}}(t) = -\int_{t_0}^{t} (\mathrm{Q}_{\mathrm{U}} - a_0)$$

$$y_{\mathrm{T}}(t) = -\int_{t_0}^{t} (\mathrm{Q}_{\mathrm{T}} - c_0)$$

we obtain, using (3) and (4), that

$$\begin{aligned} y_{\mathrm{U}}(t) &= x_{\mathrm{U}}(t) - x_{\mathrm{U}}(t_0) \\ &\quad - \int_{t_0}^{t} \sum_{k=1}^{n} \left(a_k \sin(2\pi k \frac{t}{24\mathrm{h}}) + b_k \cos(2\pi k \frac{t}{24\mathrm{h}}) \right) dt \end{aligned} \tag{5}$$

$$\begin{aligned} y_{\mathrm{T}}(t) &= x_{\mathrm{T}}(t) - x_{\mathrm{T}}(t_0) \\ &\quad - \int_{t_0}^{t} \sum_{k=1}^{n} \left(a_k \sin(2\pi k \frac{t}{24\mathrm{h}}) + b_k \cos(2\pi k \frac{t}{24\mathrm{h}}) \right) dt \end{aligned} \tag{6}$$

It is easily seen that the integration of the sines and cosines will yield a diurnal mean of zero. Hence the trend of y_{U} and y_{T} will follow the trend of x_{U} and x_{T}. When examining the trends of y_{U} and y_{T} it is possible to see *if* pollutants are deposting in the sewer since y_{U} and y_{T} will be growing, when pollutants are depositing, and falling and when the pollutants are flushed out.

If pollutants actually are deposting one approach to identify the amount of deposits in terms of UV absorption and turbidity mass (x_{U} and x_{T}) in the sewer system is to model these using simple first order ordinary differential equations:

$$\begin{aligned} \frac{dx_{\mathrm{U}}}{dt} &= a_{\mathrm{U}}(x_{\mathrm{U},0} - x_{\mathrm{U}}) + b_{\mathrm{U}}(Q_0 - Q) \\ &= -a_{\mathrm{U}} x_{\mathrm{U}} - b_{\mathrm{U}} Q + c_{\mathrm{U}}, \end{aligned} \tag{7}$$

$$\begin{aligned} \frac{dx_{\mathrm{T}}}{dt} &= a_{\mathrm{T}}(x_{\mathrm{T},0} - x_{\mathrm{T}}) + b_{\mathrm{T}}(Q_0 - Q) \\ &= -a_{\mathrm{T}} x_{\mathrm{T}} - b_{\mathrm{T}} Q + c_{\mathrm{T}}, \end{aligned} \tag{8}$$

where $c_{\mathrm{U}} = a_{\mathrm{U}} x_{\mathrm{U},0} + b_{\mathrm{U}} Q_{\mathrm{U},0}$ and $c_{\mathrm{T}} = a_{\mathrm{T}} x_{\mathrm{T},0} + b_{\mathrm{T}} Q_{\mathrm{T},0}$. The actual flow through the sewer is Q, a_{U}, b_{U}, a_{T} and b_{T} are constants. Q_0 is the global mean value of Q, and $x_{\mathrm{U},0}$ and $x_{\mathrm{T},0}$ are assumed to be the means of x_{U} and x_{U}, respectively.

The explanation of the differential equations, (7) and (8), is that when there is a small amount of deposits in the sewer and the flow is low, pollutants will be built up to an equillibrium (dependant on $x_{\mathrm{U},0}$, Q and $Q_{\mathrm{U},0}$ or $x_{\mathrm{T},0}$, Q and $Q_{\mathrm{T},0}$). When a large amount is deposited and the flow is high, the pollutants will be flushed out of the sewer resulting in higher pollutant levels in the wastewater.

Results - Discussion

From the plots of y_{U} and y_{T} in Figure 3 it is seen that both has a growing trend between the rain incidents, and a significant falling trend in a short period after the rain incidents. The conclusion is, that it is evident that deposition and flushing out of pollutants actually does occur. Hence there is reason to try to model these depositions.

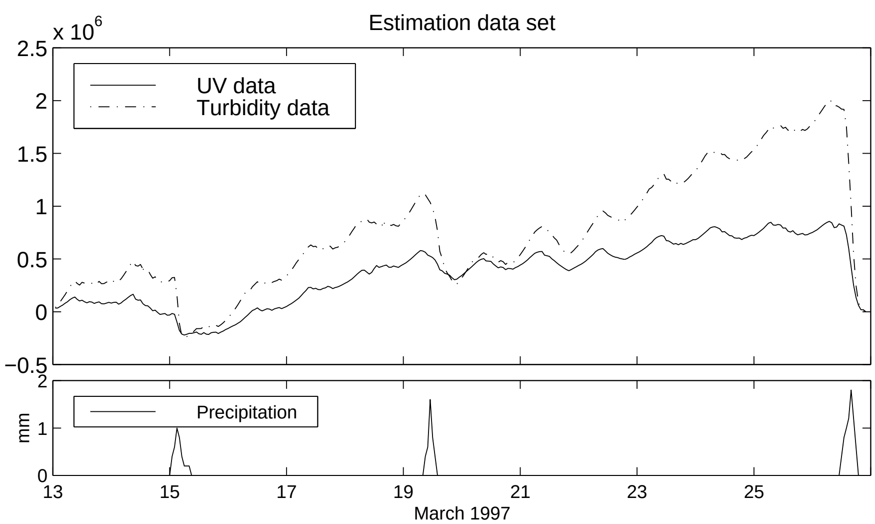

Figure 3.

In dry weather the relations between COD and UV absorption, and between

SS and turbidity was found to be:

$$\mathrm{COD} = 5.0\frac{\mathrm{mg}}{\mathrm{l} \times \mathrm{m}^{-1}}\mathrm{UV} - 26\frac{\mathrm{mg}}{\mathrm{l}}$$
$$\mathrm{SS} = 1.52\frac{\mathrm{mg}}{\mathrm{l} \times \mathrm{FTU}}\mathrm{Turb} - 7.8\frac{\mathrm{mg}}{\mathrm{l}}$$

with correlation coefficients 0.90 and 0.85 respectively. These relations are good during dry weather, but are not suitable in storm situations. Hence instead of measuring discharge during storms, we model the build-up of pollutants during dry weather. This simple approach is reliable if the dry weather load to the sewer is predictable or constant.

A second order harmonic was found to be reasonable in describing the diurnal profiles for both UV and turbidity mass flow. In Figure 4 results of the mass flow estimations are shown with the validation data set. The model is seen to describe the measurement data reasonably well.

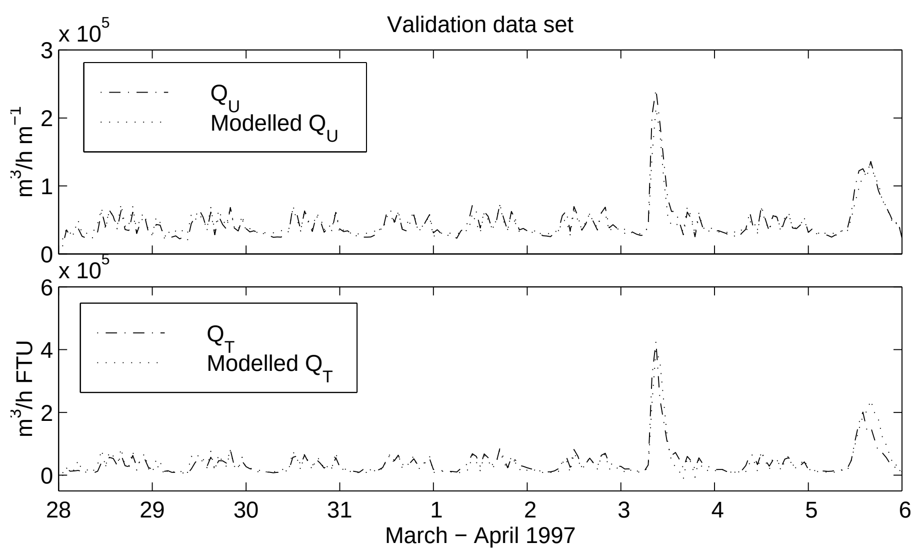

Figure 4. Real and modelled UV and turbidity mass flows.

The estimated parameters in (3), (4), (7) and (8) are shown in Table 1, and the estimated diurnal profiles for $\mathrm{Q_U}$ and $\mathrm{Q_U}$ are shown in Figure 5, and as expected the pollutant load is lowest in the night and the early morning hours and are highest in the afternoon. It is important to notice that the estimated values of c_{U} and c_{T} are dependant on the initial values of x_{U} and x_{T}, respectively.

The initial values of x_{U} were estimated to $45 \times 10^3 \mathrm{m}^3 \times \mathrm{m}^{-1}$ for the estimation data set and $52 \times 10^3 \mathrm{m}^3 \times \mathrm{m}^{-1}$ for the validation data set. The initial values of x_{T} were estimated to $90 \times 10^3 \mathrm{m}^3 \times \mathrm{FTU}$ for the estimation data set and $95 \times 10^3 \mathrm{m}^3 \times \mathrm{FTU}$ for the validation data set.

$a_0 = 44.4 \times 10^3 \mathrm{m}^3/\mathrm{h} \times \mathrm{m}^{-1}$	$c_0 = 48.2 \times 10^3 \mathrm{m}^3/\mathrm{h} \times \mathrm{FTU}$
$a_1 = -6.54 \times 10^3 \mathrm{m}^3/\mathrm{h} \times \mathrm{m}^{-1}$	$c_1 = -10.3 \times 10^3 \mathrm{m}^3/\mathrm{h} \times \mathrm{FTU}$
$b_1 = -2.40 \times 10^3 \mathrm{m}^3/\mathrm{h} \times \mathrm{m}^{-1}$	$d_1 = -2.60 \times 10^3 \mathrm{m}^3/\mathrm{h} \times \mathrm{FTU}$
$a_2 = -1.25 \times 10^3 \mathrm{m}^3/\mathrm{h} \times \mathrm{m}^{-1}$	$c_2 = -1.15 \times 10^3 \mathrm{m}^3/\mathrm{h} \times \mathrm{FTU}$
$b_2 = 3.81 \times 10^3 \mathrm{m}^3/\mathrm{h} \times \mathrm{m}^{-1}$	$d_2 = 1.98 \times 10^3 \mathrm{m}^3/\mathrm{h} \times \mathrm{FTU}$
$a_{\mathrm{U}} = 0.0821 \mathrm{h}^{-1}$	$a_{\mathrm{T}} = 0.0685 \mathrm{h}^{-1}$
$b_{\mathrm{U}} = 59.7 \mathrm{m}^{-1}$	$b_{\mathrm{T}} = 121.5 \mathrm{FTU}$
$c_{\mathrm{U}} = 81.2 \times 10^3 \mathrm{m}^3/\mathrm{h} \times \mathrm{m}^{-1}$	$c_{\mathrm{T}} = 162 \times 10^3 \mathrm{m}^3/\mathrm{h} \times \mathrm{FTU}$

Table 1.

The values of a_{U} and a_{T} shows that the UV and turbidity will build up in the sewer with the time constants $1/0.0821\mathrm{h} = 12.2\mathrm{h}$ and $1/0.0685\mathrm{h} = 14.6\mathrm{h}$. This means that after a (considerable) change in the flow, the UV and turbidity masses in the sewer will reach 63% of the equilibrium in 12.2 and 14.6 hours, respectively.

The estimations of the pollutant masses in the sewer is shown in Figure 6. It is clear that the pollutants are built up in the sewer during dry weather and flushed out during the rain incidents. During the first approximately 24 hours after the rain incident the growth is much faster than it was just before the rain, which shows that the level of UV and turbidity at the WWTP is higher during the rain periods, than under normal dry weather conditions. After the rain the levels will be lower at the WWTP, since the depots in the sewer are built up again.

Conclusions

On-line measurements of UV absorption, turbidity and wastewater flow combined with grey-box modelling can be used to identify a model for pollutant concentrations in the wastewater and the amount of deposits in the sewer sys-

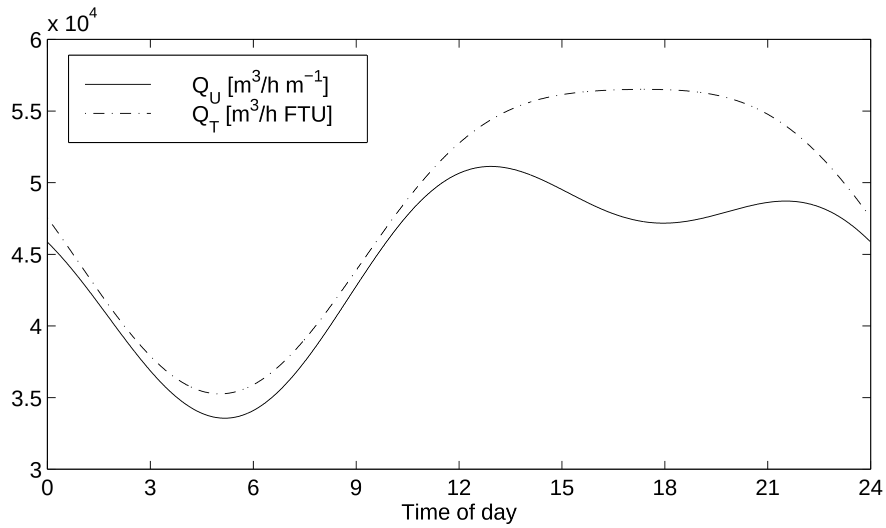

Figure 5. The estimated diurnal profiles.

tem at a given time.

Longer test periods with more variation in length of dry weather periods and rain intensity are needed for a better validation of the models and prediction methods.

When models of the build-up of pollutants are established, the combination of the models and a flow prediction (Carstensen et al., 1998) can be used to predict the pollutant concentrations in the wastewater. These predictions can be used adjust the control strategy for the sewer and the WWTP. The control actions for the sewer can typically be a choice between directing the wastewater to a detention basin, to the WWTP or directly to the recipient.

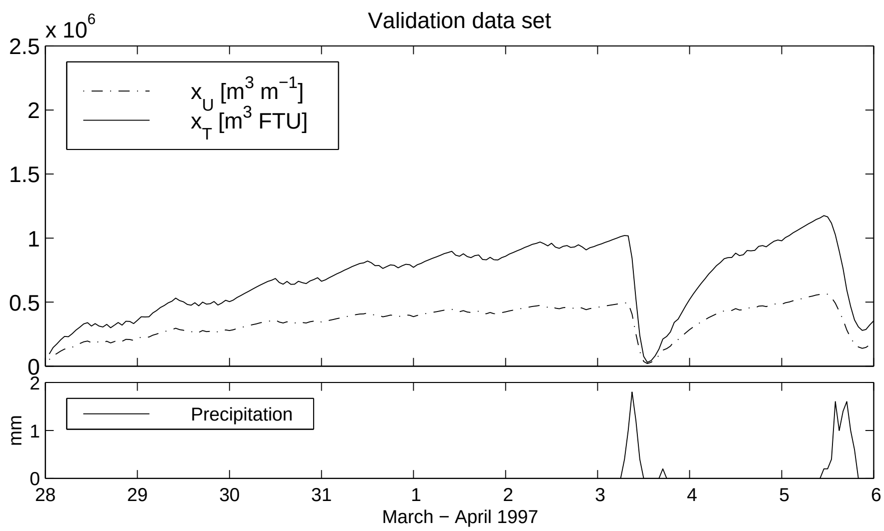

Figure 6. The estimated build up of pollutants in the sewer.

Paper B

B

Grey box modelling of first flush and incoming wastewater at a wastewater treatment plant.

Published in *Environmetrics*, ***11**(1), pp. 1–12, 2000*

Summary

On-line measurements of turbidity, UV absorption and flow in the inlet to a Danish wastewater treatment plant are used to establish a dynamic model of the deposition of pollutants in the sewer system and the pollutant mass flow to the treatment plant. The modelling is made using the grey box approach, which is a statistical method that uses known physical relations to formulate the model. The dynamics of the sewer are modelled by means of continuous time stochastic differential equations combined with dry weather diurnal pollutant mass flows.

Key words: On-line measurements; sewer systems; wastewater treatment plant; dynamic systems; grey box modelling; stochastic differential equations; first flush; diurnal pollutant load

Introduction

Modelling of sewer systems is necessary to gain a better understanding of the dynamics of the system, and to verify if deposition of pollutants occurs. If deposition occurs then the model can be used to predict and quantify the first flushes. When the dynamics of the first flushes are quantified, it can be used to calculate the necessary size of a storage basin in the sewer system or at the wastewater treatment plant.

When modelling sewer systems, these are often described using a configuration of storage volumes and pipes with different dimensions. This approach results in a mathematical model with many parameters and internal states of the stores. Unfortunately the data seldom provides sufficient information to uniquely identify all parameters.

In this paper a data based grey box modelling approach is used. A grey box model is a stochastic model which only describes the most important physical relations. The benefits of this approach are that the resulting model has few parameters and states which are possible to identify, using appropriate statistical methods. Due to the small number of parameters, few computational resources are needed to estimate the parameters, which makes the parameter estimation applicable for on-line use, e.g. for on-line control purposes (Carstensen et al., 1996).

The present work is based on on-line measurements of UV absorption, turbidity and flow. The measurements of UV absorption and turbidity are used to estimate the actual level of chemical oxygen demand (COD) and suspended solids (SS) in the wastewater (Kanaya et al., 1985; Ruban et al., 1993; Nowack and Ueberbach, 1995; Matsché and Stumwöhrer, 1996). Based on these data a model including the diurnal profiles of COD and SS mass flow as well as the amount of COD and SS deposits in the sewer, is proposed and identified. The model parameters are estimated using one set of data, and cross validated using another data set.

The deposits, which are not practically measurable, are states in the model and hence estimated by means of the procedure. By use of the model the estimated amounts of deposited pollutants in the sewer are identified and shown.

The measurement system

A measuring box, developed by Krüger A/S, Denmark, has been collecting measurements from the inlet to the wastewater treatment plant of the town of Skive in central Jutland, Denmark, in the early spring of 1997. The Krüger measuring box is a compact and portable unit which consists of a datalogger, a Dr. Lange UV absorbance sensor model LXV 109 and a Dr. Lange SOLITAXplus LXV 121 turbidity sensor. Furthermore inlet flow estimates are collected from the supervisory control and data acquisition (SCADA) system of the WWTP. The flow estimates are computed in the SCADA system on the basis of measurements from the inlet pumping station. Off-line measurements of the precipitation and laboratory analyses of COD and SS are also available.

The influent to Skive WWTP is separated into industrial and municipal wastewater. The sensors are placed in the municipal wastewater.

COD and SS

Linear relationships between the concentration of COD denoted C_{COD} and UV absorption (UV) and between the concentration of SS denoted C_{SS} and turbidity ($Turb$) have been suggested by several authors (Kanaya et al., 1985; Ruban et al., 1993; Nowack and Ueberbach, 1995; Matsché and Stumwöhrer, 1996), i.e.

$$C_{COD} = \alpha_U UV + \beta_U \tag{1}$$

$$C_{SS} = \alpha_T Turb + \beta_T \tag{2}$$

where α_U, β_U, α_T and β_T are constants. The concentrations of COD and SS are measured in $\mathrm{gO_2/m^3}$ and $\mathrm{gSS/m^3}$. The models are calibrated on the basis of laboratory measurements of C_{COD} and C_{SS} and the corresponding on-line measurements of UV and $Turb$. When the concentrations are multiplied by the wastewater flow Q (in $\mathrm{m^3/h}$) the results are the mass flows of COD and SS in $\mathrm{gO_2/h}$ and $\mathrm{gSS/h}$, respectively.

A dynamical model of the deposited pollutants

It is assumed that pollutants quantified as masses of COD and SS deposit gradually in the sewer system and on impervious areas of the catchment in dry weather (low wastewater flow). Similarly, it is assumed that the deposited pollutants are flushed out during rain incidents and into the inlet of the treatment plant. This means that the model does not explicitly describe reactions occurring in the sewers, but these processes are in part accounted for through the statistical calibration of the model.

The deposited amounts of COD and SS are denoted X_{COD} and X_{SS}, respectively. The time derivatives, dX_{COD}/dt and dX_{SS}/dt are the growth rates at which COD and SS are built up in the depots. The growth rates are assumed to be described by the first order linear differential equations:

$$\frac{dX_{COD}}{dt} = a_{COD}(X_{COD} - \bar{X}_{COD}) + b_{COD}(Q - \bar{Q}) \tag{3}$$

$$\frac{dX_{SS}}{dt} = a_{SS}(X_{SS} - \bar{X}_{SS}) + b_{SS}(Q - \bar{Q}) \tag{4}$$

where Q is the wastewater flow in the inlet and $\bar{X}_{COD}$ and $\bar{Q}$ are the mean values of X and Q. The proposed model is thus a simple first order storage model. When the parameters a_{COD}, b_{COD}, a_{SS} and b_{SS} are assumed to be negative constants, a flow larger than the mean flow will cause a decrease of the amount of deposits and a flow lower than the mean flow will cause an increase of the deposits. Likewise a deposited amount of pollutants larger than the mean will cause a decrease in the corresponding growth rate, and vice versa.

Furthermore we assume that the pollutant mass flow entering the sewer system is following a diurnal profile and that the rain water does not contain any COD and SS. The diurnal profiles are modelled by periodic functions with a 24 hour period, which are described by n-th order harmonic functions. A simple mass balance of the sewer system shows that the mass flows of COD and SS at the WWTP are the corresponding diurnal profile minus the contribution to the depots. The pollutant mass flows $Q_{COD} = Q \times COD$ and $Q_{SS} = Q \times SS$ in the inlet to the WWTP are then modelled by:

$$Q_{COD} = a_0 + \sum_{k=1}^{n} \left(a_k \sin(2\pi k \frac{t}{24\text{h}}) + b_k \cos(2\pi k \frac{t}{24\text{h}}) \right) - \frac{dX_{COD}}{dt} \quad (5)$$

$$Q_{SS} = c_0 + \sum_{k=1}^{n} \left(c_k \sin(2\pi k \frac{t}{24\text{h}}) + d_k \cos(2\pi k \frac{t}{24\text{h}}) \right) - \frac{dX_{SS}}{dt} \quad (6)$$

where a_0, a_k, b_k, c_0, c_k and d_k ($1 \leq k \leq n$), are the parameters of the harmonic functions. Combining (3) with (5) and (4) with (6) leads to:

$$\begin{aligned} Q_{COD} = & -a_{COD}(X_{COD} - \bar{X}_{COD}) - b_{COD}(Q - \bar{Q}) \\ & + a_0 + \sum_{k=1}^{n} \left(a_k \sin(2\pi k \frac{t}{24\text{h}}) + b_k \cos(2\pi k \frac{t}{24\text{h}}) \right) \end{aligned} \quad (7)$$

$$\begin{aligned} Q_{SS} = & -a_{SS}(X_{SS} - \bar{X}_{SS}) - b_{SS}(Q - \bar{Q}) \\ & + c_0 + \sum_{k=1}^{n} \left(c_k \sin(2\pi k \frac{t}{24\text{h}}) + d_k \cos(2\pi k \frac{t}{24\text{h}}) \right) \end{aligned} \quad (8)$$

In order to use a matrix notation we introduce $\boldsymbol{X}, \boldsymbol{U}$ and $\boldsymbol{Y}$ as the state vector, the input vector and the observation vector, respectively; i.e.:

$$\boldsymbol{X} = [X_{COD} - \bar{X}_{COD}, X_{SS} - \bar{X}_{SS}]' \quad (9)$$

$$\boldsymbol{U} = [Q - \bar{Q}, 1, \sin(2\pi \frac{t}{24\text{h}}), \cos(2\pi \frac{t}{24\text{h}}), \dots, \cos(2\pi k \frac{t}{24\text{h}})]' \quad (10)$$

$$\boldsymbol{Y} = [Q_{COD}, Q_{SS}]' \quad (11)$$

and the matrices $\boldsymbol{A}$, $\boldsymbol{B}$, $\boldsymbol{C}$ and $\boldsymbol{D}$ defined by:

$$\boldsymbol{A} = \begin{bmatrix} -a_{COD} & 0 \\ 0 & -a_{SS} \end{bmatrix} \tag{12}$$

$$\boldsymbol{B} = \begin{bmatrix} -b_{COD} & 0 & 0 & 0 & \dots & 0 \\ -b_{SS} & 0 & 0 & 0 & \dots & 0 \end{bmatrix} \tag{13}$$

$$\boldsymbol{C} = \begin{bmatrix} a_{COD} & 0 \\ 0 & a_{SS} \end{bmatrix} \tag{14}$$

$$\boldsymbol{D} = \begin{bmatrix} b_{COD} & a_0 & a_1 & b_1 & a_2 & b_2 & \dots & a_k & b_k \\ b_{SS} & c_0 & c_1 & d_1 & c_2 & d_2 & \dots & c_k & d_k \end{bmatrix} \tag{15}$$

After addition of a noise term (3) and (4) can now be described by the stochastic differential equation:

$$d\boldsymbol{X} = \boldsymbol{A}\boldsymbol{X}dt + \boldsymbol{B}\boldsymbol{U}dt + d\boldsymbol{w}(t) \tag{16}$$

where the stochastic process $\boldsymbol{w}(t)$ is assumed to be a vector Wiener process. The noise term is included to describe the deviations between the model equations (3) and (4) and the true system.

The observation equation in the matrix notation is found by combining (3) with (5) and (4) with (6):

$$\boldsymbol{Y}(t) = \boldsymbol{C}\boldsymbol{X}(t) + \boldsymbol{D}\boldsymbol{U}(t) + \boldsymbol{e}(t) \tag{17}$$

Here the term $\boldsymbol{e}(t)$ is the measurement error, which is assumed to be a zero mean Gaussian white noise sequence independent of $\boldsymbol{w}(t)$.

The parameter estimation method

This section briefly describes the method used to estimate the parameters of the stochastic differential equation (16) for the dynamics of the sewer system. The estimation method is a maximum likelihood method for estimating parameters in stochastic differential equations based on discrete time data. For a more detailed description of the method we refer to Madsen and Melgaard (1991) or Melgaard and Madsen (1993).

The observations are given in discrete time, and, in order to simplify the notation, we assume that the time index t belongs to the set $\{0, 1, 2, ..., N\}$, where N is the number of observations. Introduce

$$\mathcal{Y}(t) = [\boldsymbol{Y}(t), \boldsymbol{Y}(t-1), \ldots, \boldsymbol{Y}(1), \boldsymbol{Y}(0)]' \tag{18}$$

i.e. $\mathcal{Y}(t)$ is a vector containing all the observations up to and including time t.

Using the matrix notation the continuous time stochastic differential equation describing the dynamics of the sewer system can be written as the so-called Itô differential equation (Øksendal, 1995)

$$d\boldsymbol{X}(t) = f(\boldsymbol{X}, \boldsymbol{U}, t)dt + \boldsymbol{G}(\boldsymbol{U}, t)d\boldsymbol{w}(t) \tag{19}$$

where $\boldsymbol{X}$ is the state vector, $\boldsymbol{U}$ an input (e.g. control) vector, $\boldsymbol{w}$ a vector standard Wiener process (see e.g. Kloeden and Platen (1995)), and f and $\boldsymbol{G}$ are known functions. The matrix $\boldsymbol{G(U,t)}$ describes any input or time dependent variation related to how the variation generated by the Wiener process enters the system.

For the observations we assume the discrete time relation

$$\boldsymbol{Y}(t) = h(\boldsymbol{X}, \boldsymbol{U}, t) + \boldsymbol{e}(t) \tag{20}$$

where $\boldsymbol{e}(t)$ is assumed to be a Gaussian white noise sequence independent of $\boldsymbol{w}$. All the unknown parameters, denoted by the vector $\boldsymbol{\theta}$, are embedded in the continuous-discrete time state space model (equations (19) and (20)).

The likelihood function is the joint probability density of all the observations assuming that the parameters are known, i.e.

$$\begin{aligned} L'(\boldsymbol{\theta}; \mathcal{Y}(N)) &= p(\mathcal{Y}(N)|\boldsymbol{\theta}) \\ &= p(\boldsymbol{Y}(N)|\mathcal{Y}(N-1), \boldsymbol{\theta})p(\mathcal{Y}(N-1)|\boldsymbol{\theta}) \\ &= \left(\prod_{t=1}^{N} p(\boldsymbol{Y}(t)|\mathcal{Y}(t-1), \boldsymbol{\theta})\right)p(\boldsymbol{Y}(0)|\boldsymbol{\theta}) \end{aligned} \tag{21}$$

where successive applications of the rule $P(A \cap B) = P(A|B)P(B)$ are used to express the likelihood function as a product of conditional densities.

In order to evaluate the likelihood function it is assumed that all the conditional densities are Gaussian. In the case of a linear state space model as described by (16) and (17), it is easily shown that the conditional densities are actually Gaussian (Madsen and Melgaard, 1991). In the more general non-linear case the Gaussian assumption is an approximation.

The Gaussian distribution is completely characterized by the mean and covariance. Hence, in order to parameterize the conditional distribution, we introduce the conditional mean and the conditional covariance as

$$\begin{aligned} \hat{\boldsymbol{Y}}(t|t-1) &= E[\boldsymbol{Y}(t)|\mathcal{Y}(t-1), \boldsymbol{\theta}] \quad \text{and} \\ \boldsymbol{R}(t|t-1) &= V[\boldsymbol{Y}(t)|\mathcal{Y}(t-1), \boldsymbol{\theta}] \end{aligned} \tag{22}$$

respectively. It should be noted that these correspond to the one-step prediction and the associated covariance, respectively. Furthermore, it is convenient to introduce the one-step prediction error (or innovation)

$$\boldsymbol{\epsilon}(t) = \boldsymbol{Y}(t) - \hat{\boldsymbol{Y}}(t|t-1) \tag{23}$$

For calculating the one-step prediction and its variance, an iterated extended Kalman filter is used. The extended Kalman filter is simply based on a linearization of the system equation (19) around the current estimate of the state (see Gelb (1974)). The iterated extended Kalman filter is obtained by local iterations of the linearization over a single sample period.

Using (21) – (23) the conditional likelihood function (conditioned on $\boldsymbol{Y}(0)$) becomes

$$\begin{aligned} &L(\boldsymbol{\theta}; \mathcal{Y}(N)) \\ &= \prod_{t=1}^{N} \Big((2\pi)^{-m/2} \det \boldsymbol{R}(t|t-1)^{-1/2} \exp(-\tfrac{1}{2}\boldsymbol{\epsilon}(t)' \boldsymbol{R}(t|t-1)^{-1} \boldsymbol{\epsilon}(t)) \Big) \end{aligned} \tag{24}$$

where m is the dimension of the $\boldsymbol{Y}$ vector. Traditionally the logarithm of the conditional likelihood function is considered

$$\begin{aligned} &\log L(\boldsymbol{\theta}; \mathcal{Y}(N)) \\ &= -\tfrac{1}{2} \sum_{t=1}^{N} \big(\log \det \boldsymbol{R}(t|t-1) + \boldsymbol{\epsilon}(t)' \boldsymbol{R}(t|t-1)^{-1} \boldsymbol{\epsilon}(t) \big) + \text{const} \end{aligned} \tag{25}$$

The maximum likelihood estimate (ML-estimate) is the set $\hat{\boldsymbol{\theta}}$, which maximizes the likelihood function. Since it is not, in general, possible to optimize the likelihood function analytically, a numerical method has to be used. A reasonable method is the quasi-Newton method.

An estimate of the uncertainty of the parameters is obtained by the fact that the ML-estimator is asymptotically normally distributed with mean $\boldsymbol{\theta}$ and covariance

$$\boldsymbol{D} = \boldsymbol{H}^{-1} \tag{26}$$

where the matrix $\boldsymbol{H}$ is given by

$$\{h_{lk}\} = -E\left[\frac{\partial^2}{\partial\theta_l \partial\theta_k} \log L(\boldsymbol{\theta}; \mathcal{Y}(N))\right] \tag{27}$$

An estimate of $\boldsymbol{D}$ is obtained by equating the observed value with its expectation and applying

$$\{h_{lk}\} \approx -\left(\frac{\partial^2}{\partial\theta_l \partial\theta_k} \log L(\boldsymbol{\theta}; \mathcal{Y}(N))\right)_{|\theta=\hat{\theta}} \tag{28}$$

The above equation can be used for estimating the variance of the parameter estimates. The variances serves as a basis for calculating t-test values for test under the hypothesis that the parameter is equal to zero. Finally, the correlation between the parameter estimates is readily found based on the covariance matrix $\boldsymbol{D}$.

Results and Discussion

In dry weather the relations between COD and UV absorption and between SS and turbidity were found by regression analysis to be:

$$C_{COD} = 5.0\frac{\mathrm{g}}{\mathrm{m}^3\mathrm{m}^{-1}}UV - 26\frac{\mathrm{g}}{\mathrm{m}^3} \tag{29}$$

$$C_{SS} = 1.52\frac{\mathrm{g}}{\mathrm{m}^3\mathrm{FTU}}Turb - 7.8\frac{\mathrm{g}}{\mathrm{m}^3} \tag{30}$$

with degrees of explanation $R^2 = 0.90$ and $R^2 = 0.85$, respectively. In dry weather equations (29) and (30) describe the relations well, and it is assumed that it is reasonable to extrapolate to rainy situations. More thorough research will have to be carried out to refine the relationships between the measurements of UV absorption and turbidity, and COD and SS, respectively. This investigation could include flow dependent parameter values. Such an approach will increase the need for laboratory analysis of COD and SS enormously.

The parameters in the model were estimated using the CTLSM program (Madsen and Melgaard, 1991; Melgaard and Madsen, 1991). Different orders of the harmonic functions were tried, and it was found that a second order harmonic was reasonable in describing the diurnal profiles for both COD and SS mass flow. The estimated parameters are shown in Table 1, together with the estimated standard deviations of the parameter estimates.

It was found that c_2 was not significantly different from zero, and it was therefore excluded from the final estimation.

In the model presented it is not possible to estimate the mean level of the non-measured deposited pollutants $\bar{X}_{COD}$ and $\bar{X}_{SS}$. In the estimations these were fixed at zero, meaning that X_{COD} and X_{SS} are differences from unknown mean values. This does not put any limitations on the use of the model, as it is still possible to quantify the amount of pollutants in a first flush.

Validation of the resulting model was done by cross-validation, i.e. by applying the model on a data set (the validation data set), which differs from that used for the parameter estimation. Using all the estimated parameter values, except for the initial states, the initial values of the states for the validation data set were found by the estimation software. In Figures 1 and 2 the measured and simulated pollutant mass flows are shown. They are seen to be in good agreement. Furthermore tests on the white noise assumption based on the autocorrelations and on the cumulative residual periodograms were carried out. It was seen that the white noise assumptions were not perfectly satisfied, but since the cross-validations shown in Figures 1 and 2 are very fine, it is concluded that the model describes the data well.

In Figures 3 and 4 the estimated amounts of deposited COD and SS are shown for the estimation data set and for the validation data set, and it is clear that COD and SS are deposited in dry weather periods and flushed out during rain incidents. From Figure 4 it appears that the amount of COD first flush during the rain incident on April 3rd is approximately $2500\ \mathrm{kgO_2}$ and that the SS first flush is approximately $1800\ \mathrm{kgSS}$. A comparison of these amounts with

Parameter	a_{COD}	b_{COD}	a_0	a_1	b_1	a_2	b_2
Unit	h^{-1}	$\frac{kgO_2}{m^3}$	$\frac{kgO_2}{h}$	$\frac{kgO_2}{h}$	$\frac{kgO_2}{h}$	$\frac{kgO_2}{h}$	$\frac{kgO_2}{h}$
Estimate	-0.05432	-0.2969	198.3	-26.58	-16.05	-6.710	20.76
Standard deviation	0.00378	0.0041	1.2	1.50	1.62	1.560	1.47

Parameter	a_{SS}	b_{SS}	c_0	c_1	d_1	c_2	d_2
Unit	h^{-1}	$\frac{kgSS}{m^3}$	$\frac{kgSS}{h}$	$\frac{kgSS}{h}$	$\frac{kgSS}{h}$	$\frac{kgSS}{h}$	$\frac{kgSS}{h}$
Estimate	-0.03597	-0.1962	62.14	-12.27	-6.008	–	2.713
Standard deviation	0.00259	0.0032	0.71	1.09	1.061	–	1.054

Table 1. Maximum likelihood estimates of the parameters of the system.

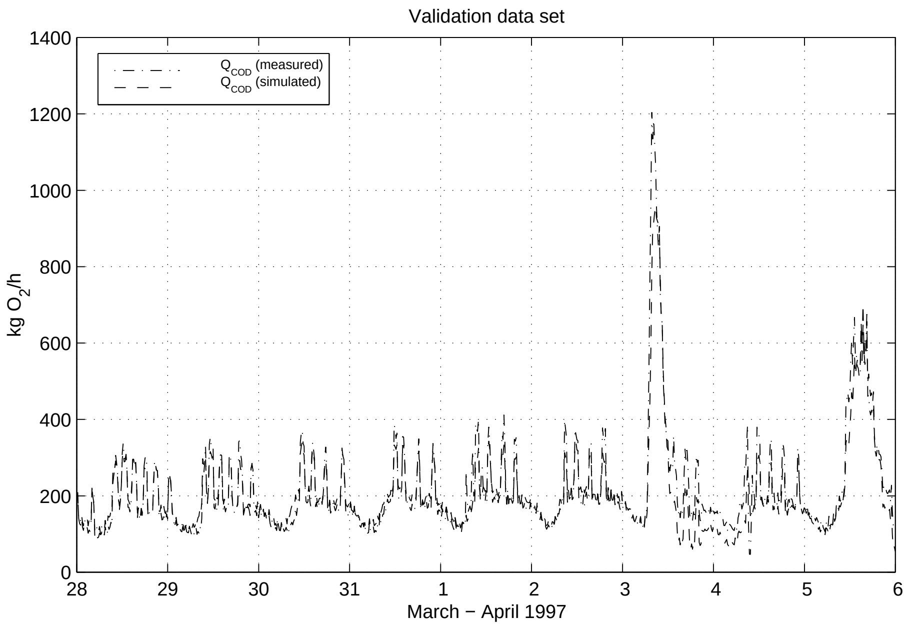

Figure 1. Measured and simulated COD mass flow - validation data set.

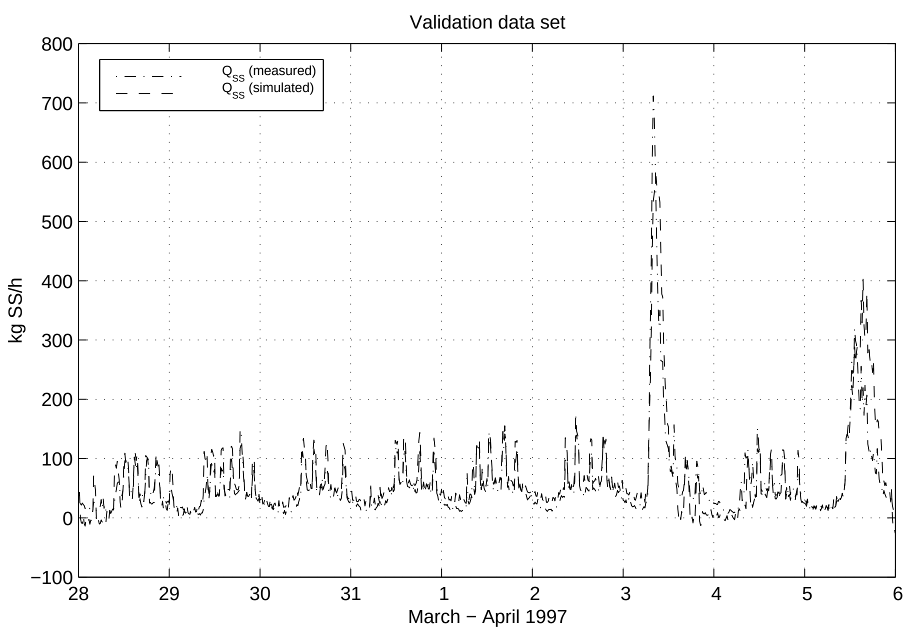

Figure 2. Measured and simulated SS mass flow - validation data set.

the mean loads of COD and SS to the WWTP of $5030\ \mathrm{kgO_2/24h}$ and $1527\ \mathrm{kgSS/24h}$ shows that this first flush contains approximately half a 24-hour load of COD and 20% more than a 24-hour load of SS. This is considered realistic, as it is expected that COD stabilizes in the sewer depots. When COD stabilizes in the sewer the amount of COD in a first flush compared to the normal load of COD will be smaller than the amount of SS compared to the normal load of SS, as SS are not expected to stabilize between rain incidents.

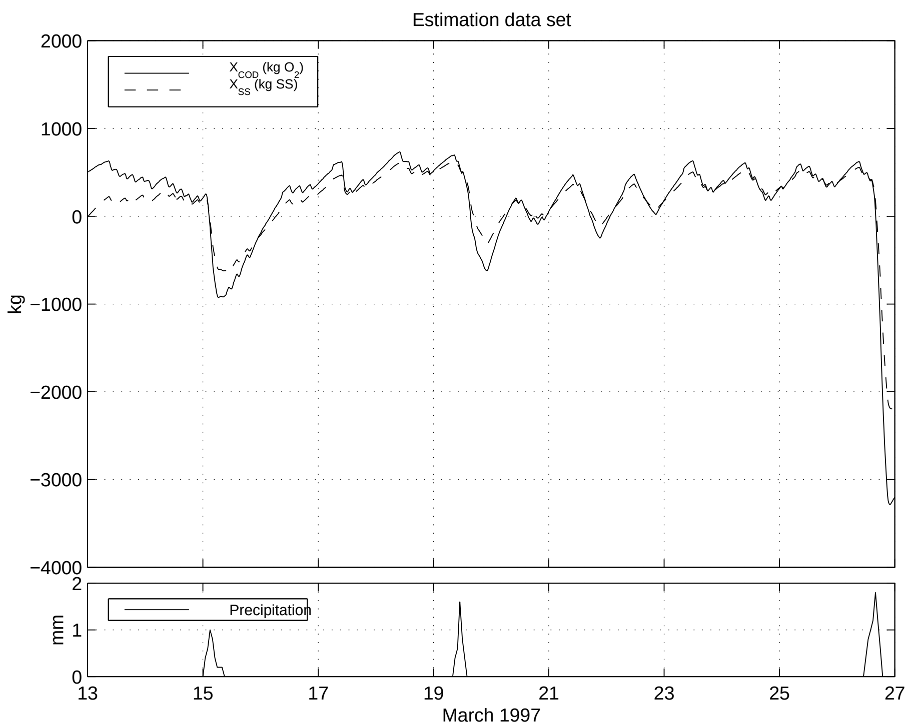

Figure 3. Estimated amounts of COD and SS deposits in the sewer system - estimation data set.

The time constants $\tau_{COD} = -1/a_{COD}$ and $\tau_{SS} = -1/a_{SS}$ are found to be $\tau_{COD} = 18.4\mathrm{h}$ and $\tau_{SS} = 27.8\mathrm{h}$. This means that after a considerable change in the flow, the masses of COD and SS in the sewer depots will reach 63% of the equilibrium in 18.4 and 27.8 hours, respectively. The time constants are thus found to be reasonable.

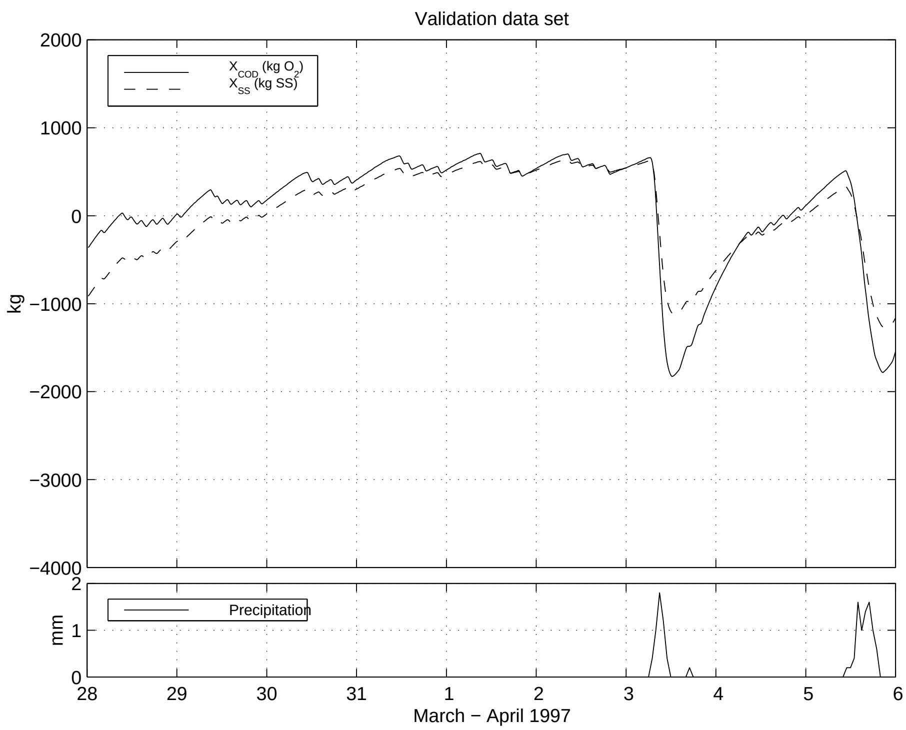

Figure 4. Estimated amounts of COD and SS deposits in the sewer system - validation data set.

Conclusion

In this paper a stochastic grey box model of the deposition of pollutants in the sewer system and on impervious areas of the catchment is proposed. Furthermore, the model provides a characterization of the influent wastewater to the WWTP. The parameters of the model are estimated using the maximum likelihood method. The modelling is based on measurements of concentrations of COD and SS, which are calculated from measurements of UV absorption and turbidity. It is concluded that the models, which relate the measurements of UV absorption and turbidity to COD and SS concentrations, describe the relations well in dry weather situations, and it is assumed that it is reasonable to extrapolate to rainy conditions.

Using the grey box approach, it is possible to identify a model for a complex dynamical system based on simple physical assumptions combined with statistical modelling tools. The model is formulated in continuous time with discrete time measurements and due to the rather small number of parameters, the model is operational for on-line applications.

The model makes it possible to estimate the amount of COD and SS in a first flush during a rain incident. It is found that these amounts are dependent on the time interval since the previous rain event and on the intensity of the current rain.

Acknowledgements

The authors wish to thank Skive WWTP for its cooperation during the data collection and for making the laboratory analyses, and Henrik A. Thomsen and Kenneth Kisbye for their kind assistance in the data collection. Thanks are also due to the Danish Academy of Technical Sciences for funding the project in which the present work has been carried out, under grant EF-623.

Paper C

Grey-box modelling of pollutant loads from a sewer system.

Published in *UrbanWater*, ***1****(1), pp. 71–78, 1999*

C

Abstract

Using a compact measuring unit with on-line meters for UV absorption and turbidity, it is possible to determine concentrations of organic load (chemical oxygen demand and suspended solids) anywhere in a sewer system. When measurements of the flow are available as well, the pollutant mass flow at the measuring point can be calculated.

The measured data are used to estimate different models describing the load of pollutants in the sewer. A comparison of the models shows that a grey-box model is most informative and best in terms measured by the multiple correlation coefficient. The grey-box model is a state-space model, where the state represents the actual amount of deposition in the sewer, and the output from the model is the pollutant mass flow to the wastewater treatment plant. The model is formulated by means of stochastic differential equations. Harmonic functions are used to describe the dry weather diurnal load profiles. It is found that the accumulation of deposits in the sewer depends on previous rain events and flows.

By means of on-line use of the grey-box models, it is possible to predict the amount of pollutants in a first flush at any time, and hence from the capacity of the plant to decide if and when the available detention basin is to be used for storage of wastewater. The mass flow models comprise an important improvement of the integrated control of sewer and wastewater treatment plant including control of equalisation basins in the sewer system. Further improvements are expected by the introduction of an additive model where dry weather situations and storm situations are modelled separately before addition to the resulting model.

Key words: Pollutant deposition, sewer system, first flush, grey-box models, statistical identification, on-line measurements.

Introduction

On-line measurements of organic pollution in terms of biological, chemical or total oxygen demand (BOD, COD or TOD) and suspended solids (SS) by means of UV absorbance and turbidity sensors are now well described (Dobbs et al., 1972; Mrkva, 1975; Kanaya et al., 1985; Ruban et al., 1993; Nowack and Ueberbach, 1995; Matsché and Stumwöhrer, 1996; Reynolds and Ahmad, 1997; Wass et al., 1997). When on-line measurements of COD and SS are available a better characterization of the wastewater can be achieved, and this leads to a better understanding of the processes in the sewer system.

The sewer system is often modelled by means of deterministic modelling as a configuration of storage volumes connected with pipes of different dimensions (Mark et al., 1995; Dempsey et al., 1997; Heip et al., 1997; van Luijtelaar and Rebergen, 1997). As these models are formulated as a large collection of differential equations with many parameters, it is difficult to estimate the parameters on the basis of available measurements.

Data based models are also common in the literature (Capodaglio, 1994; Delleur and Gyasi-Agyei, 1994; Ruan and Wiggers, 1997; Young et al., 1997). These models have few parameters, which can then be estimated on the basis of available data. However, as the models are most often formulated in discrete time, the parameter estimates depend on the sampling time.

In this paper a data based grey-box modelling approach is used. A grey-box model is a physically based macroscopic model with stochastic terms to count in uncertainties in model formulation and measurement values. The introduction of stochastic terms enables maximum likelihood estimation of the model parameters. The maximum likelihood method provides estimates of the variances of the parameter estimates, which are used to evaluate the uncertainty of the parameters. The proposed models are formulated here in continuous time. Measurements of pollutant mass flows in the inlet to a wastewater treatment plant (WWTP) are modelled by means of models of differing complexity. Pollutant deposition in the sewer can for instance be included, to make it possible to quantify the amounts of pollutants in a first flush.

The measurement system

A compact portable measuring box, developed by Krüger A/S, Denmark, has been used to collect measurements of UV absorption and turbidity from the inlet to the Aalborg East wastewater treatment plant in Northern Jutland, Den-

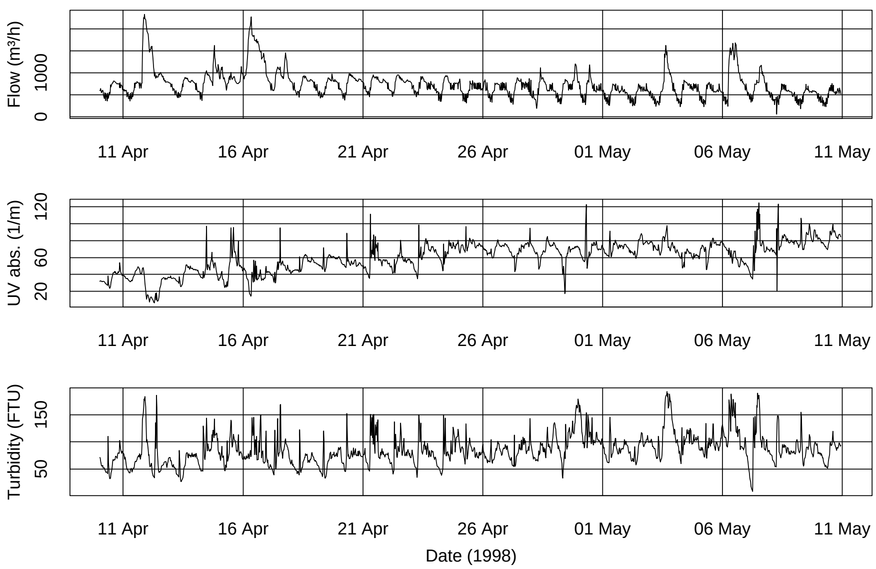

Figure 1. The measurements of flow, UV absorbance and turbidity.

mark, in the late 1997 and in the beginning of 1998. The Krüger measuring box consists of a Grant SQ-1003 datalogger, a Dr. Lange UV absorbance sensor model LSV 109 and a Dr. Lange SOLITAXplus LSV 121 turbidity sensor. The Aalborg East WWTP is equipped with the STAR control system (Nielsen and Önnerth, 1995; Önnerth and Bechmann, 1995) which supplies estimates of the inlet flow, based on measurements from the inlet pumping station. Figure 1 shows the data used in the present work. Laboratory analyses of COD and SS are also available.

Models of the pollution concentrations and fluxes

The relationships between on-line measurements of UV absorbance (A) and turbidity (T) and laboratory analyses of COD and SS concentrations (C_{COD} and C_{SS}, respectively) are assumed to be:

$$C_{\mathrm{COD}} = \alpha_{\mathrm{COD}} A + \beta_{\mathrm{COD}} \quad (1)$$

$$C_{\mathrm{SS}} = \alpha_{\mathrm{SS}} T + \beta_{\mathrm{SS}} \quad (2)$$

where α_{COD}, β_{COD}, α_{SS} and β_{SS} are parameters, which have to be estimated on the basis of measurements of C_{COD}, C_{SS}, A and T, as the parameters depend on the actual operating conditions and the wastewater composition (Dobbs et al., 1972; Mrkva, 1975; Kanaya et al., 1985; Ruban et al., 1993; Nowack and Ueberbach, 1995; Matsché and Stumwöhrer, 1996; Reynolds and Ahmad, 1997; Wass et al., 1997). When these parameters are estimated, it is possible to consider the observation at time t of pollution flux:

$$y(t) = Q(t)C(t) \tag{3}$$

with $Q(t)$ and $C(t)$ denoting the flow and the pollution concentration (C_{COD} or C_{SS}), respectively. This quantity can be modelled using:

$$y(t) = \hat{y}(t) + \epsilon(t) \tag{4}$$

Here $\hat{y}(t)$ is the predictable part of the model, and the residual $\epsilon(t)$ is a stochastic part, which is the difference between the data observed and the prediction obtained from the model.

The first approach considered is to model the pollution flux using a fixed diurnal profile expressed as an n-th order harmonic function with a 24 hour period (model 1):

$$\hat{y}(t) = a_0 + \sum_{k=1}^{n} \left(a_k \sin(2\pi k \frac{t}{24\mathrm{h}}) + b_k \cos(2\pi k \frac{t}{24\mathrm{h}}) \right) \tag{5}$$

where a_0, a_k, and b_k ($1 \leq k \leq n$), are the unknown parameters.

Another approach is to model the flux as a mean value and a term proportional to the flow (model 2):

$$\hat{y}(t) = c_0 + c_1 Q(t) \tag{6}$$

where c_0 and c_1 are positive parameters.

These two approaches can be combined to (model 3):

$$\hat{y}(t) = a_0 + \sum_{k=1}^{n} \left(a_k \sin(2\pi k \frac{t}{24\mathrm{h}}) + b_k \cos(2\pi k \frac{t}{24\mathrm{h}}) \right) + cQ(t) \tag{7}$$

Note that the parameter values of the Fourier expansion in equations (5) and (7) are in general not the same, as some of the harmonic variation in $y(t)$ is most likely explained by the harmonic variation of $cQ(t)$.

These approaches all result in static models.

The final approach considered is model 4 which is a dynamic model formulated as a state-space model. This model takes the deposition of pollutants in the sewer system and on impervious areas of the catchment area into account.

The model is based on the assumption that pollutants deposit gradually in dry weather and that the deposited pollutants are flushed out during rain incidents and into the inlet of the treatment plant. Let $x(t)$ denote the deposition of pollutants at time t. Then a simple first order linear ordinary differential equation:

$$\frac{\mathrm{d}\hat{x}}{\mathrm{d}t} = a(\hat{x} - \bar{x}) + b(Q - \bar{Q}) \tag{8}$$

can be used to describe the dynamics of the pollution deposition. The time derivative of $\hat{x}$ is the estimated growth rate at which pollution is built up in the sewer, and $\bar{x}$ and $\bar{Q}$ are the mean values of $\hat{x}$ and Q. The parameters a and b are assumed to be negative, and hence a flow larger than the average flow during the period will decrease the growth rate and a flow lower than the mean flow will increase the growth rate. Similarly a deposited amount larger than the mean will decrease the growth rate, and vice versa.

The pollution flux observed at the measuring point in the inlet to the WWTP, is assumed to consist of a fixed diurnal profile, which describes the pollutants that enter the sewer system, minus a contribution to the depositions in the sewer. This is formulated in the observation equation:

$$\begin{aligned}\hat{y}(t) &= a_0 + \sum_{k=1}^{n}\left(a_k \sin(2\pi k\frac{t}{24\mathrm{h}}) + b_k \cos(2\pi k\frac{t}{24\mathrm{h}})\right) - \frac{\mathrm{d}\hat{x}}{\mathrm{d}t} \\ &= a_0 + \sum_{k=1}^{n}\left(a_k \sin(2\pi k\frac{t}{24\mathrm{h}}) + b_k \cos(2\pi k\frac{t}{24\mathrm{h}})\right) \\ &\quad - a(\hat{x} - \bar{x}) - b(Q - \bar{Q})\end{aligned} \tag{9}$$

Besides a better description of the available data, this approach also provides information about the practically unmeasureable amount of deposits in the sewer and impervious areas of the catchment. Hence, besides the parameter estimates, the model also provides an estimate of $x - \bar{x}$. This means that the model does not give information about the actual deposition level x, but only about the difference from the mean level of deposition. This does not pose any practical limitations on the use of the model, as, for instance, it is still possible to quantify the amount of pollutants in a first flush.

All the proposed pollution flux models can be applied to both SS and COD flux.

Estimation methods

The parameters of the concentration models (1) and (2) as well as the parameters of the static pollution flux models (5), (6), and (7), can be estimated by ordinary least squares methods, as these models are all linear in the parameters.

The method used to estimate the parameters of the dynamic pollution flux model (4) and (8) – (9) is a maximum likelihood method for estimating parameters in stochastic differential equations based on discrete time data given by (4). For a more detailed description of the method refer to Madsen and Melgaard (1991) or Melgaard and Madsen (1993).

In order to use the maximum likelihood method, some stochastic terms have to be introduced. Hence, the first order differential equation (8) turns into a stochastic differential equation, where the continuous time equation describing the dynamics of the pollution deposition can be written as the so-called Itô differential equation (Øksendal, 1995)

$$dx(t) = f(x, u, t)dt + g(u, t)dw(t) \tag{10}$$

where x is the state variable, u an input (e.g. control) variable, w a standard Wiener process (see e.g. Kloeden and Platen (1995)), and f and g are known functions. The function $g(u, t)$ describes any input or time dependent variation related to how the variation generated by the Wiener process enters the system. Note, that in order to illustrate the flexibility of the method equation (10) represents a generalization of the ordinary state equation (8).

For the observations we assume the discrete time relation

$$y(t) = h(x, u, t) + e(t) \tag{11}$$

where $e(t)$ is assumed to be a Gaussian white noise sequence independent of w, which can be seen as a generalization of (4) and (9). All the unknown parameters, denoted by the vector $\boldsymbol{\theta}$, are embedded in the continuous-discrete time state space model (equations (10) and (11)).

The observations are given in discrete time, and, in order to simplify the notation, we assume that the time index t belongs to the set $\{0, 1, 2, ..., N\}$, where N is the number of observations. Introducing

$$\mathcal{Y}(t) = [y(t), y(t-1), \ldots, y(1), y(0)]' \tag{12}$$

i.e. $\mathcal{Y}(t)$ is a vector containing all the observations up to and including time t, the likelihood function is the joint probability density of all the observations assuming that the parameters are known, i.e.

$$\begin{aligned} L'(\boldsymbol{\theta}; \mathcal{Y}(N)) &= p(\mathcal{Y}(N)|\boldsymbol{\theta}) \\ &= p(y(N)|\mathcal{Y}(N-1), \boldsymbol{\theta})p(\mathcal{Y}(N-1)|\boldsymbol{\theta}) \\ &= \left(\prod_{t=1}^{N} p(y(t)|\mathcal{Y}(t-1), \boldsymbol{\theta})\right)p(y(0)|\boldsymbol{\theta}) \end{aligned} \tag{13}$$

where successive applications of the rule $P(A \cap B) = P(A|B)P(B)$ are used to express the likelihood function as a product of conditional densities.

In order to evaluate the likelihood function it is assumed that all the conditional densities are Gaussian. In the case of a linear state space model as described by (4) and (8) – (9), it is easily shown that the conditional densities are actually Gaussian (Madsen and Melgaard, 1991). In the more general non-linear case the Gaussian assumption is an approximation.

The Gaussian distribution is completely characterized by the mean and covariance. Hence, in order to parameterize the conditional distribution, we introduce the conditional mean and the conditional variance as

$$\begin{aligned} \hat{y}(t|t-1) &= E[y(t)|\mathcal{Y}(t-1), \boldsymbol{\theta}] \quad \text{and} \\ R(t|t-1) &= V[y(t)|\mathcal{Y}(t-1), \boldsymbol{\theta}] \end{aligned} \tag{14}$$

respectively. It should be noted that these correspond to the one-step prediction and the associated variance, respectively. Furthermore, it is convenient to introduce the one-step ahead prediction error (or innovation)

$$\epsilon(t) = y(t) - \hat{y}(t|t-1) \tag{15}$$

For calculating the one-step ahead prediction and its variance, an iterated extended Kalman filter is used. The extended Kalman filter is simply based on a linearization of the system equation (10) around the current estimate of the state (see Gelb (1974)). The iterated extended Kalman filter is obtained by local iterations of the linearization over a single sample period.

Using (13) – (15) the conditional likelihood function (conditioned on $y(0)$) becomes

$$L(\boldsymbol{\theta}; \mathcal{Y}(N)) = \prod_{t=1}^{N} \left(\frac{1}{\sqrt{2\pi}\sqrt{R(t|t-1)}} \exp(-\frac{\epsilon(t)^2}{2R(t|t-1)}) \right) \tag{16}$$

Traditionally, the logarithm of the conditional likelihood function is considered

$$\log L(\boldsymbol{\theta}; \mathcal{Y}(N)) = -\tfrac{1}{2} \sum_{t=1}^{N} \left(\log R(t|t-1) + \frac{\epsilon(t)^2}{R(t|t-1)} \right) + \text{const} \tag{17}$$

The maximum likelihood estimate (ML-estimate) is the set $\hat{\boldsymbol{\theta}}$, which maximizes the likelihood function. Since it is not, in general, possible to optimize the likelihood function analytically, a numerical method has to be used. A reasonable method is the quasi-Newton method.

An estimate of the uncertainty of the parameters is obtained by the fact that the ML-estimator is asymptotically normally distributed with mean $\boldsymbol{\theta}$ and covariance

$$\boldsymbol{D} = \boldsymbol{H}^{-1} \tag{18}$$

where the matrix $\boldsymbol{H}$ is given by

$$\{h_{lk}\} = -E\left[\frac{\partial^2}{\partial\theta_l \partial\theta_k} \log L(\boldsymbol{\theta}; \mathcal{Y}(N)) \right] \tag{19}$$

An estimate of $\boldsymbol{D}$ is obtained by equating the observed value with its expectation and applying

$$\{h_{lk}\} \approx -\left(\frac{\partial^2}{\partial\theta_l \partial\theta_k} \log L(\boldsymbol{\theta}; \mathcal{Y}(N))\right)_{|\theta=\hat{\theta}} \tag{20}$$

The above equation can be used for estimating the variance of the parameter estimates. The variances serve as a basis for calculating t-test values for test under the hypothesis that the parameter is equal to zero. Finally, the correlation between the parameter estimates is readily found, based on the covariance matrix $\boldsymbol{D}$.

The estimation methods are implemented in the CTLSM program, which are available from http://www.imm.dtu.dk/~hm/.

Results and discussion

The parameters of equations (1) and (2) are found by linear regression. It turned out that β_{COD} and β_{SS} were insignificant, and therefore they were eliminated in the final estimation. The estimated parameters and their standard deviations are shown in Table 1. The degrees of explanations (multiple correlation coefficients) of the COD and SS concentration models are $R^2 = 0.98$ and $R^2 = 0.97$, respectively.

Parameter	α_{COD}	β_{COD}	α_{SS}	β_{SS}
Unit	$\frac{\mathrm{gO_2/m^3}}{\mathrm{m^{-1}}}$	$\mathrm{gO_2/m^3}$	$\frac{\mathrm{gSS/m^3}}{\mathrm{FTU}}$	$\mathrm{gSS/m^3}$
Estimate	10.57	–	3.05	–
Standard deviation	0.40	–	0.13	–

Table 1. Parameters of equations (1) and (2). The β parameters are insignificant and are therefore not estimated.

For the models, which include a diurnal profile modelled as a harmonic function (models 1, 3, and 4), it was found that second order harmonic functions were suitable, as the higher order coefficients were insignificant. In Tables 2 and 3 it can be seen that some of the parameters of the harmonic functions are

Table 2. Parameter estimates of the COD flux models.

Model 1	Parameter	a_0	a_1	b_1	a_2	b_2		
	Unit	$\frac{kgO_2}{h}$	$\frac{kgO_2}{h}$	$\frac{kgO_2}{h}$	$\frac{kgO_2}{h}$	$\frac{kgO_2}{h}$		
	Estimate	443.5	-148.6	-39.22	17.94	53.94		
	Standard deviation	3.8	5.34	5.34	5.34	5.34		
Model 2	Parameter	c_0	c_1					
	Unit	$\frac{kgO_2}{h}$	$\frac{kgO_2}{m^3}$					
	Estimate	190.1	0.3464					
	Standard deviation	10.3	0.0130					
Model 3	Parameter	a_0	a_1	b_1	a_2	b_2	c	
	Unit	$\frac{kgO_2}{h}$	$\frac{kgO_2}{h}$	$\frac{kgO_2}{h}$	$\frac{kgO_2}{h}$	$\frac{kgO_2}{h}$	$\frac{kgO_2}{m^3}$	
	Estimate	270.8	-114.3	-29.29	19.25	36.04	0.2361	
	Standard deviation	9.4	5.07	4.79	4.76	4.85	0.0120	
Model 4	Parameter	a	b	a_0	a_1	b_1	a_2	b_2
	Unit	h^{-1}	$\frac{kgO_2}{m^3}$	$\frac{kgO_2}{h}$	$\frac{kgO_2}{h}$	$\frac{kgO_2}{h}$	$\frac{kgO_2}{h}$	$\frac{kgO_2}{h}$
	Estimate	-0.08775	-0.4448	444.4	-93.50	1.403	24.67	22.69
	Standard deviation	0.00864	0.0175	3.0	4.65	4.690	4.12	4.34

Table 3. Parameter estimates of the SS flux models.

Model 1	Parameter	a_0	a_1	b_1	a_2	b_2		
	Unit	$\frac{\mathrm{kgSS}}{\mathrm{h}}$	$\frac{\mathrm{kgSS}}{\mathrm{h}}$	$\frac{\mathrm{kgSS}}{\mathrm{h}}$	$\frac{\mathrm{kgSS}}{\mathrm{h}}$	$\frac{\mathrm{kgSS}}{\mathrm{h}}$		
	Estimate	198.8	-65.91	-16.62	-10.55	32.10		
	Standard deviation	3.3	4.70	4.70	4.70	4.70		
Model 2	Parameter	c_0	c_1					
	Unit	$\frac{\mathrm{kgSS}}{\mathrm{h}}$	$\frac{\mathrm{kgSS}}{\mathrm{m}^3}$					
	Estimate	-77.11	0.3772					
	Standard deviation	5.25	0.0066					
Model 3	Parameter	a_0	a_1	b_1	a_2	b_2	c	
	Unit	$\frac{\mathrm{kgSS}}{\mathrm{h}}$	$\frac{\mathrm{kgSS}}{\mathrm{h}}$	$\frac{\mathrm{kgSS}}{\mathrm{h}}$	$\frac{\mathrm{kgSS}}{\mathrm{h}}$	$\frac{\mathrm{kgSS}}{\mathrm{h}}$	$\frac{\mathrm{kgSS}}{\mathrm{m}^3}$	
	Estimate	-67.96	-12.96	-1.268	-8.536	4.445	0.3647	
	Standard deviation	5.60	3.01	2.846	2.830	2.882	0.0071	
Model 4	Parameter	a_{SS}	b_{SS}	a_0	a_1	b_1	a_2	b_2
	Unit	h^{-1}	$\frac{\mathrm{kgSS}}{\mathrm{m}^3}$	$\frac{\mathrm{kgSS}}{\mathrm{h}}$	$\frac{\mathrm{kgSS}}{\mathrm{h}}$	$\frac{\mathrm{kgSS}}{\mathrm{h}}$	$\frac{\mathrm{kgSS}}{\mathrm{h}}$	$\frac{\mathrm{kgSS}}{\mathrm{h}}$
	Estimate	-0.01192	-0.4147	204.3	-3.945	4.002	-6.357	-0.1627
	Standard deviation	0.00090	0.0086	1.7	2.663	2.429	2.339	2.476

insignificant, as their estimated values are smaller or comparable in absolute values to their estimated standard deviations. Especially b_1 of COD flux model 3, b_1 of SS flux model 3 and b_2 of SS flux model 4 are very uncertain. Usually insignificant parameters should be excluded from the final estimation, to make the estimation of the remaining parameters better. However, we have chosen to include these parameters for comparison with the other models.

Comparison plots of measured and modelled pollution fluxes of the 4 models are shown in Figures 2, 3, 4, and 5. Note, that the modelled pollution fluxes shown in the figures are not one-step ahead predictions, but simulations from the estimated models. The simulations are based only on the measured input to the models, which is time of day (models 1, 3, and 4) and inlet flow (models 2, 3, and 4). In Tables 2 and 3 the parameter estimates of the proposed models are listed, and in Table 4 the correlations between measured and simulated fluxes R^2 of the models are listed.

Model	R^2	
	COD model	SS model
1	0.39	0.15
2	0.32	0.69
3	0.51	0.69
4	0.61	0.76

Table 4. Degrees of explanation of the different models.

When comparing Figures 2, 3, 4 and 5, it is seen that the simple harmonic model 1 is good at describing most of the dry weather situations, but not the wet weather situations. Models 2, 3 and 4 are better than model 1 at following the peaks in pollution flux in wet weather, as they include a term proportional to the flow. Besides a better correlation between measured and modelled pollutant fluxes expressed by the degree of explanation R^2, application of the dynamic model provides information about the pollutant depositions in the sewer. In Figure 6 the estimated deviations from the mean levels of COD and SS deposits are shown. From this figure it is seen that pollutants build up in the sewer during dry weather periods and are flushed out during rain. The amounts of deposits in a first flush can also be quantified on the basis of Figure 6: The first and second rain incidents contain approximately 3000 kgO_2 (COD) and 6000 kgSS which are 14% and 63% of the diurnal load of COD and SS, respectively. As it is expected that deposited COD stabilizes in the sewer this is considered realistic. The stabilization of COD will lead to a smaller amount of COD in a first flush compared to the normal load of COD than the amount of SS compared to the normal load of SS, as deposited SS are not expected to stabilize in the sewer.

The time constants of the dynamic COD and SS models are $-1/a = 11.4\mathrm{h}$ and $-1/a = 83.9\mathrm{h}$, respectively. This means that after a considerable change in the flow, the COD and SS depositions will reach 63% of the steady state level in 11.4 and 83.9 hours, respectively. The dynamics of the COD deposition is thus about 7 times faster than the dynamics of the SS deposition.

As the data used for estimating the models are dominated by dry weather situations, the fluxes are underestimated during rainful events. A separation of the models into dry weather models and storm models, which are added to each other, might be a significant improvement.

Conclusions

Linear relationships between UV absorption and COD and between turbidity and SS are derived. These relationships are used to compute the COD and SS concentrations from on-line measurements of UV absorption and turbidity. Using available measurements of the flow in the inlet to Aalborg East WWTP the pollution flows of COD and SS are used to estimate models of differing complexity. It is shown that the estimated dynamic grey-box models, which include the deposition and flush out of pollutant masses in the sewer, describe the data better than the other models proposed. Furthermore, these dynamic models estimate the amounts of deposits in the sewer at any time. Hereby the amounts of pollutants in a first flush are found. This information is very useful when control algorithms for the use of the available detention basin at the WWTP are designed. However, when the models are to be used to enable better operational control of available detention basins, predictions of the wastewater flow to the WWTP are required. When flow forecasts are available, the models suggested can be used to predict the pollutant load with the same time horizon as the flow predictions.

With degrees of explanation (multiple correlation coefficients) $R^2 = 0.76$ and

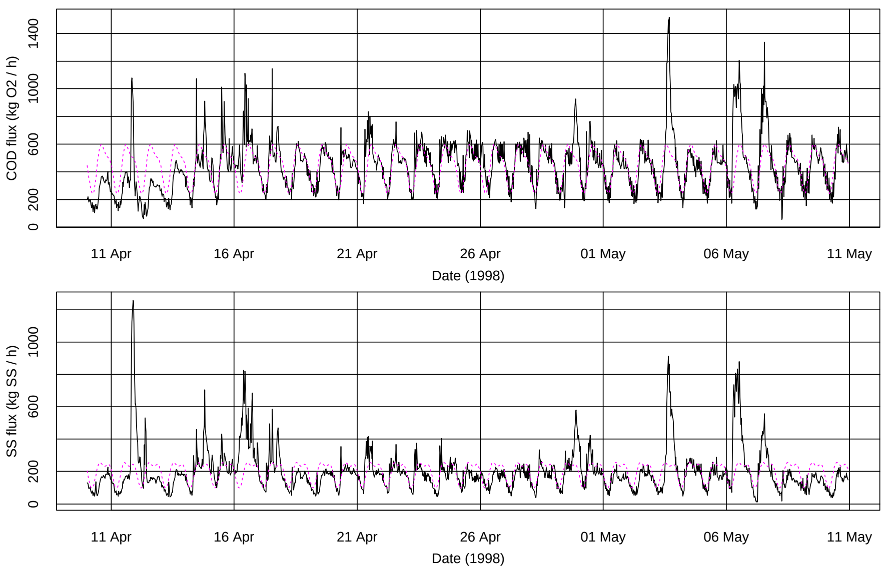

Figure 2. The pollutant flux modelled as a diurnal profile. Solid lines: measured flux, dashed lines: modelled flux.

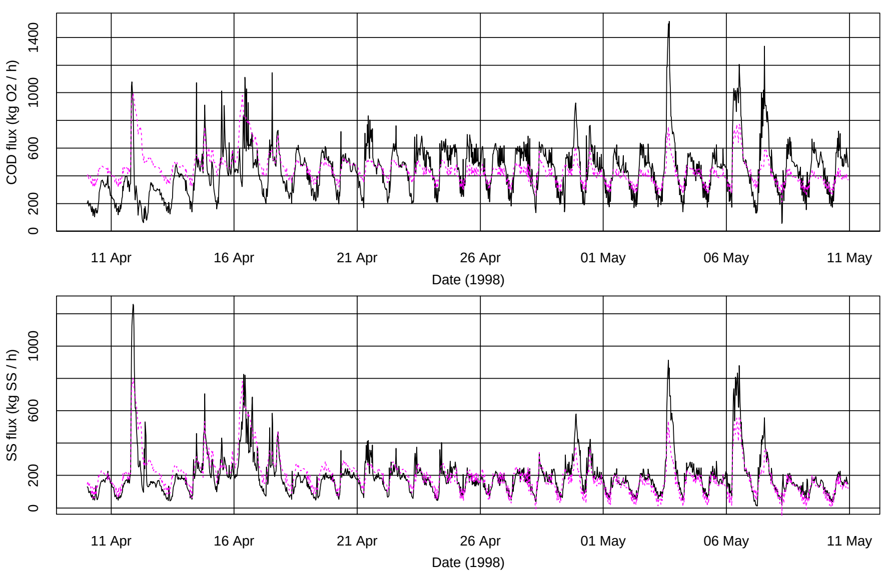

Figure 3. The pollutant flux modelled as proportional to the flow. Solid lines: measured flux, dashed lines: modelled flux.

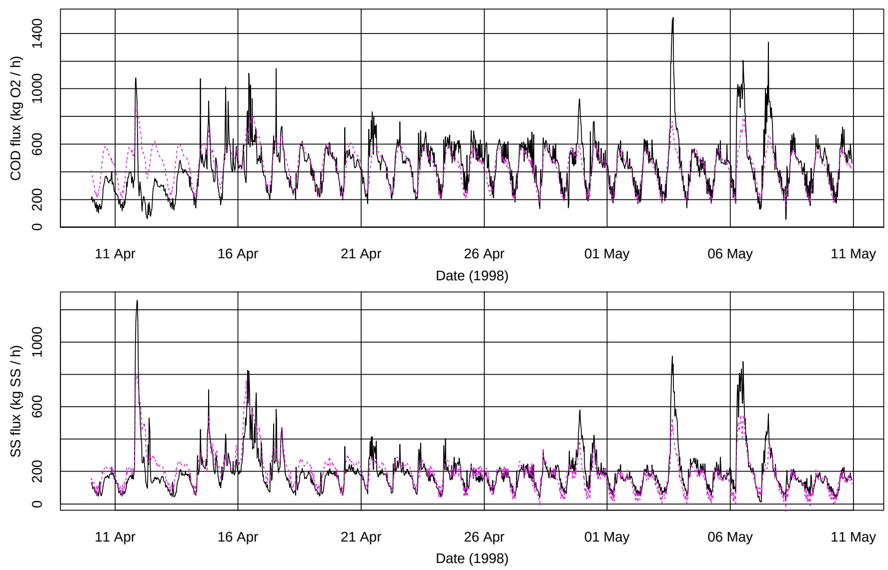

Figure 4. The pollutant flux modelled as a diurnal profile plus a term proportional to the flow. Solid lines: measured flux, dashed lines: modelled flux.

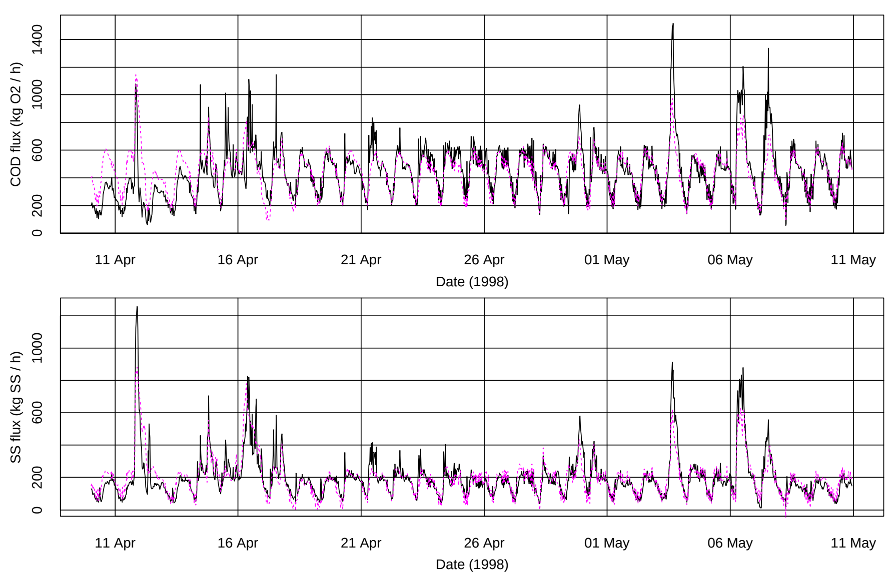

Figure 5. The pollutant flux modelled by a dynamic grey-box model. Solid lines: measured flux, dashed lines: modelled flux.

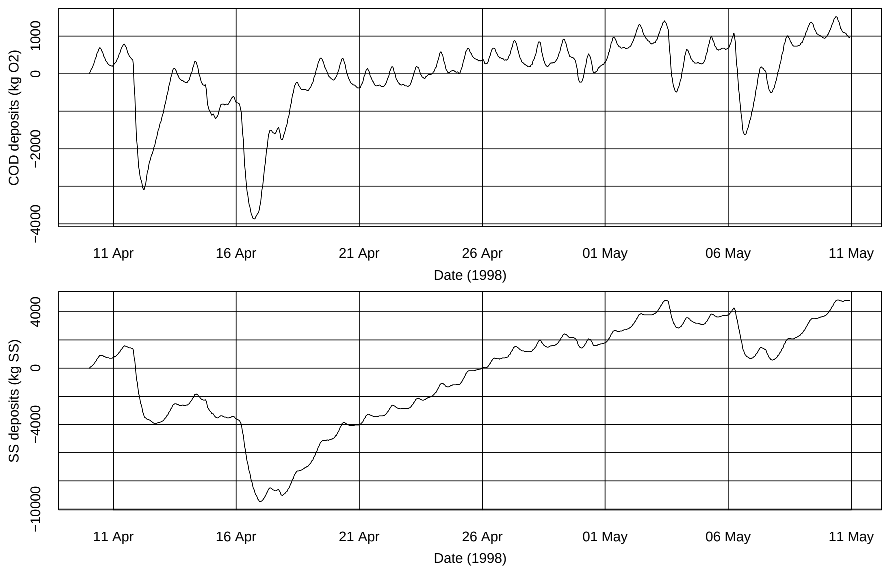

Figure 6. Estimated depositions of COD and SS in the sewer and on impervious areas.

$R^2 = 0.61$ for the dynamic grey-box COD and SS flux models, respectively, there are still variations in the data that are not described by the models. Hence, there is still a need to develop better models. Improvements could be a separation into dry weather models and storm models, and the introduction of limitations on the depositions in the sewer and on impervious areas. However, introduction of limitations on the depositions will require measurement data that covers the limits sufficiently to estimate the parameters that describe the bounds.

Acknowledgements

The authors wish to thank the staff of Aalborg East WWTP, especially Pernille Iversen, for their cooperation during the data collection and for making the laboratory analyses. Thanks are also due to the Danish Academy of Technical Sciences for funding the project in which the present work has been carried out, under grant EF-623.

Paper D

Modelling and test of Aeration Tank Settling ATS.

Published in *Proceedings of the 8th IAWQ Conference on Design, Operation and Economics of Large Wastewater Treatment Plants* pp. 199–206.

International Association on Water Quality, IAWQ, Budapest University of Technology, Department of Sanitary and Environmental Engineering

D

Abstract

The use of aeration tank settling during high hydraulic loads on large wastewater treatment plants has previously been demonstrated as a reliable technique and proven valuable. The paper proposes a simplified deterministic model to predict the efficiency of the method. It is shown that a qualitatively correct model can be established. The simplicity of the model allows for on-line identification of the necessary parameters, so that no maintenance is needed for use of the on-line model for control.

The practical implementation on 3 plants indicates that implementation of STAR with ATS control gives 50% increase of plant capacity for 3% extra cost.

Key words: Wastewater treatment, modelling, on-line control, hydraulic capacity, stormwater control, activated sludge.

Introduction

The settling in aeration tanks is often a problem in activated sludge wastewater treatment plants. Especially for low loaded plants or during anoxic conditions during nutrient removal correct mixing intensity is important. Traditionally, these problems are solved by introduction of mixers or by installation of excess aeration capacity in the tanks to assure homogeneity in the reaction tanks.

During recent years more controllers are accepting partly settling in the aeration tanks during intermitting aeration, as presented at IAWQ ICA Workshop 1997. Other controls are today emphasizing on intentional settling in the aeration tank (Bundgaard et al., 1996) to increase the hydraulic capacity of the plant. As Wett et al. (1997) demonstrated, introduction of mixing in the denitrifying clarifiers has no effect on the reaction rates. Similar experiences have been reported in aeration tanks with intentional settling (Bundgaard et al., 1996).

As there is no negative effect on reaction rates by no mixing and the hydraulic capacity can be increased, there is a potential to save energy and improve plant capacity by use of aeration tank settling in activated sludge plants. Thus, many mixers might be saved in future plants.

To be able to design the controllers for these processes, it is necessary to be able to predict when and how much sludge settling will occur in the tanks during stop of aeration. Then it is possible to model the effect on transport of sludge to clarifiers, and hence the hydraulic capacity of the plant can be calculated. To adjust the capacity to predicted needs, the periods of settling can be adjusted, and in alternating plants the settling can be further expanded by intermediate phases where settling is taking place in the whole volume as shown in Figure 1.

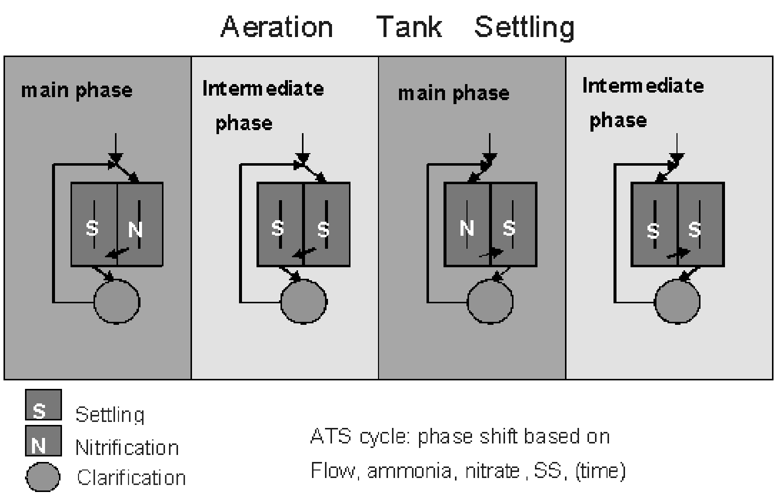

Figure 1. Dynamic phase length control schemes for STAR control.

In the following a simple model for settling in aeration tanks is proposed. The model is a little different for alternating and recirculating systems. However, the aim is to describe a model, which can be used for design and adjustments of the control strategies and which can obtain 30 – 100 percent extension of the hydraulic capacity for the plants.

Theory for modelling

The sludge settling starts when the turbulence in the tanks is reduced after stopping both aeration and mixing. When the settling starts, the formula for hindered settling dependent on the mixed liquor suspended solids, MLSS, in the interface is proposed as a two-layer model with dynamic layer heights. The upper layer is assumed to be clear water while the lower layer is assumed to contain all the initial sludge content which concentrates as the sludge layer height decreases during the settling period.

The settling rate model for sludge proposed by Vesilind (1979) and quantified by Härtel and Pöpel (1992) is used:

$$v_{\mathrm{SS}} = v_{\mathrm{S,0}}\,\mathrm{e}^{-n_{\mathrm{v}} SS} \tag{1}$$

where:

v_{SS} and $v_{\mathrm{S,0}}$ are the actual and the unhindered settling rate of sludge particles, respectively, and n_{v} is an empiric concentration effect factor.

The modelling of the sludge blanket depth, d_{SB}, can be done by integration of the settling rate over time:

$$d_{\mathrm{SB}} = \int_{t_0}^{t} v_{\mathrm{SS}} dt \tag{2}$$

The relevant sludge concentration starts at the MLSS value in the aerated tank and increases during the settling as sludge concentrates towards the bottom.

The starting time t_0 is when the turbulence is reduced.

To predict the outlet SS from the tanks in non-ideal full-scale plants the details of the inlet, outlet and tank geometrical design must be included in the model.

As a first simple model for SS in the top weir outlet of the aeration tank and inlet to the clarifier, SS_{out}, can be made as a calculation of suction depth, d_{suct}.

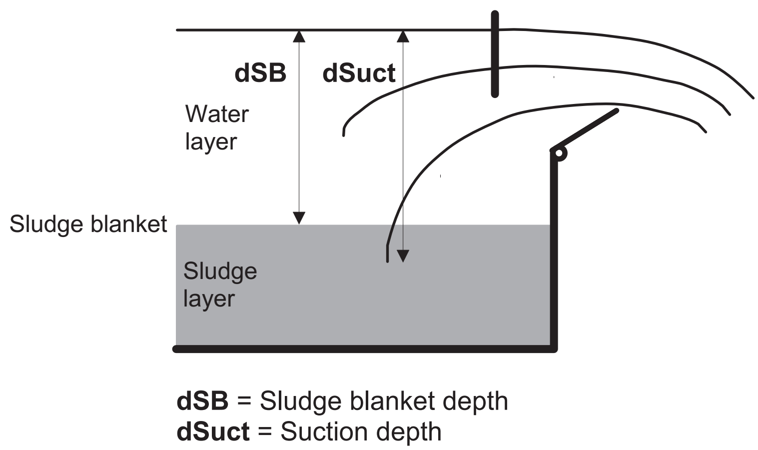

Figure 2. Parameter definition for modelling effluent SS.

The suction depth is predicted for the specific outlet and the concentration is modelled as:

$$SS_{\text{out}} = \frac{d_{\text{suct}} - d_{\text{SB}}}{d_{\text{suct}}} SS_{\text{bl}} \tag{3}$$

Of course, the suction depth is varying with the flow rate, and the distribution of the actual flow is not proportional with the depth. These unmeasurable factors are modelled by data fitting to full-scale measurements.

Physical model

Alternating systems

In the alternating system typically two tanks are available. As a rule only the last tank before the clarifier is relevant for settling. The inlet will normally be from an adjoining tank as seen in Figure 3, and the inlet velocity and distribution is of paramount importance for the efficiency of the settling as well as the outlet distribution as it is in other clarifier designs.

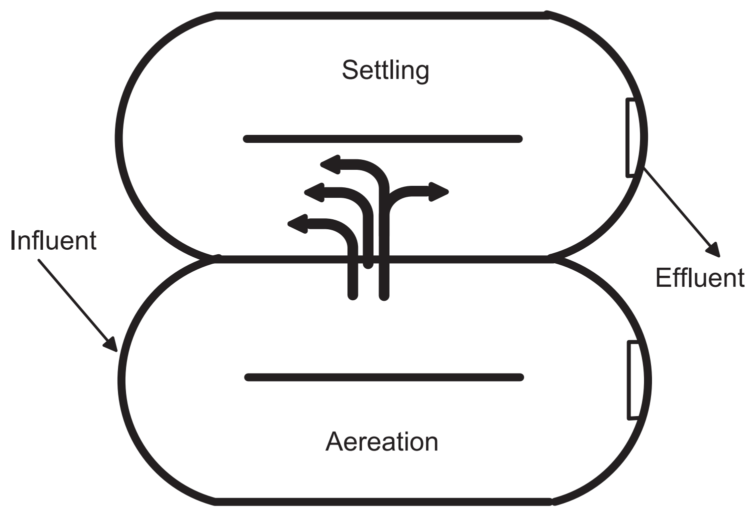

Figure 3. Physical description of outlet modelling in settling aeration tanks in an alternating plant.

Apart from simple ideal settling the model must include the reduced efficiency of the aeration tank as clarifier because inlet and outlet is not optimal. Further the storage of sludge on the bottom will limit the capacity for settling after some time in the same phase, as there is no sludge removal from the aeration tanks during the phases.

The inlet turbulence must be adequate enough to distribute the incoming water sufficiently in the tank under settling operation to avoid short-circuiting. For the modelling, the limitation in settling efficiency is simplest described by reducing the efficient volume of the aeration settling tank.

The outlet is more important for the time distribution of the aeration tank efficiency for settling. The outlet is assumed to be via a weir, and the suction depth is a function of outflow. As shown in Figure 2 the concentration of sludge in the outlet is dependent on the sludge blanket level and the SS concentration under the sludge blanket that is sucked out in the effluent from the tank.

The sludge build-up and concentration profile on the bottom is modelled as a single layer model, but to be able to fit the model to practical experiments a virtual bottom is assumed, and the sludge concentration below the sludge blanket and the virtual bottom is assumed homogeneous.

With these assumptions we have a simple model for the concentration out of an aeration tank at any time dependent on present and previous load and on the period since the settling started as shown in Figure 7.

Recirculating plants

In recirculating plants the settling can take place in the effluent part of the aeration tank. Apart from the stopping of the aerators in intervals, the priority can be to stop the effluent end aeration grids as shown in Figure 4 to obtain settling in the outlet end. The return of sludge can use the existing recirculation system.

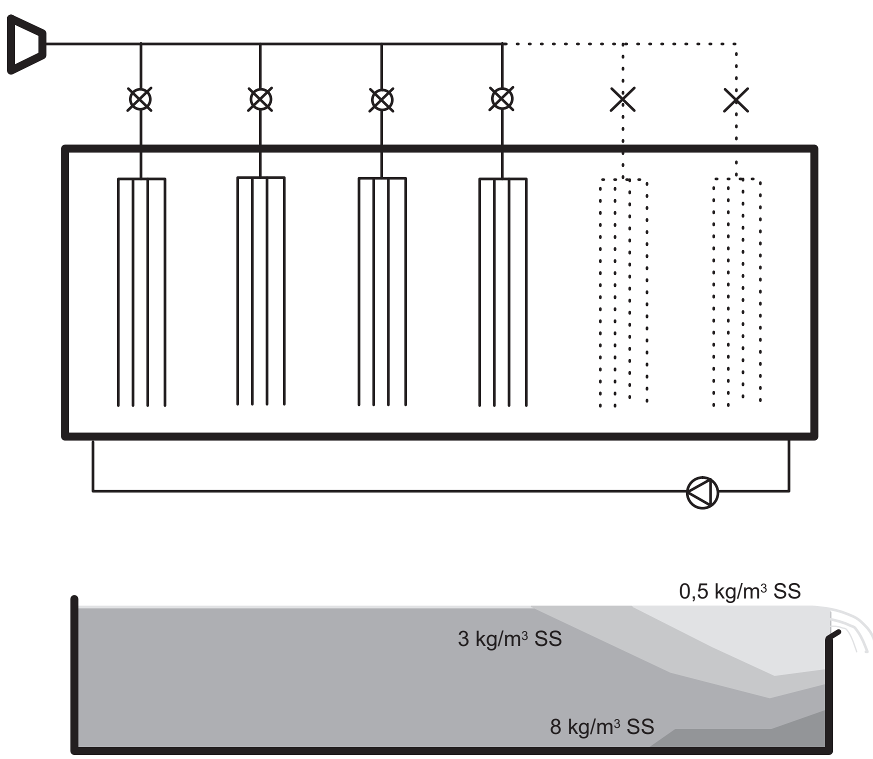

Figure 4. Physical description of outlet modelling in a recirculating plant.

Plant capacity

The capacity of the clarifiers is often the limiting factor during rain events. In stationary situations, the capacity of the clarifiers, according to normal design rules (like the ATV rules), is inverse proportional to the sludge volume index, SVI, and the concentration of suspended solids, SS. Billmeier (1986) describes the steady state hydraulic capacity of the clarifiers as

$$Q = \frac{V_{\text{clarifier}}}{SS_{\text{out}} SVI k} = \frac{K}{SS_{\text{out}}} \tag{4}$$

where k is a proportionality factor, specific for a given plant design, and

$$K = \frac{V_{\text{clarifier}}}{SVI k} \tag{5}$$

is a plant specific value for a given sludge quality.

Hence, at a plant with a given clarifier volume and sludge volume index, the hydraulic capacity of the plant is inverse proportional to the suspended solid concentration out of the aeration tank as shown above.

By introducing the aeration tank settling (ATS) operation before and during rain, the necessary clarifier volume is reduced as illustrated in Figure 5 taken from Nielsen et al. (1996).

Practical test

To test the model, the data from a full-scale application at Aalborg East WWTP shown in Figure 6 are used.

At present this configuration is used on 3 alternating plants serving approx 700.000 pe in Scandinavia. At minor rain events the model and reality look

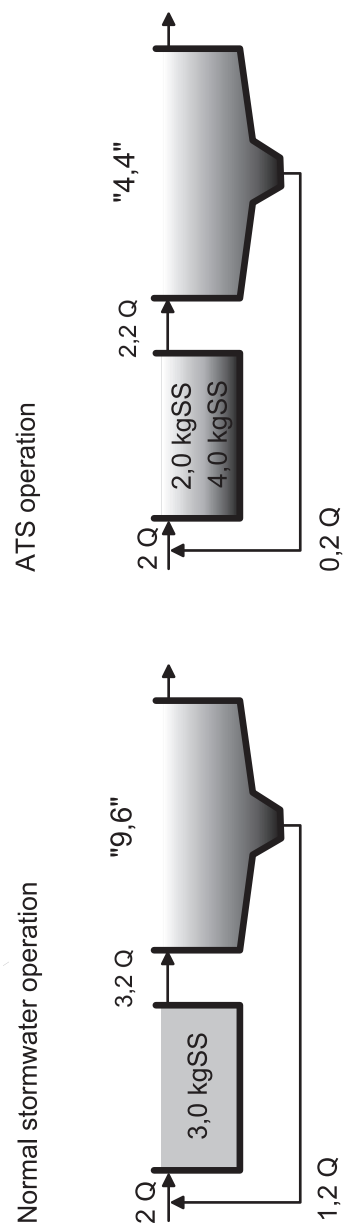

Figure 5. Required settler volume for two control control schemes (Nielsen et al., 1996).

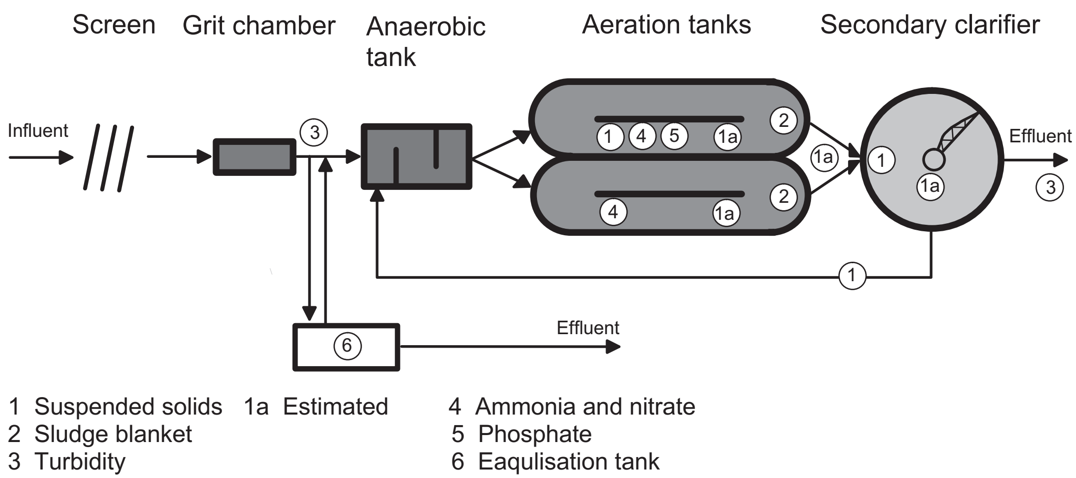

Figure 6. Description of the Aalborg East alternating WWTP.

as shown in Figure 7 below. Compared to conventional extension of clarifier volume, the use of control to extend the capacity can be achieved by typically 1/10 of the cost.

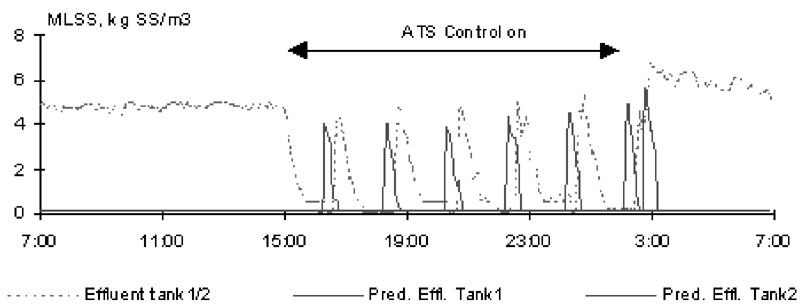

Figure 7. Measured and modelled MLSS out of the aeration tanks.

The modelled and measured MLSS out of aeration tanks during storm events with settling in the aeration tanks are shown in Figure 7.

As it can be seen the modelled MLSS is nearly 45 minutes ahead of measured values. This is due to delay from: 1) SCADA system, 2) Rotation in horizontal channels and 3) delay from stop of micro-turbulence after stop of aeration and mixers, all of which are not included in the model.

Equal results are experienced from other alternating plants. Control has been introduced on a recirculating system at the Sydkysten WWTP, but they have not been documented on-line yet. However, it has been experienced that the return sludge flow must be reduced proportionally by the length of the aerator stop periods to maintain constant concentration in return sludge (Nielsen and Önnerth, 1995), so a significant but smaller effect will be obtained.

Discussion

It is seen that the proposed model is qualitatively correct. Its quantification is sufficient for most control, however there are some empirical constants, which are only adjustable from practical fitting based on on-line data. Although these constants are explained above, as having a physical meaning, they are only found from data fitting to experiences during rain events.

However, experiences show that the model can be transferred from one plant to another. Only small adjustments, and update to actual MLSS concentration and SVI is needed, hence practical experiences from one plant can be transferred to another similar plant, and the on-line update can be obtained from the first rain event experiences.

By use of the model and the prediction of flow from rain gauges or sewer system it is possible to predict the needed efficiency of the ATS control and optimize the organic versus hydraulic capacity of the plant.

Conclusion

Aeration tank settling is a robust and reliable technique, which by use of models can be designed and controlled to perform efficiently, in alternating plants to increase their hydraulic capacity with 30 - 100% within a few hours.

The use of the same model methodology can predict the hydraulic capacity for recirculating plants. When further experiences of the methodology of the settling sludge and recirculation of the sludge are collected from full-scale, the standard design technique will be extended to cover most plug flow and other recirculating activated sludge plants too.

Acknowledgements

We thank our co-operators within the EUREKA projects MUST and SIMBIOSE from the Department of Mathematical Modelling, Department of Environmental Science and Engineering at the Technical University of Denmark, for their support and co-operation.

Paper E

Grey-box modelling of aeration tank settling.

Submitted.

E

Abstract

A model of the concentrations of suspended solids (SS) in the aeration tanks and in the effluent from these during Aeration Tank Settling (ATS) operation is established. The model is based on simple SS mass balances, a model of the sludge settling and a simple model of how the SS concentration in the effluent from the aeration tanks depends on the actual concentrations in the tanks and the sludge blanket depth.

The model is formulated in continuous time by means of stochastic differential equations with discrete-time observations. The parameters of the model are estimated using a maximum likelihood method from data from an alternating BioDenipho wastewater treatment plant (WWTP).

The model is an important tool for analyzing ATS operation and for selecting the appropriate control actions during ATS, as the model can be used to predict the SS amounts in the aeration tanks as well as in the effluent from the aeration tanks.

Key words: Aeration Tank Settling, mass balance, grey-box models, statistical identification, on-line measurements.

Introduction

With the introduction of advanced optimising control systems at wastewater treatment plants (Nielsen and Önnerth, 1995; Önnerth and Bechmann, 1995) the demand for mathematical models of the important processes in wastewater treatment plants is increased. The Aeration Tank Settling (ATS) principle introduces settling periods in aeration tanks of alternating plants and enables increased amounts of suspended solids (SS) to be stored in the aeration tanks during rain storms. ATS increases the hydraulic capacity of the WWTP, but complicates the prediction of the SS concentration in the effluent from the aeration tanks, compared to dry weather operation. During dry weather operation the aeration tanks are fully mixed, and the SS concentrations in the effluent are equal to the SS concentrations in the tanks, but during ATS operation the effluent comes from an aeration tank where the sludge settles. Hence, the SS concentrations in and out of the aeration tanks are not equal during ATS operation.

To minimize the amounts of SS in the effluent, predictive models of the SS concentrations are needed. In Nielsen et al. (1999), a model of SS in the aeration tanks and in the effluent from these is proposed. The model consists of 3 submodels: 1) A simple mass balance model for the SS concentrations in the aeration tanks, 2) a sludge settling model and 3) a model for the SS concentration in the effluent from the aeration tanks. Here, the model is reformulated by means of stochastic differential equations, and the parameters are estimated by a maximum likelihood method.

Vesilind (1968, 1979) proposed a sludge settling velocity model of exponential form. During recent years, several refinements to the original model have been proposed, see e.g. Grijspeerdt et al. (1995); Dupont and Dahl (1995); Ekama et al. (1997). In the proposed models several layers in the settling tank are incorporated to permit the calculation of SS profiles over the tank depth and predict the SS concentrations in the return sludge and in the effluent from the clarifier.

Here, the original Vesilind model combined with a simple suction depth model is used to enable prediction of the SS concentration in the effluent from the aeration tank. In order to make the model applicable for real time control purposes, only two layers of variable height in the aeration tank are considered.

Dry weather and ATS operation

In an alternating WWTP, the aeration tanks are composed of pairs of interconnected tanks. The wastewater is directed to one of the tanks, through the connection between the tanks and out of the second tank. In dry weather situations the tanks are fully mixed to enable optimal nutrient removal. The incoming wastewater is directed to an aeration tank with anoxic conditions, and thus with denitrification. The other tank from which the effluent is taken is aerated and is hence a tank with nitrification. Depending on the state of the processes in the aeration tanks, the flow path is changed.

During rain storms ATS operation is activated. When the WWTP is in ATS operation, the aeration scheme is changed so that the influent is directed to an aerobic nitrification tank, and the effluent is taken from an anoxic denitrification tank. When the mixers are switched off in the anoxic tank, settling occurs. When the sludge settles in the tank that discharges to the clarifier, the SS concentration in the effluent is lower than the average concentration in the aeration tank. Hereby more SS can be kept in the aeration tanks compared to dry weather operation at the same time as the SS load to the clarifier is decreased.

It is crucial that as much SS as possible is kept in the aeration tanks during the rain storm and not transported to the clarifier, as an increased SS concentration in the aeration tank effluent will limit the hydraulic capacity of the clarifiers, and thus lead to an SS increase in the effluent to the receiving waters.

By introducing intermediate phases with settling and anoxic conditions in both tanks, the SS concentrations in the effluent from the aeration tanks can be further reduced. By proper control of the flow path and the settling, the SS concentration out of the aeration tanks can be optimized, so that the control does not limit the organic capacity of the plant unnecessarily.

Based on measurements and predictions of the influent flow to the WWTP the ATS operation is activated. The use of flow predictions makes it possible to prepare the plant for the increased storm flow, before the storm water actually enters the WWTP. At Aalborg West WWTP, from where the data used here originates, the influent flow prediction horizon is approximately one hour. Before the influent flow is increased, the recirculation of sludge from the secondary clarifiers to the aeration tanks is increased. Hereby SS is decreased in the clarifiers and increased in the aeration tanks. Furthermore, the hydraulic load to the aeration tanks and clarifiers is increased. When the storm water arrives at the plant, the recirculation flow is decreased to a lower level.

Theory

In Figure 1 the flow through the aeration tanks and clarifiers is illustrated. The black and grey lines illustrate alternative flow paths through the aeration tanks. The influent flow and the recirculation flow are denoted Q_{i} and Q_{r}, respectively. X_{ssi}, X_{ssr} and X_{ssoutat} denote SS concentrations in the influent, the return sludge and the effluent from the aeration tanks to the secondary

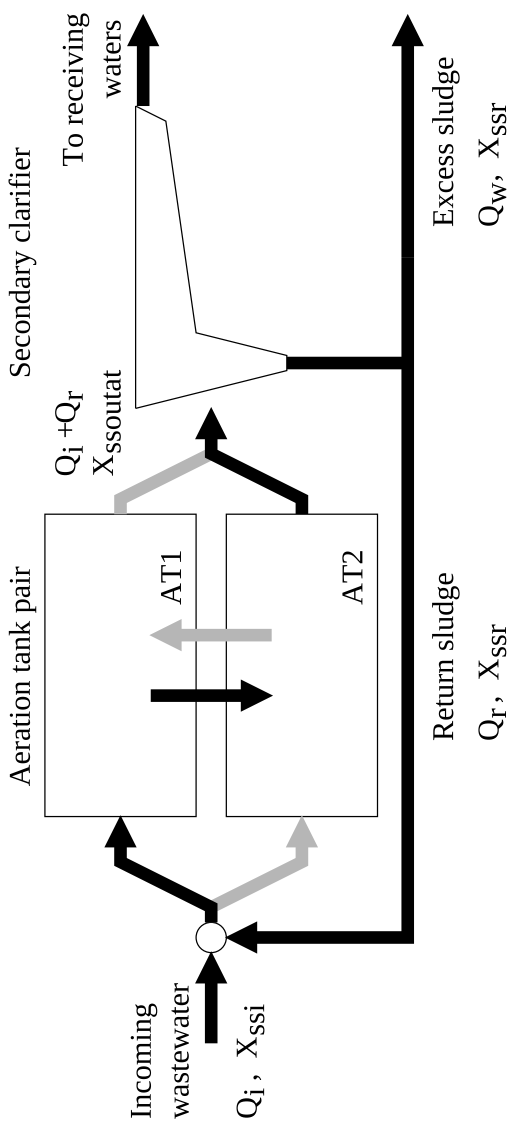

Figure 1. Flow path through aeration tank pair in an alternating WWTP.

clarifers. The dynamics of the water amounts in the aerations tanks are not considered, i.e. it is assumed that the flows to and from each of the aeration tanks are the same ($Q_\mathrm{i} + Q_\mathrm{r}$). Furthermore, the SS concentration in the flow between the two aeration tanks is assumed to be the average SS concentration in the feeding tank. When the feeding tank is fully mixed, this assumption is fulfilled, but when settling occurs it is an approximation.

The mass balance equations for each of the aeration tanks depend on the actual flow path designated f_p. When $f_\mathrm{p} = 1$ the influent flow is directed to aeration tank 1, and the effluent flow is taken from tank 2. f_p is 0 when the opposite flow path is applied. With V_at, X_ssm1 and X_ssm2 denoting the volume of each of the equally sized aeration tanks and the average SS concentrations in tank 1 and 2, respectively, the mass balance equations can be established.

For $f_\mathrm{p} = 1$ the mass balance equations for the aeration tanks are:

$$\frac{dX_\mathrm{ssm1}}{dt} = \frac{Q_\mathrm{i}X_\mathrm{ssi} + Q_\mathrm{r}X_\mathrm{ssr} - (Q_\mathrm{i} + Q_\mathrm{r})X_\mathrm{ssm1}}{V_\mathrm{at}} \quad (1)$$

$$\frac{dX_\mathrm{ssm2}}{dt} = \frac{(Q_\mathrm{i} + Q_\mathrm{r})X_\mathrm{ssm1} - (Q_\mathrm{i} + Q_\mathrm{r})X_\mathrm{ssoutat}}{V_\mathrm{at}} \quad (2)$$

For $f_\mathrm{p} = 0$ the mass balance equations are:

$$\frac{dX_\mathrm{ssm1}}{dt} = \frac{(Q_\mathrm{i} + Q_\mathrm{r})X_\mathrm{ssm2} - (Q_\mathrm{i} + Q_\mathrm{r})X_\mathrm{ssoutat}}{V_\mathrm{at}} \quad (3)$$

$$\frac{dX_\mathrm{ssm2}}{dt} = \frac{(Q_\mathrm{i}X_\mathrm{ssi} + Q_\mathrm{r}X_\mathrm{ssr}) - (Q_\mathrm{i} + Q_\mathrm{r})X_\mathrm{ssm2}}{V_\mathrm{at}} \quad (4)$$

The flow path variable can be used to combine equation (1) with (3) and equation (2) with (4) into one equation per aeration tank:

$$\begin{aligned}\frac{dX_\mathrm{ssm1}}{dt} = {} & f_\mathrm{p}\frac{Q_\mathrm{i}X_\mathrm{ssi} + Q_\mathrm{r}X_\mathrm{ssr} - (Q_\mathrm{i} + Q_\mathrm{r})X_\mathrm{ssm1}}{V_\mathrm{at}} \\ & + (1 - f_\mathrm{p})\frac{(Q_\mathrm{i} + Q_\mathrm{r})X_\mathrm{ssm2} - (Q_\mathrm{i} + Q_\mathrm{r})X_\mathrm{ssoutat}}{V_\mathrm{at}}\end{aligned} \quad (5)$$

and:

$$\begin{aligned}\frac{dX_\mathrm{ssm2}}{dt} = {} & f_\mathrm{p}\frac{(Q_\mathrm{i} + Q_\mathrm{r})X_\mathrm{ssm1} - (Q_\mathrm{i} + Q_\mathrm{r})X_\mathrm{ssoutat}}{V_\mathrm{at}} \\ & + (1 - f_\mathrm{p})\frac{(Q_\mathrm{i}X_\mathrm{ssi} + Q_\mathrm{r}X_\mathrm{ssr}) - (Q_b + Q_\mathrm{r})X_\mathrm{ssm2}}{V_\mathrm{at}}\end{aligned} \quad (6)$$

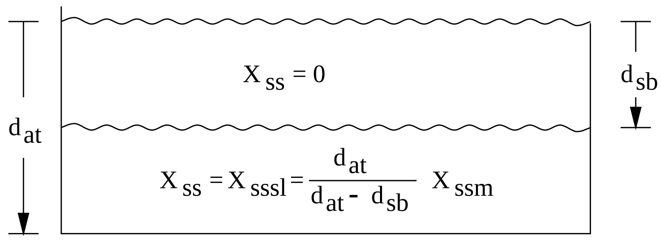

Figure 2. Two layer model of settling in an aeration tank.

When mixing is stopped in an aeration tank, the suspended solids settle. A simple two layer model, where the water in the layer above the sludge blanket is assumed to be clear water, and the layer under the sludge blanket is assumed to contain all the SS fully mixed, is used. The settling velocity for the sludge blanket is modelled according to Vesilind (1968) as:

$$\frac{dd_{\mathrm{sb}}}{dt} = V_0\,\mathrm{e}^{-n_{\mathrm{v}} X_{\mathrm{sssl}}} \tag{7}$$

where d_{sb} and X_{sssl} denote the sludge blanket depth and the SS concentration in the sludge layer, respectively, see Figure 2, and V_0 and n_{v} are sludge volume index (SVI) dependent parameters. For simplicity we use the expressions found by Härtel and Pöpel (1992):

$$\begin{aligned} V_0 &= (17.4\,\mathrm{e}^{-0.0113 SVI} + 3.931)\frac{\mathrm{m}}{\mathrm{h}} \\ n_{\mathrm{v}} &= (-0.9834\,\mathrm{e}^{-0.00581 SVI} + 1.043)\frac{\mathrm{l}}{\mathrm{g}} \end{aligned} \tag{8}$$

If sludge blanket depth measurements are available, V_0 and n_{v} can be estimated.

As the volume of the sludge layer is $(d_{\mathrm{at}} - d_{\mathrm{sb}})V_{\mathrm{at}}/d_{\mathrm{at}}$, the average SS concentration in the sludge layer is:

$$X_{\mathrm{sssl}} = \frac{d_{\mathrm{at}}}{d_{\mathrm{at}} - d_{\mathrm{sb}}} X_{\mathrm{ssm}} \tag{9}$$

where X_{ssm} is the average SS concentration in the aeration tank.

When the tank is fully mixed, the sludge blanket depth is 0. When mixing is switched on d_{sb} tends towards zero, which is modelled by:

$$\frac{dd_{\text{sb}}}{dt} = -\frac{1}{\tau_{\text{mix}}} d_{\text{sb}} \tag{10}$$

where τ_{mix} is a mixing capacity dependent time constant.

Introduce the mixing signals m_1 and m_2 for aeration tank 1 and 2, respectively. The mixing signals are 1 when the corresponding aeration tank is mixed and 0 otherwise. The signals can then be used to combine the settling equation (7) with the mixing equation (10) for each of the aeration tanks:

$$\begin{aligned}\frac{dd_{\text{sb1}}}{dt} &= l(m_1)(-\frac{1}{\tau_{\text{mix}}} d_{\text{sb1}}) \\ &\quad + (1 - l(m_1)) V_0 \, \mathrm{e}^{-n_{\text{v}} X_{\text{sssl1}}}\end{aligned} \tag{11}$$

and:

$$\begin{aligned}\frac{dd_{\text{sb2}}}{dt} &= l(m_2)(-\frac{1}{\tau_{\text{mix}}} d_{\text{sb2}}) \\ &\quad + (1 - l(m_2)) V_0 \, \mathrm{e}^{-n_{\text{v}} X_{\text{sssl2}}}\end{aligned} \tag{12}$$

Here, the aeration tank number is introduced on the sludge blanket depth and average SS concentration variables so that d_{sb1}, d_{sb2}, X_{sssl1} and X_{sssl1} designates the sludge blanket depths and average SS concentrations in aeration tank 1 and 2, respectively.

The SS concentration in the effluent from an aeration tank is modelled as a function of the suction depth, d_{suct} and the SS concentration in the sludge layer:

$$X_{\text{ssoutat}} = \begin{cases} \frac{d_{\text{suct}} - d_{\text{sb}}}{d_{\text{suct}}} X_{\text{sssl}} & \text{for } d_{\text{suct}} \geq d_{\text{sb}} \\ 0 & \text{otherwise} \end{cases} \tag{13}$$

The suction depth is expected to depend on the flow and is modelled as:

$$d_{\text{suct}} = d_0 \left(\frac{Q_{\text{i}} + Q_{\text{r}}}{Q_0} \right)^{b_{\text{suct}}} \tag{14}$$

where d_0 and b_{suct} are positive parameters and $Q_0 = 1000 \text{ m}^3/\text{h}$. Combining

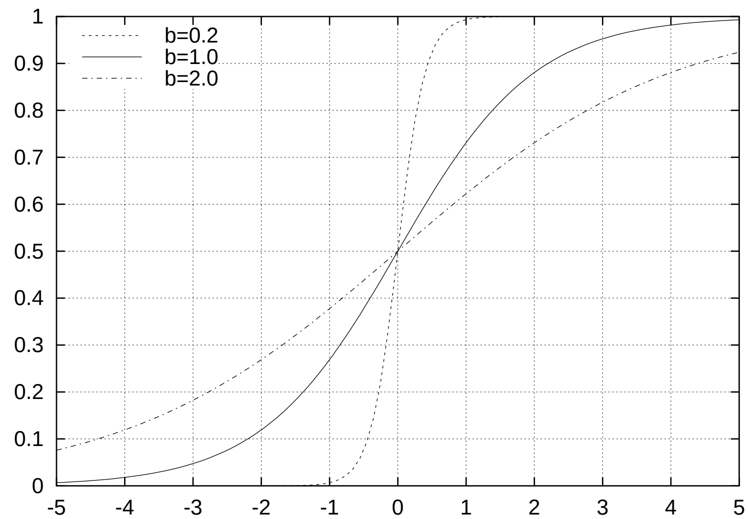

Figure 3. The logistic function for $a = 0$ and different b values.

(9) and (13) yields

$$\begin{aligned} X_{\text{ssoutat}} &= \frac{d_{\text{suct}} - d_{\text{sb}}}{d_{\text{suct}}} \frac{d_{\text{at}}}{d_{\text{at}} - d_{\text{sb}}} X_{\text{ssm}} \\ &= \frac{1 - d_{\text{sb}}/d_{\text{suct}}}{1 - d_{\text{sb}}/d_{\text{at}}} X_{\text{ssm}} \qquad \text{for } d_{\text{suct}} > d_{\text{sb}} \end{aligned} \tag{15}$$

To enable smooth changes in X_{ssoutat} when the point $d_{\text{suct}} = d_{\text{sb}}$ is passed a smooth threshold function is introduced. Here, the logistic function:

$$l(x) = l(x, a, b) = \frac{1}{1 + \mathrm{e}^{\frac{a-x}{b}}} \tag{16}$$

is used. For $x = a$ the logistic function is 0.5, i.e. the value of a determines the midpoint of the switch between 0 and 1. By appropriate selection of a and b the change between 0 and 1 of $l(x, a, b)$ can be controlled. In Figure 3 the logistic function is shown for $a = 0$ and 3 different values of b. In the following $b > 0$ is assumed.

The logistic function (16) is used to calculate X_{ssoutat} while the flow path variable is used select the discharge tank:

$$\begin{aligned} X_{\text{ssoutat}} = f_{\text{p}} &\left(l(d_{\text{suct}} - d_{\text{sb2}}) \frac{1 - d_{\text{sb2}}/d_{\text{suct}}}{1 - d_{\text{sb2}}/d_{\text{at}}} X_{\text{ssm2}} \right) \\ &(1 - f_{\text{p}}) \left(l(d_{\text{suct}} - d_{\text{sb1}}) \frac{1 - d_{\text{sb1}}/d_{\text{suct}}}{1 - d_{\text{sb1}}/d_{\text{at}}} X_{\text{ssm1}} \right) \end{aligned} \tag{17}$$

As d_{suct} is only dependent on the flow, there is no need to consider different suction depths for each of the aeration tanks.

In order to use a matrix notation, introduce the state vector $\boldsymbol{X}$, the input vector $\boldsymbol{U}$ and the observation vector $\boldsymbol{Y}$:

$$\begin{aligned} \boldsymbol{X} &= [X_{\text{ssm1}}, X_{\text{ssm2}}, d_{\text{sb1}}, d_{\text{sb2}}]' \\ \boldsymbol{U} &= [f_{\text{p}}, m_1, m_2, X_{\text{ssr}}, Q_{\text{i}}, Q_{\text{r}}]' \\ \boldsymbol{Y} &= [X_{\text{ssm2}}, X_{\text{ssoutat}}]' \end{aligned} \tag{18}$$

Here, it is assumed that aeration tank 2 is equipped with a suspended solids sensor.

By use of the vector function $\boldsymbol{f}(\boldsymbol{X}, \boldsymbol{U}, t)$ the mass balances and sludge blanket depth equations can be expressed in a vector differential equation:

$$\frac{d\boldsymbol{X}(t)}{dt} = \boldsymbol{f}(\boldsymbol{X}, \boldsymbol{U}, t) \tag{19}$$

where $\boldsymbol{f}(\boldsymbol{X}, \boldsymbol{U}, t)$ is easily constructed from equations (5)–(12) and (18).

The measurements are described by the observation equation

$$\boldsymbol{Y}(t) = \boldsymbol{h}(\boldsymbol{X}, \boldsymbol{U}, t) \tag{20}$$

where $\boldsymbol{h}(\boldsymbol{X}, \boldsymbol{U}, t)$ is constructed from equations (17) and (18).

To count in uncertainties in the model formulation and to enable use of the maximum likelihood parameter estimation method, stochastic noise terms are introduced. Hence, equation (19) turns into a stochastic differential equation, where the continuous time equations describing the mass balances and the sludge blanket depths in the aeration tanks can be written as the so-called Itô differential equation (Øksendal, 1995):

$$d\boldsymbol{X}(t) = \boldsymbol{f}(\boldsymbol{X}, \boldsymbol{U}, t)\, dt + \boldsymbol{G}(\boldsymbol{X}, \boldsymbol{U}, t)\, d\boldsymbol{w}(t) \tag{21}$$

where the stochastic process $\boldsymbol{w}(t)$ is assumed to be a standard vector Wiener process (see e.g. Kloeden and Platen (1995)). The function $\boldsymbol{G}(\boldsymbol{X},\boldsymbol{U},t)$ describes any state, input or time dependent variation related to how the variation generated by the Wiener process enters the system.

Here, $\boldsymbol{G}$ is assumed to be a constant diagonal matrix:

$$\boldsymbol{G}(\boldsymbol{X},\boldsymbol{U},t) = \boldsymbol{G} = \begin{bmatrix} \sigma_{\text{ss}} & 0 & 0 & 0 \\ 0 & \sigma_{\text{ss}} & 0 & 0 \\ 0 & 0 & \sigma_{\text{sb}} & 0 \\ 0 & 0 & 0 & \sigma_{\text{sb}} \end{bmatrix} \tag{22}$$

Hereby, the covariance of $\boldsymbol{G}\,d\boldsymbol{w}(t)$ becomes

$$\boldsymbol{\Sigma} = \boldsymbol{G}\boldsymbol{G}' = \begin{bmatrix} \sigma_{\text{ss}}^2 & 0 & 0 & 0 \\ 0 & \sigma_{\text{ss}}^2 & 0 & 0 \\ 0 & 0 & \sigma_{\text{sb}}^2 & 0 \\ 0 & 0 & 0 & \sigma_{\text{sb}}^2 \end{bmatrix} \tag{23}$$

The observation uncertainties are included in the observation equation:

$$\boldsymbol{Y}(t) = \boldsymbol{h}(\boldsymbol{X},\boldsymbol{U},t) + \boldsymbol{e}(t) \tag{24}$$

where the term $\boldsymbol{e}(t)$ is the measurement error, which is assumed to be a zero mean Gaussian white noise sequence independent of $\boldsymbol{w}(t)$ and with covariance matrix:

$$V(\boldsymbol{e}(t)) = \begin{bmatrix} \sigma_{\text{ss2}}^2(t) & 0 \\ 0 & \sigma_{\text{ssoutat}}^2(t) \end{bmatrix} \tag{25}$$

Estimation method

The method used to estimate the parameters of the model (21)–(22) and (24) is a maximum likelihood method for estimating parameters in stochastic differential equations based on discrete-time data given by (24). For a more detailed description of the method refer to Madsen and Melgaard (1991) or Melgaard and Madsen (1993).

All the unknown parameters, denoted by the vector $\boldsymbol{\theta}$, are embedded in the continuous-discrete time state space model (21) and (24).

The measurements are given in discrete time, and, in order to simplify the notation, it is assumed that the time index t belongs to the set $\{0, 1, 2, ..., N\}$, where N is the number of observations. Introducing

$$\mathcal{Y}(t) = [\boldsymbol{Y}(t), \boldsymbol{Y}(t-1), \ldots, \boldsymbol{Y}(1), \boldsymbol{Y}(0)]' \tag{26}$$

i.e. $\mathcal{Y}(t)$ is a vector containing all the observations up to and including time t, the likelihood function is the joint probability density of all the observations assuming that the parameters are known, i.e.

$$\begin{aligned} L'(\boldsymbol{\theta}; \mathcal{Y}(N)) &= p(\mathcal{Y}(N)|\boldsymbol{\theta}) \\ &= p(\boldsymbol{Y}(N)|\mathcal{Y}(N-1), \boldsymbol{\theta}) p(\mathcal{Y}(N-1)|\boldsymbol{\theta}) \\ &= \left(\prod_{t=1}^{N} p(\boldsymbol{Y}(t)|\mathcal{Y}(t-1), \boldsymbol{\theta}) \right) p(\boldsymbol{Y}(0)|\boldsymbol{\theta}) \end{aligned} \tag{27}$$

where successive applications of the rule $P(A \cap B) = P(A|B)P(B)$ are used to express the likelihood function as a product of conditional densities.

In order to evaluate the likelihood function it is assumed that all the conditional densities are Gaussian. In the case of a linear state space model, it is easily shown that the conditional densities actually are Gaussian (Madsen and Melgaard, 1991). In the more general non-linear case, as described by (21) and (24), the Gaussian assumption is an approximation.

The Gaussian distribution is completely characterized by the mean and covariance. Hence, in order to parameterize the conditional densities in (27), we introduce the conditional mean and the conditional covariance as

$$\begin{aligned} \hat{\boldsymbol{Y}}(t|t-1) &= E[\boldsymbol{Y}(t)|\mathcal{Y}(t-1), \boldsymbol{\theta}] \quad \text{and} \\ \boldsymbol{R}(t|t-1) &= V[\boldsymbol{Y}(t)|\mathcal{Y}(t-1), \boldsymbol{\theta}] \end{aligned} \tag{28}$$

respectively. It should be noted that these correspond to the one-step prediction and the associated covariance, respectively. Furthermore, it is convenient to introduce the one-step prediction error (or innovation)

$$\boldsymbol{\epsilon}(t) = \boldsymbol{Y}(t) - \hat{\boldsymbol{Y}}(t|t-1) \tag{29}$$

For calculating the one-step prediction and its variance, an iterated extended Kalman filter is used. The extended Kalman filter is simply based on a linearization of the system equation (21) around the current estimate of the state (see Gelb (1974)). The iterated extended Kalman filter is obtained by local iterations of the linearization over a single sample period.

Using (27) – (29) the conditional likelihood function (conditioned on $\boldsymbol{Y}(0)$) becomes

$$\begin{aligned} &L(\boldsymbol{\theta}; \mathcal{Y}(N)) \\ &= \prod_{t=1}^{N} \Big((2\pi)^{-m/2} \det \boldsymbol{R}(t|t-1)^{-1/2} \exp(-\tfrac{1}{2} \boldsymbol{\epsilon}(t)' \boldsymbol{R}(t|t-1)^{-1} \boldsymbol{\epsilon}(t)) \Big) \end{aligned} \tag{30}$$

where m is the dimension of the $\boldsymbol{Y}$ vector. Traditionally the logarithm of the conditional likelihood function is considered

$$\begin{aligned} &\log L(\boldsymbol{\theta}; \mathcal{Y}(N)) \\ &= -\tfrac{1}{2} \sum_{t=1}^{N} \Big(\log \ \det \boldsymbol{R}(t|t-1) + \boldsymbol{\epsilon}(t)' \boldsymbol{R}(t|t-1)^{-1} \boldsymbol{\epsilon}(t) \Big) + \text{const} \end{aligned} \tag{31}$$

The maximum likelihood estimate (ML-estimate) is the set $\hat{\boldsymbol{\theta}}$, which maximizes the likelihood function. Since it is not, in general, possible to optimize the likelihood function analytically, a numerical method has to be used. A reasonable method is the quasi-Newton method.

An estimate of the uncertainty of the parameters is obtained by the fact that the ML-estimator is asymptotically normally distributed with mean $\boldsymbol{\theta}$ and covariance

$$\boldsymbol{D} = \boldsymbol{H}^{-1} \tag{32}$$

where the matrix $\boldsymbol{H}$ is given by

$$\{h_{lk}\} = -E\left[\frac{\partial^2}{\partial\theta_l \partial\theta_k} \log L(\boldsymbol{\theta}; \mathcal{Y}(N)) \right] \tag{33}$$

An estimate of $\boldsymbol{D}$ is obtained by equating the observed value with its expectation and applying

$$\{h_{lk}\} \approx -\left(\frac{\partial^2}{\partial\theta_l \partial\theta_k} \log L(\boldsymbol{\theta}; \mathcal{Y}(N)) \right)_{|\theta=\hat{\theta}} \tag{34}$$

The above equation can be used for estimating the variances of the parameter estimates. The variances serves as a basis for calculating t-test values for tests under the hypothesis that the parameter is equal to zero. Finally, the correlation between the parameter estimates is readily found based on the covariance matrix $\boldsymbol{D}$.

Unreliable measurements are handled by adjusting the variance of $\boldsymbol{e}(t)$. When an unreliable observation is encountered, the corresponding observation variance is considerably increased. As the extended Kalman filter uses the observation noise variance and the intensity of the Wiener process, that count for state noise, the unreliable observations are taken into account by the estimation procedure.

Results and discussion

Aalborg West WWTP, from where the data used for the estimations originates, has three aeration tank pairs, which are controlled in an identical way, except for a time delay between the tank pairs. The master tank pair consists of aeration tanks 5 and 6, of which tank 6 is equipped with an SS sensor. The flow path and mixing of tanks 3 and 4 are delayed $T_d = 12$ min in relation to tanks 5 and 6, and tank 1 and 2 are delayed further T_d. To include all 6 aeration tanks in the model, it is extended with equations for the 4 additional tanks. The flows to and from each tank pair are reduced to a third of the total flows, and the time delay between the tank pairs is taken into account in the flow path and mixing signals to the respective tank pairs. The resulting SS concentration out of the aeration tanks is the average of the SS concentrations out of the 3 tank pairs. The Aalborg West WWTP model is thus a 12 state non-linear model with 2 observations, X_{ssm6} and X_{ssoutat}.

The measurements of the average SS concentration in aeration tank 6 are only reliable when the tank is fully mixed. This is taken into account by adjusting the variance of $\boldsymbol{e}(t)$ according to the mixing of aeration tank 6. When the tank is not mixed, $\sigma^2_{\text{ss6}}(t)$ is large (ideally ∞) compared to the value of $\sigma^2_{\text{ss6}}(t)$ when the tank is mixed.

Aalborg West WWTP is equipped with a STAR (Superiour Tuning And Reporting) control system (Nielsen and Önnerth, 1995; Önnerth and Bechmann, 1995), which optimizes the operation of the plant. In the STAR system, measurements are fetched and control actions are computed every 6 minutes. This turned out to be a too short sampling time for the estimation procedure, hence, the data was re-sampled to a longer sampling period. Furthermore, it turned out that there was a significant time delay between the input variables (the flow direction, the mixing signals and the flows and concentrations to the aeration tanks) and the output variables (SS concentrations in aeration tank 6 and out of the aeration tanks). The time delay was found to be 0.8 h, and the new sampling interval selected was 0.2 h.

The parameters of the model were estimated on one data set and the resulting model was cross validated on another data set. It was not possible to estimate the sludge settling model parameters V_0 and n_v and the parameters of the suction depth model d_0 and b_suct simultaneously. This is due to the fact that these two sub-models are closely correlated, as a change in the sludge settling model will be compensated by an equivalent change in the suction depth model. The SVI for the estimation data set was 142, hence the sludge settling parameters found from (8) are

$$V_0 = 7.43 \text{ m/h} \quad \text{and} \quad n_v = 0.612 \text{ m}^3\text{/kg SS} \tag{35}$$

The SVI for the validation data set was 177, which gives the corresponding sludge settling parameters

$$V_0 = 6.29 \text{ m/h} \quad \text{and} \quad n_v = 0.691\text{m}^3\text{/kg SS} \tag{36}$$

By inspecting the data before the estimation was carried out, systematic errors in the SS concentration measurements were observed. As it is not possible from the available measurements to detect which of the measurements that are correct, it was decided to use X_ss6 as the reference. The errors on the measurements of X_ssoutat were included in the model as offset errors, even though other methods could be applied. For the errors in the return sludge measurements both an additive and a multiplicative form were tried out. It was found that both types gave similar results, and the multiplicative form was used in the final estimations. The bias on X_ssoutat designated $X_\mathrm{ssout,b}$ and the factor on X_ssr designated $X_\mathrm{ssr,f}$ were estimated simultaneously with the other parameters.

The influent SS concentration X_ssi was sought estimated as constant during the period considered. This parameter was, however, found to be insignificant, and therefore excluded from the final estimation.

The estimated parameters as well as their estimated standard deviations are

Parameter	d_0	b_{suct}	$X_{\mathrm{ssr,f}}$	$X_{\mathrm{ssout,b}}$	σ^2_{ss}	σ^2_{sb}	σ^2_{ss6}	$\sigma^2_{\mathrm{ssoutat}}$
Unit	m	–	–	g/l	$(\mathrm{g/l})^2$	m^2	$(\mathrm{g/l})^2$	$(\mathrm{g/l})^2$
Estimate	1.005	0.164	1.129	0.143	0.0259	1.34	$1.91\ 10^{-4}$	$1.78\ 10^{-7}$
Standard deviation	0.015	0.022	0.009	0.014	0.0038	0.09	$0.28\ 10^{-4}$	$2.08\ 10^{-7}$

Table 1. Maximum likelihood estimates of the parameters of the model.

shown in Table 1. All the parameters except $\sigma^2_{\text{ssoutat}}$ are estimated with small standard deviations. The estimate of $\sigma^2_{\text{ssoutat}}$ is thus uncertain.

The measured and modelled SS concentrations are shown in Figures 4 and 5, for a part of the estimation data set and the validation data set, respectively. The mixing signal for aeration tank 6 is included in the X_{ss6} graphs to indicate the validity of the X_{ss6} measurements, as these are only reliable when mixing is on. Note that the modelled SS concentrations are simulations based only on the input variables to the model, and not one-step ahead predictions, which use the measurements of the output variables at every time step to predict the output at the next time step.

For the validation data set the V_0 and n_{v} parameters for both $SVI = 142$ (the estimation data set value) and $SVI = 177$ (the validation data set value) were tried. The best result was obtained with the parameter values for the estimation data set, hence, these values were used to make the graphs. The fact that the values of V_0 and n_{v} for the estimation data set performed better with the validation data set indicates that the sludge settling model, the suction depth model and the X_{ssoutat} model are interdependent. These should thus be regarded as a single sub-model, and not independent sub-models. The model is found to perform well as regards the SS concentrations in aeration tank 6 for both the estimation data set and the validation data set. The simulated SS concentrations in the effluent from the aeration tanks are not as good for the validation data set as for the estimation data set. This indicates that the combined model consisting of the sludge settling model, the suction depth model and the X_{ssoutat} model could be refined.

The estimation method relies on the assumption that the observation noise is white. The validity of this assumption is checked by use of cumulative residual periodograms, see Figs. 6 and 7. As only the observations of X_{ss6} in aerated periods are reliable, the non-aerated periods result in residuals that can not be considered to be generated by a white noise process. Hence, the cumulative residual periodograms are shown only for the X_{ssoutat} observations. The confidence limits for the periodograms are calculated using the Kolmogorov-Smirnov test principle (Kendall and Stuart, 1979; Box and Jenkins, 1976). As the periodograms are between the confidence limits, the X_{ssoutat} residuals can be considered to be white noise. Note that the confidence band for the validation data is wider than for the estimation data. This is caused by the fact that the estimation data set contains more observations than the validation data set.

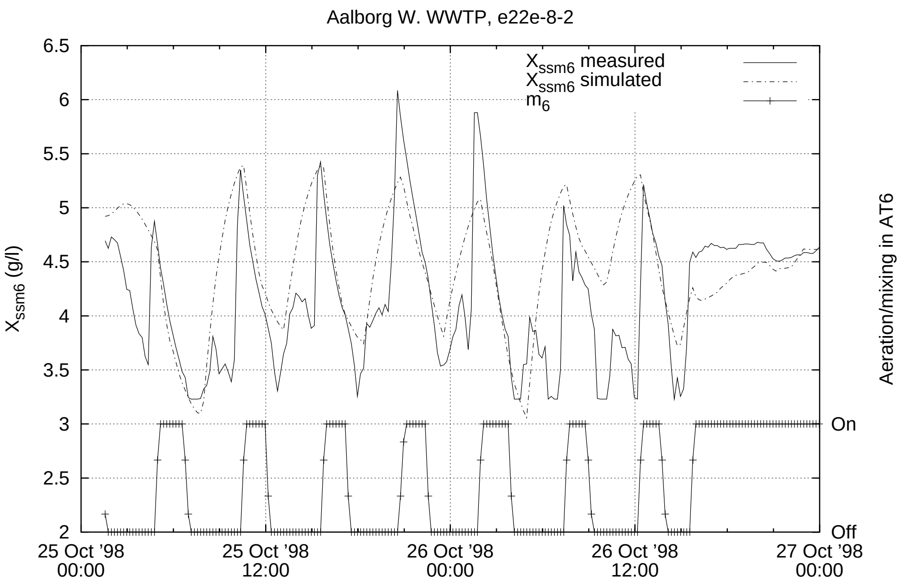

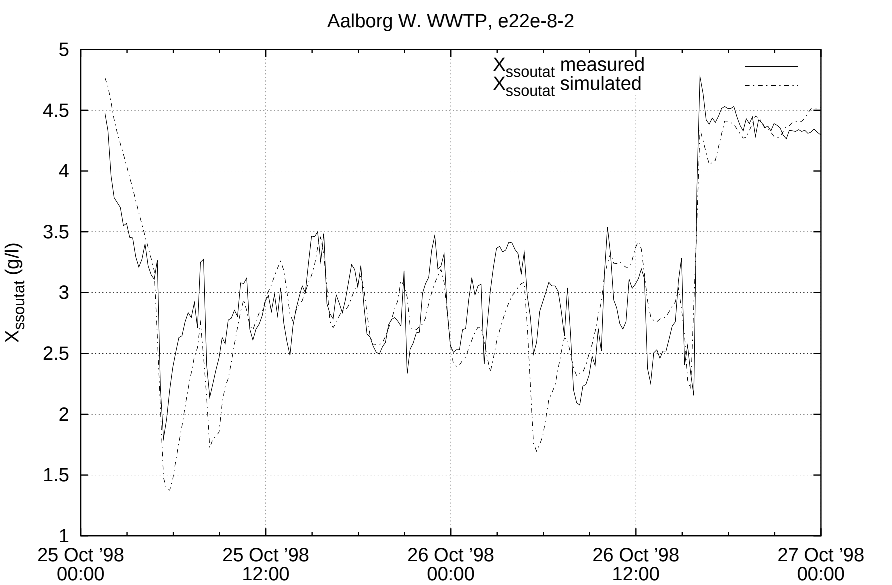

Figure 4. Measured and simulated SS concentrations in aeration tank 6 and in the effluent from the aeration tanks, estimation data set.

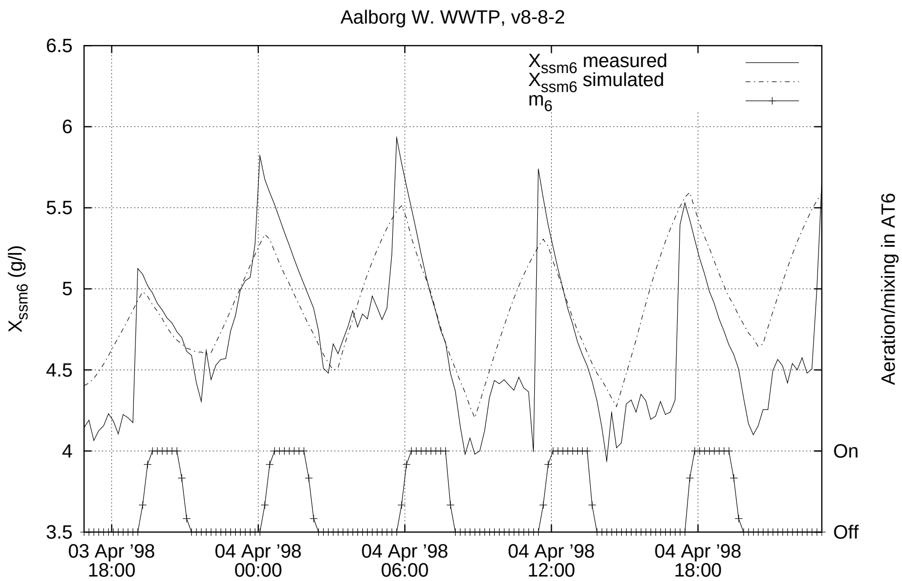

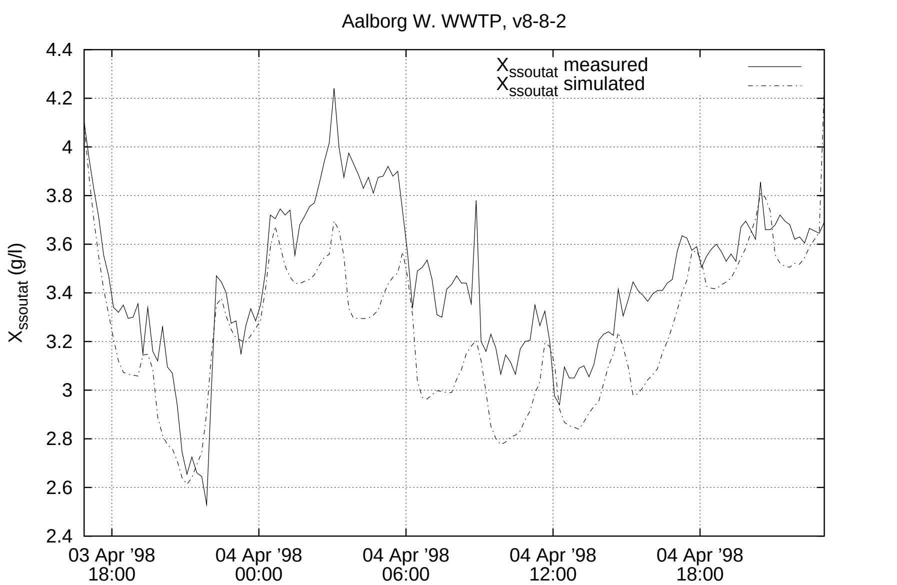

Figure 5. Measured and simulated SS concentrations in aeration tank 6 and in the effluent from the aeration tanks, validation data set.

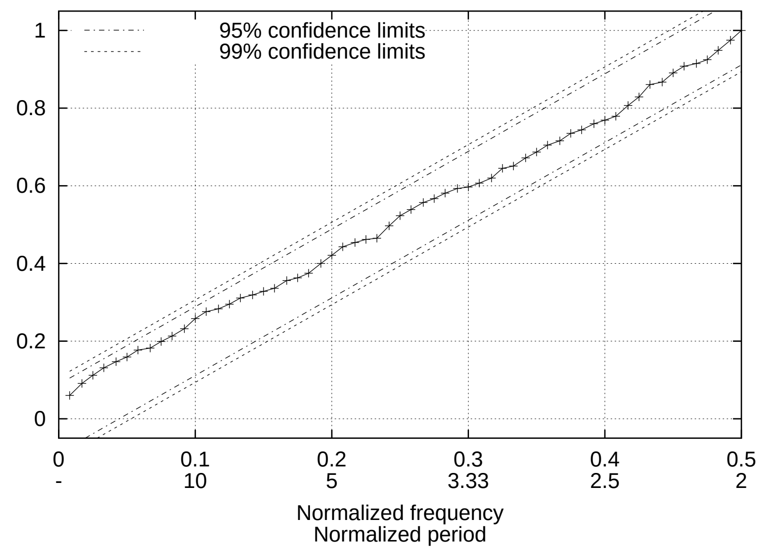

Figure 6. Cumulative residual periodogram for X_{ssoutat} with 95% and 99% confidence limits, estimation data set.

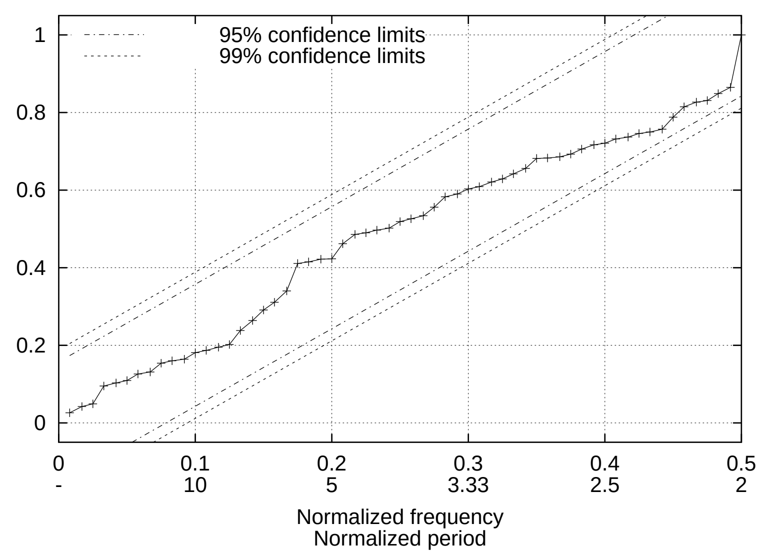

Figure 7. Cumulative residual periodogram for X_{ssoutat} with 95% and 99% confidence limits, validation data set.

Conclusions

A model for the SS concentrations in and out of the aeration tanks in an alternating WWTP is proposed, and the parameters are estimated using the maximum likelihood method.

The estimated model shows good agreement between simulated and measured SS concentrations in the aeration tanks and in the effluent from these at Aalborg West WWTP. However, improvements are still possible. The sub-models for the sludge settling velocity, the suction depth and the SS concentration out of the aeration tanks are subjects for refinements, and the model should be tested under conditions with more flow variation as well as at other WWTPs. Furthermore, the inclusion of the secondary clarifiers in the model is an important improvement, as the objective is to keep the effluent to the receiving waters to a minimum.

Due to time delays in the aeration tanks the model simulations are 0.8 h ahead of the measurements. Combined with an influent flow forecast horizon of approximately 1 h, the SS concentrations out of the aeration tanks can be predicted almost 2 h ahead. This horizon is considered to be sufficient for selecting the optimal control action.

The proposed model is a valuable tool for designing control algorithms for ATS. By applying the models, it is possible to forecast the SS concentration in the effluent from the aeration tanks. The predictions can be used to choose the best control action, i.e. whether to change the flow direction and switch aeration and mixing on or off, within the limitations, caused by the nutrient removal processes.

Acknowledgements

The authors wish to thank the staff of Aalborg West WWTP and the municipality of Aalborg, for their cooperation and permission to use the data from the WWTP. Thanks are also due to Krüger A/S and the Danish Academy of Technical Sciences for funding the project in connection with which the present work has been carried out, under grant EF-623.

Paper F

Effects and control of Aeration Tank Settling.

Submitted.

F

Abstract

Aeration Tank Settling (ATS) operation is introduced at alternating wastewater treatment plants (WWTPs) to increase the hydraulic capacity during rain storms. A recently developed dynamic grey-box model of ATS as well as a dynamic model of dry weather operation is used to quantify the benefits of ATS operation in terms of increased hydraulic capacity on a large Danish alternating Bio Denipho WWTP.

A real time control algorithm for optimal selection of operating mode based on model predictions of the SS concentrations in the aeration tanks is proposed.

The economic value of ATS operation is estimated by a calculation of the price of a detention basin capable of handling nearly the same amount of water as the increased hydraulic capacity entails.

Key words: Aeration Tank Settling, model based predictive control, grey-box models

Introduction

In an alternating wastewater treatment plant (WWTP) the aeration tanks are composed of pairs of interconnected tanks. The influent to the aeration tanks is directed to one of the tanks, through the connection between the tanks and out of the second tank to the secondary clarifier. During dry weather periods, the tanks are always fully mixed to enable optimal nutrient removal. The tank which receives the incoming wastewater is in anoxic denitrification mode, while the other tank, which delivers effluent to the secondary clarifier, is operated in aerobic nitrification mode.

During rain storms, the wet weather flow often exceeds the capacity of the clarifier, and the usual approach to this situation is to store the excess water in detention basins and/or bypass the biological treatment part of the WWTP. Another approach is to handle the excess water in the biological part of the WWTP by increasing the secondary clarifier volume, e.g. by using available storm water tanks for sedimentation (Carrette et al., 1999). Yet another way to

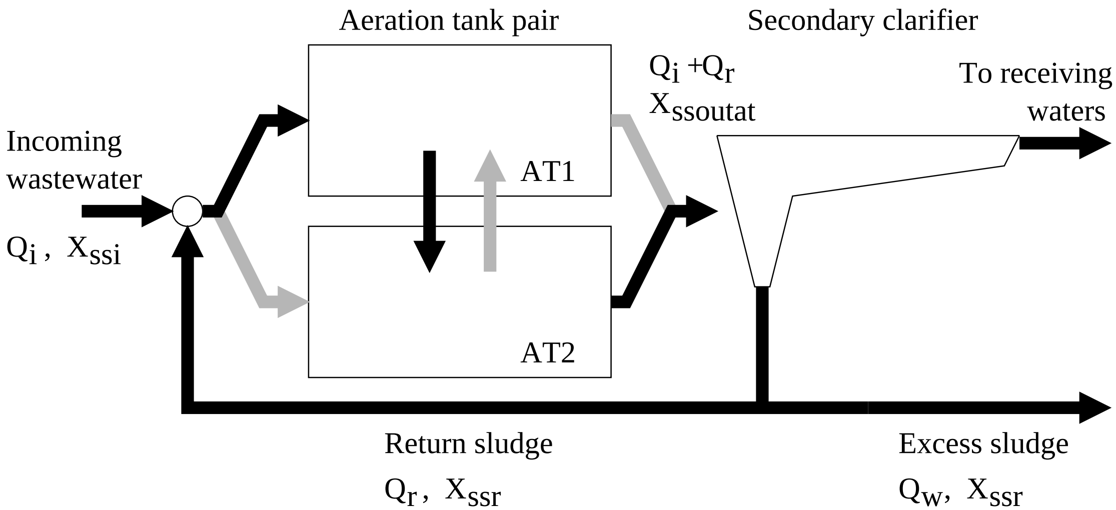

Figure 1. Flow path through aeration tank pair in an alternating WWTP.

increase the hydraulic capacity of the biological treatment during rain storms is to introduce aeration tank settling (ATS) operation[1] (Bundgaard et al., 1996; Nielsen et al., 1996, 1999).

When ATS is active, the aeration scheme is changed, so that the aeration tank that receives influent is aerated and the other tank not. By stopping the mixers in the non aerated tank, sludge settling is made possible, which enables an increased amount of SS to be held in the aeration tanks. Hereby, the SS load to the secondary clarifier can be reduced, and hence the hydraulic capacity increased. The effect of ATS can be increased by introducing an intermediate phase with settling periods in the tank that receives influent, to start the sludge settling before the flow path is switched. ATS operation thus consists of the four phases illustrated in Figure 2.

The benefits of ATS are better wastewater treatment during wet weather periods and economics compared to building storm water tanks (Boonen et al., 1999).

When a rain storm can be predicted ahead of the arrival of the storm water at the WWTP, the prediction horizon can be used to transport SS from the secondary clarifer to the aeration tanks, and hereby further increase the effect of ATS control.

The selection of the lengths of the periods with aeration in one of the tanks (main phases) and the periods with no aeration at all (intermediate phases) during ATS is a trade off between two objectives: 1) to keep as much suspended solids in the aeration tanks as possible, and 2) to obtain optimal aeration capacity. Long main and intermediate phase lengths fulfil the first objective, while shorter main phases and no intermediate phases satisfy the second objective. Hence, it is important to choose the phase lengths to ensure that the needed hydraulic capacity is available with minimum limitation of aeration capacity. To utilize the available hydraulic capacity of a given plant with given sludge characteristics and sludge amounts, the sludge storage capacity of the clarifier must be used. It is assumed that the sludge storage capacity can be quantified in terms of how much sludge from the aeration tanks that can be stored in the clarifier without limiting the hydraulic capacity.

[1] ATS is patented by Krüger A/S

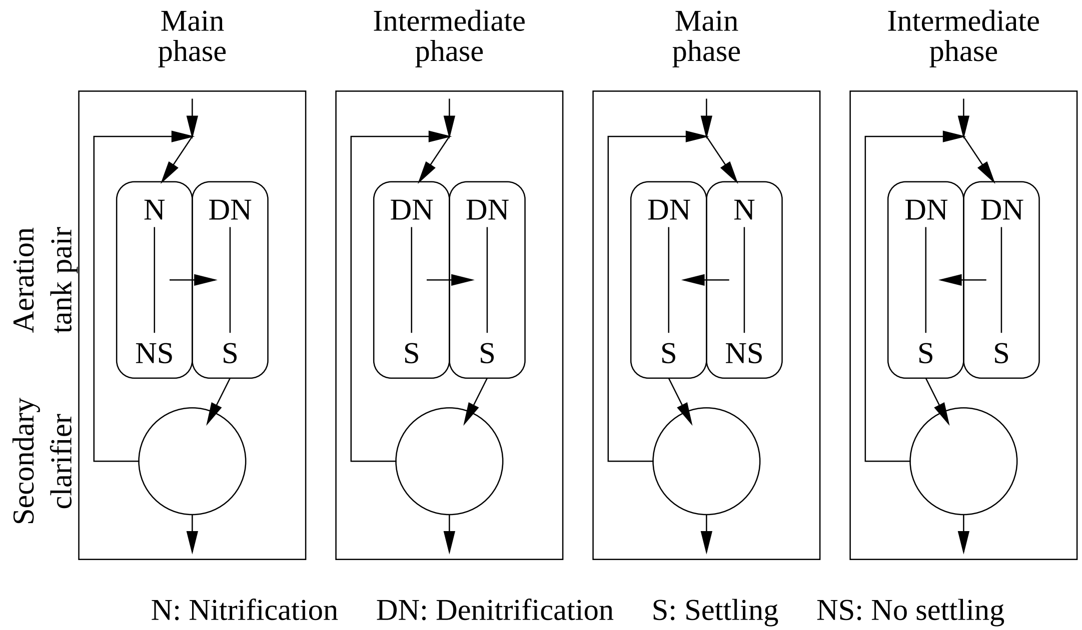

Figure 2. Phases of ATS operation.

Theory

A grey-box model of the suspended solids (SS) concentrations in and out of the aeration tanks of an alternating WWTP during ATS operation has recently been developed (Bechmann et al., 1999c; Nielsen et al., 1999). The model consists of 3 submodels: 1) A simple mass balance for the SS concentrations in the aeration tanks, 2) a sludge settling model, and 3) a model for the SS concentration in the effluent from the aeration tanks.

In Figure 1 an aeration tank pair composed of the aeration tanks AT1 and AT2 as well as the secondary clarifier is illustrated. The mean SS concentrations in AT1 and AT2 are designated X_{ssm1} and X_{ssm2}, while X_{ssi}, X_{ssoutat} and X_{ssr} denote the SS concentrations in the incoming wastewater, in the effluent from the aeration tanks to the secondary clarifer, and in the return sludge flow, respectively. Q_{i}, Q_{r}, and Q_{w}, denote the incoming wastewater flow, the return sludge flow and the excess sludge flow, respectively.

When the incoming wastewater is directed to AT1, and the effluent is taken from AT2, the mass balance equations are:

$$\frac{dX_{\text{ssm1}}}{dt} = \frac{Q_{\text{i}}X_{\text{ssi}} + Q_{\text{r}}X_{\text{ssr}} - (Q_{\text{i}} + Q_{\text{r}})X_{\text{ssm1}}}{V_{\text{at}}} \quad (1)$$

$$\frac{dX_{\text{ssm2}}}{dt} = \frac{(Q_{\text{i}} + Q_{\text{r}})X_{\text{ssm1}} - (Q_{\text{i}} + Q_{\text{r}})X_{\text{ssoutat}}}{V_{\text{at}}} \quad (2)$$

where V_{at} is the volume of each of the equally sized aeration tanks.

For the opposite flow direction, the mass balance equations are

$$\frac{dX_{\text{ssm1}}}{dt} = \frac{(Q_{\text{i}} + Q_{\text{r}})X_{\text{ssm2}} - (Q_{\text{i}} + Q_{\text{r}})X_{\text{ssoutat}}}{V_{\text{at}}} \quad (3)$$

$$\frac{dX_{\text{ssm2}}}{dt} = \frac{(Q_{\text{i}}X_{\text{ssi}} + Q_{\text{r}}X_{\text{ssr}}) - (Q_{b} + Q_{\text{r}})X_{\text{ssm2}}}{V_{\text{at}}} \quad (4)$$

The sludge settling in an aeration tank is modelled by a simple two layer model, where the layer above the sludge blanket is assumed to be clear water, and the layer under the sludge blanket contains all the SS fully mixed, see Figure 3. The sludge blanket settling velocity is modelled according to Vesilind (1968):

$$\frac{dd_{\text{sb}}}{dt} = V_0\,\mathrm{e}^{-n_{\text{v}}X_{\text{sssl}}} \quad (5)$$

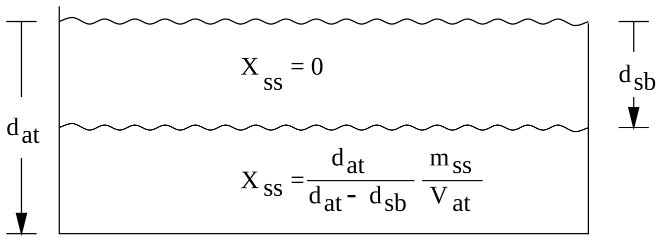

Figure 3. Two layer model of settling in an aeration tank.

where d_{sb} and X_{sssl} denote the sludge blanket depth and the SS concentration in the sludge layer, respectively.

The average SS concentration in the sludge layer is

$$X_{\text{sssl}} = \frac{d_{\text{at}}}{d_{\text{at}} - d_{\text{sb}}} X_{\text{ssm}} \tag{6}$$

where X_{ssm} is the average SS concentration in the aeration tank and d_{at} is the aeration tank depth.

The SS concentration in the effluent from the aeration tank is assumed to depend on the suction depth d_{suct}, and the X_{sssl}:

$$X_{\text{ssoutat}} = \frac{d_{\text{suct}} - d_{\text{sb}}}{d_{\text{suct}}} X_{\text{sssl}} \tag{7}$$

where d_{suct} is flow dependent and modelled as:

$$d_{\text{suct}} = d_0 \left(\frac{Q_{\text{i}} + Q_{\text{r}}}{Q_0} \right)^{b_{\text{suct}}} \tag{8}$$

where d_0 and b_{suct} are positive parameters, and $Q_0 = 1000\ \text{m}^3/\text{h}$ is a normalizing constant.

Introduce the loss of mean SS concentration in the aeration tanks during the period from $t = t_0$ to $t = t_1$:

$$\Delta_{\text{ssat}} = \bar{X}_{\text{ssm}}(t_0) - \bar{X}_{\text{ssm}}(t_1) \tag{9}$$

where

$$\bar{X}_{\text{ssm}}(t) = \frac{X_{\text{ssm1}}(t) + X_{\text{ssm2}}(t)}{2} \tag{10}$$

is the average SS concentration in the aeration tanks at time t.

When it is assumed that the SS amounts that enter the aeration tanks from the influent and that come from sludge growth are equal to the SS amounts removed from the system with the excess sludge and with the effluent to the recepient, the increase in the SS concentration in the secondary clarifier is:

$$\Delta_{\mathrm{sssc}} = \frac{V_{\mathrm{at}}}{V_{\mathrm{sc}}} \Delta_{\mathrm{ssat}} \tag{11}$$

where V_{at} and V_{sc} denote the total volume of the aeration tanks and the secondary clarifer, respectively.

From (11) it can be seen that Δ_{ssat} is a measure of the increase of SS in the secondary clarifier. At a given operating point (return sludge flow, effluent flow, sludge characteristcs etc.) the secondary clarifier is only capable of handling a limited increase of SS, before the SS concentration in the effluent to the receiving waters is increased to an unacceptable level. Hence, Δ_{ssat} must be limited to a certain level, dependent on the WWTP considered and its operational state.

Dry weather operation

During dry weather operation the aeration tanks are fully mixed, hence, $X_{\mathrm{ssoutat}} = X_{\mathrm{ssm2}}$ when the effluent is taken from aeration tank 2, and $X_{\mathrm{ssoutat}} = X_{\mathrm{ssm1}}$ when the opposite flow path is used. Thus, when the wastewater is directed to aeration tank 1 and effluent is taken from aeration tank 2, the dry weather mass balance equations are

$$\frac{dX_{\mathrm{ssm1}}}{dt} = \frac{Q_{\mathrm{i}}X_{\mathrm{ssi}} + Q_{\mathrm{r}}X_{\mathrm{ssr}} - (Q_{\mathrm{i}} + Q_{\mathrm{r}})X_{\mathrm{ssm1}}}{V_{\mathrm{at}}} \tag{12}$$

$$\frac{dX_{\mathrm{ssm2}}}{dt} = \frac{(Q_{\mathrm{i}} + Q_{\mathrm{r}})X_{\mathrm{ssm1}} - (Q_{\mathrm{i}} + Q_{\mathrm{r}})X_{\mathrm{ssm2}}}{V_{\mathrm{at}}} \tag{13}$$

Note that the mass balance equations for AT1 during ATS operation (equation (1)) and during dry weather operation (equation (12)) are the same, but that the corresponding equations for AT2 (equations (2) and (13)) are not the same.

When it is assumed that the SS concentrations in the two aeration tanks as well as their time derivatives are approximately equal, ie:

$$X_{\text{ssm}} = X_{\text{ssm1}} = X_{\text{ssm2}} \tag{14}$$

$$\frac{dX_{\text{ssm}}}{dt} = \frac{dX_{\text{ssm1}}}{dt} = \frac{dX_{\text{ssm2}}}{dt} \tag{15}$$

the addition of (12) and (13) yields

$$\frac{dX_{\text{ssm}}}{dt} = \frac{Q_{\text{i}}X_{\text{ssi}} + Q_{\text{r}}X_{\text{ssr}} - (Q_{\text{i}} + Q_{\text{r}})X_{\text{ssm}}}{2V_{\text{at}}} \tag{16}$$

which for constant Q_{i}, Q_{r}, X_{ssi}, X_{ssr} and V_{at} has the solution

$$X_{\text{ssm}}(t) = \frac{Q_{\text{i}}X_{\text{ssi}} + Q_{\text{r}}X_{\text{ssr}}}{Q_{\text{i}} + Q_{\text{r}}} \left(1 - \mathrm{e}^{-\frac{Q_{\text{i}}+Q_{\text{r}}}{2V_{\text{at}}}(t-t_0)}\right) + X_{\text{ssm}}(t_0)\,\mathrm{e}^{-\frac{Q_{\text{i}}+Q_{\text{r}}}{2V_{\text{at}}}(t-t_0)} \tag{17}$$

Hence, the loss of SS concentration in the aeration tanks during dry weather operation during the period from $t = t_0$ to $t = t_1$ is

$$\begin{aligned} \Delta_{\text{ssat}} &= X_{\text{ssm}}(t_0) - X_{\text{ssm}}(t_1) \\ &= \left(X_{\text{ssm}}(t_0) - \frac{Q_{\text{i}}X_{\text{ssi}} + Q_{\text{r}}X_{\text{ssr}}}{Q_{\text{i}} + Q_{\text{r}}}\right)\left(1 - \mathrm{e}^{-\frac{Q_{\text{i}}+Q_{\text{r}}}{2V_{\text{at}}}(t_1-t_0)}\right) \end{aligned} \tag{18}$$

The steady state solution to (16) is easily found to be

$$X_{\text{ssm,ss}} = \frac{Q_{\text{i}}X_{\text{ssi}} + Q_{\text{r}}X_{\text{ssr}}}{Q_{\text{i}} + Q_{\text{r}}} \tag{19}$$

with the corresponding SS concentration loss

$$\Delta_{\text{ssat}} = X_{\text{ssm}}(t_0) - \frac{Q_{\text{i}}X_{\text{ssi}} + Q_{\text{r}}X_{\text{ssr}}}{Q_{\text{i}} + Q_{\text{r}}} \tag{20}$$

Choice of operating mode

During a storm situation the main objective is to avoid sludge flight to the recepient, and the secondary objective is to enable optimal biological treatment of the incoming wastewater. Hence, the operating mode that prevents unacceptable SS concentrations in the effluent and enables best possible biological treatment should be chosen. This choice can be made on the basis of predictions of the loss of SS concentration in the aeration tanks for the possible operating modes. The model of ATS operation can be used to predict the loss by simulation for a sufficient time to reach steady state conditions, while equation (20) is used to predict the dry weather operation loss. When the acceptable loss for the WWTP considered is known, e.g. from experience from previous rain storms, the optimal operating mode can be selected. As the SS concentration loss predictions can be computed offline for different combinations of flows, concentrations and operating modes, the real time control algorithm can be established by feedback from Q_{i}, Q_{r}, X_{ssr} and the initial SS concentrations in the aeration tanks, e.g. implemented in a look-up table.

Results and discussion

The Aalborg West WWTP in Northern Jutland, Denmark, was used to estimate the model for the ATS operation (Bechmann et al., 1999c), and hence it is used for the analyses carried out here.

The maximum loss of average SS concentration in the aeration tanks during dry weather operation as well as ATS operation was calculated for varying flows Q_{i} and Q_{r}, varying return sludge concentrations X_{ssr} and varying initial average concentrations in the aeration tanks. The simulations of ATS operation were run for a time span of approximately 24 hours in order to enable the ATS operation to reach steady state conditions.

In Bechmann et al. (1999c) it was found that the SS concentration of the wastewater entering the aeration tanks was insignificant. Therefore X_{ssi} was fixed at 0 in all the computations.

In Figure 4 the SS concentration losses for different operating modes are shown as a function of the influent flow. The initial SS concentration in the aeration tanks was $\bar{X}_{\mathrm{ssat}} = 4$ g/m^3, the return sludge concentration was $X_{\mathrm{ssr}} = 10$ g SS/m^3, and the return flow was $Q_{\mathrm{r}} = 2500$ m^3/h, as these values are typical for a rain situation at Aalborg West WWTP. At this plant, the acceptable loss is empirically found to be $\Delta_{\mathrm{ssat}} = 0.7$ g SS/m^3, hence a horizontal line for this value is included in the figure. Note that the influent flow varies from low dry weather flow to very strong storm flow (2000 m^3/h to 16,000 m^3/h), and that

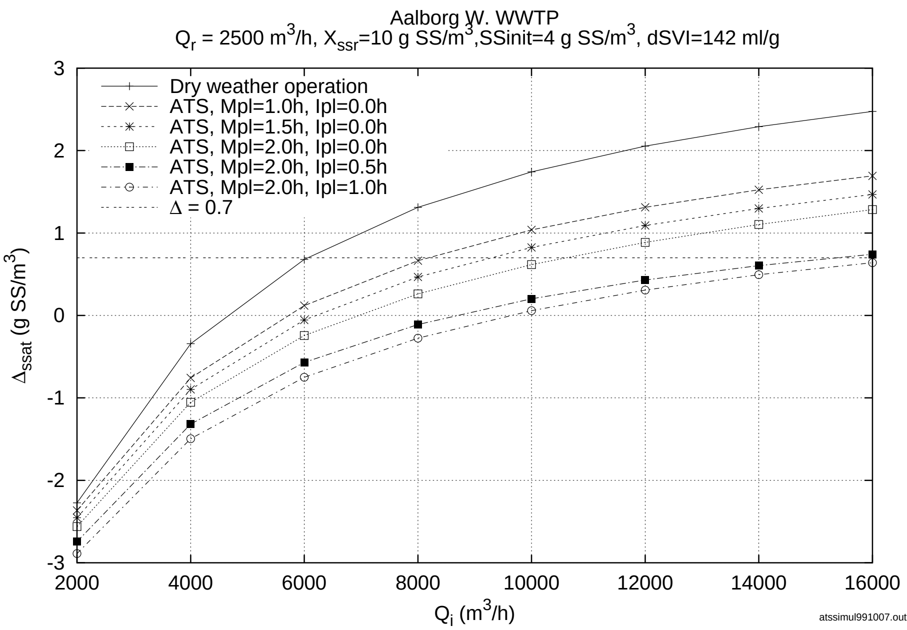

Figure 4. Loss of SS concentration in the aeration tanks for different operating modes. Mpl and Ipl denote the lengths of the main and intermediate phases of ATS operation, respectively.

the upper physical limit of the plant is approximately 12,000 m^3/h. When the flow exceeds this limit, the WWTP is flooded.

The uppermost curve in Figure 4 is the dry weather operation curve. The 5 curves below are all for ATS operation, with increasing ATS efficiency towards the lowest curve. Each of the 5 ATS curves represents an ATS operating mode, in terms of lengths of main and intermediate phases. The ATS efficiency increases with increasing phase lengths. The first three ATS curves represent operating modes with no intermediate phases but with increasing main phase lengths. In the last two ATS operation curves, intermediate phases are introduced. It is clearly seen that the introduction of a 0.5 hour intermediate phase increases the efficiency considerably. However, 1 hour intermediate phases do not result in the same increase as the first 0.5 hour intermediate phases. This is because the sludge settles faster in the first 0.5 hour of a settling phase than in the next 0.5 hour, as the SS concentration in the sludge layer increases as the sludge settles, c.f. equations (5) and (6).

When the operating mode is to be chosen, the algorithm is to select the operating mode with the uppermost curve in Figure 4, but not above the $\Delta_{\text{ssat}} = 0.7$ g SS/m^3 limit. Then the best possible biological treatment without sludge flight will be performed.

From Figure 4 it is seen that the hydraulic capacity of Aalborg West WWTP during dry weather operation is 6000 m^3/h. The lightest version of ATS operation with a main phase length of 1 hour and no intermediate phase increases the hydraulic capacity to 8000 m^3/h and the strongest version of ATS operation with a 2-hour main phase and a 1-hour intermediate phase increases the hydraulic capacity to beyond 16,000 m^3/h, which is far more than the physical limit of 12,000 m^3/h.

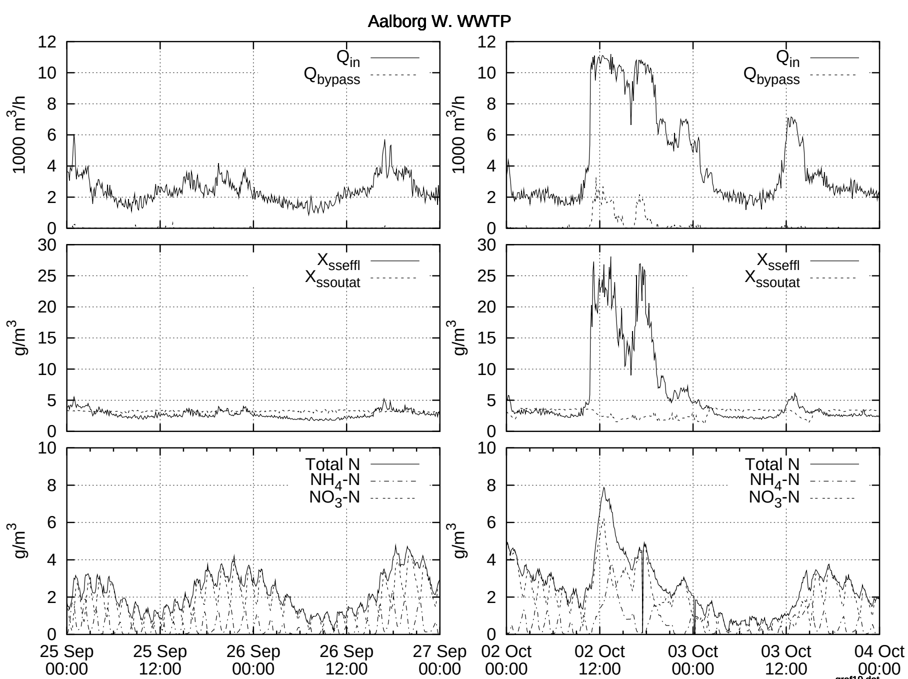

Figure 5. Results from 2 different weekends. Left plot: a dry weather weekend. Right plot: a wet weather weekend.

In Figure 5 measurements from two weekends are shown. To the left is a dry weather weekend with dry weather operation of the plant and to the right a wet weather example with ATS operation during some of the period (from October 2nd 10:14 to October 3rd 14:08, and October 3rd 11:44 to 14:08). The algorithm controlling the phase lengths of ATS operation is an earlier developed version than the one proposed here. The uppermost graphs show the influent flow to the aeration tanks as well as Q_{bypass}, which is the part of the total inflow to the WWTP that bypasses the biological treatment. In the middle graphs, the SS concentration in the effluent from the aeration tanks and in the effluent from the WWTP are shown. In the bottom graphs the ammonia and nitrate concentrations in aeration tank 6, as well as the total nitrogen concentration (the sum of the ammonia and nitrate concentrations) in this tank are shown. The wet weather example shows that the WWTP is actually capable of handling a flow of approximately 11000 m^3/h. Part of the total inflow to the WWTP bypassed the biological tanks so that the plant was not flooded. Furthermore, it can be seen that the storm situation with ATS operation causes the ammonia, nitrate and hence total nitrogen concentrations to increase to levels considerable higher than during dry weather. However, the nitrogen concentrations are below the Danish criteria for the plant (8 g total nitrogen per m^3 on an average).

Economic advantages of ATS operation

Assuming that the combined system of sewers and a WWTP should be able to handle the increase in the influent flow from 6000 m^3/h to 12,000 m^3/h for, say, 5 hours. Then the detention basin volume required is

$$5 \text{ h} \cdot 6000 \text{ m}^3/\text{h} = 30,000 \text{ m}^3 \tag{21}$$

The cost of building detention basins is estimated to be between 100 and 500 Euro per m^3, hence, a 30,000 m^3 detention basin costs between 3,000,000 and 15,000,000 Euro!

Conclusions

ATS operation can be used to increase the hydraulic capacity of the WWTP and hereby decrease the need for bypassing the biological treatment facilities of the WWTP or adding detention basins. Compared to constructing (additional) detention basins the cost benefit of introducing ATS operation is extremely good. Furthermore, ATS operation does not require extra space (which is not necessarily available), does not require cleaning facilities, and does not smell bad when not in operation.

Furthermore this paper has shown how dynamic models of ATS and dry weather operation can be used offline to establish and update a lookup table to select the optimal operation strategy at the actual operating conditions in a real time control system.

The model types used here can be applied to other types of plants and operation modes, cf. Boonen et al. (1999); Carrette et al. (1999); Nielsen et al. (1999), and hence to develop optimal control algorithms for different plants.

Incorporation of flow and pollution flux predictions of the influent to the WWTP enables further on-line optimization of the operation, as it is then not necessary to control the ATS phase lengths according to steady state conditions, but only according to the predicted conditions.

To predict the limiting value of the loss in the SS concentrations in the aeration tanks and thus the corresponding increase in the SS concentrations in the secondary clarifier experience with the WWTP considered is required. The inclusion of a model of the clarifier to enable better prediction of the SS concentrations in the clarifier and when sludge flight will take place can further increase the benefits of ATS operation, as it is expected that a clarifier model will make it possible to operate the WWTP even closer to the point where sludge flight occurs.

Acknowledgements

The authors wish to thank the staff of Aalborg West WWTP and the municipality of Aalborg for their cooperation and permission to use the data from the WWTP. Thanks are also due to Krüger A/S and the Danish Academy of Technical Sciences for funding the project in connection with which the present work has been carried out, under grant EF-623.

Bibliography

Ashley, R. M. and Crabtree, R. W. (1992). Sediment origins, deposition and build-up in combined sewer systems. *Water Science and Technology*, **25**(8), 1–12.

Bechmann, H., Madsen, H., Poulsen, N. K., and Nielsen, M. K. (2000). Grey box modelling of first flush and incoming wastewater at a wastewater treatment plant. *Environmetrics*, **11**(1), 1–12.

Bechmann, H., Nielsen, M. K., Madsen, H., and Poulsen, N. K. (1998). Control of sewer systems and wastewater treatment plants using pollutant concentration profiles. *Water Science and Technology*, **37**(12), 87–93.

Bechmann, H., Nielsen, M. K., Madsen, H., and Poulsen, N. K. (1999a). Grey-box modelling of pollutant loads from a sewer system. *UrbanWater*, **1**(1), 71–78.

Bechmann, H., Nielsen, M. K., Poulsen, N. K., and Madsen, H. (1999b). Effects and control of aeration tank settling operation. Submitted.

Bechmann, H., Nielsen, M. K., Poulsen, N. K., and Madsen, H. (1999c). Grey-box modelling of aeration tank settling. Submitted.

Berthouex, P. M. and Box, G. E. (1996). Time series models for forecasting wastewater treatment plant performance. *Water Research*, **30**(8), 1865–1875.

Bertrand-Krajewski, J.-L., Chebbo, G., and Saget, A. (1998). Distribution of pollutant mass vs volume in stormwater discharges and the first flush phenomenon. *Water Research*, **32**(8), 2341–2356.

Billmeier, E. (1986). Einfluss der Rücklaufführung auf das Absetzverhalten belebter Schlämme. *GWF-Wasser/Abwasser*, **127**(5).

Boonen, I., Bruynooghe, H., Carrette, R., Bixio, D., and Ockier, P. (1999). Renovation of the WWTP Bruges. In *8th IAWQ Conference on Design, Operation and Economics of Large Wastewater Treatment plants*, pp. 207–214. International Association on Water Quality, IAWQ, Budapest University of Technology, Department of Sanitary and Environmental Engineering.

Box, G. E. P., Jenkins, G. M., and Reinsel, G. C. (1994). *Time Series Analysis: Forecasting and Control*. Prentice-Hall, Inc.

Box, G. E. P. and Jenkins, J. M. (1976). *Time Series Analysis: Forecasting and Control*. Holden–Day, San Francisco.

Bundgaard, E., Nielsen, M. K., and Henze, M. (1996). Process development by full-scale on-line tests and documentation. *Water Science and Technology*, **33**(1), 281–287.

Capodaglio, A. G. (1994). Transfer function modelling of urban drainage systems, and potential uses in real-time control applications. *Water Science and Technology*, **29**(1–2), 409–417.

Capodaglio, A. G., Novotny, V., and Fortina, L. (1992). Modelling wastewater treatment plants through time series analysis. *Environmetrics*, **3**(1), 99–120.

Carrette, R., Bixio, D., Thoeye, C., and Ockier, P. (1999). Storm operation strategy: high-flow activated sludge process operation. In *8th IAWQ Conference on Design, Operation and Economics of Large Wastewater Treatment plants*, pp. 215–222. International Association on Water Quality, IAWQ, Budapest University of Technology, Department of Sanitary and Environmental Engineering.

Carstensen, J. and Harremoës, P. (1997). Time series modelling of overflow structures. *Water Science and Technology*, **36**(8–9), 45–50.

Carstensen, J., Nielsen, M., and Strandbæk, H. (1998). Prediction of hydraulic load for urban storm control of a municipal WWT plant. *Water Science and Technology*, **37**(12), 363–370.

Carstensen, J., Nielsen, M. K., and Harremoës, P. (1996). Predictive control of sewer systems by means of grey-box models. *Water Science and Technology*, **34**(3–4), 189–194.

Chow, V. T., Maidment, D. R., and Mays, L. W. (1988). *Applied Hydrology*. McGraw-Hill.

Conradsen, K. (1984a). *An Introduction to Statistics*, volume 2. Department of Mathematical Modelling, Technical University of Denmark, 4th edition. (In Danish: En Introduktion til Statistik).

Conradsen, K. (1984b). *An Introduction to Statistics*, volume 1. Department of Mathematical Modelling, Technical University of Denmark, 5th edition. (In Danish: En Introduktion til Statistik).

Crabtree, R. W., Ashley, R., and Gent, R. (1995). Mousetrap: Modelling of real sewer sediment characteristics and attached pollutants. *Water Science and Technology*, **31**(7), 43–50.

Deletic, A. (1998). The first flush load of urban surface runoff. *Water Research*, **32**(8), 2462–2470.

Delleur, J. W. and Gyasi-Agyei, Y. (1994). Prediction of suspended solids in urban sewers by transfer function model. *Water Science and Technology*, **29**(1–2), 171–179.

Dempsey, P., Eadon, A., and Morris, G. (1997). SIMPOL: A simplified urban pollution modelling tool. *Water Science and Technology*, **36**(8–9), 83–88.

Dobbs, R. A., Wise, R. H., and Dean, R. B. (1972). The use of ultra-violet absorbance for monitoring the total organic content of water and wastewater. *Water Research*, **6**, 1173–1180.

Dupont, R. and Dahl, C. (1995). A one-dimensional model for a secondary settling tank including density current and short-circuiting. *Water Science and Technology*, **31**(2), 215–224.

Dupont, R. and Sinkjær, O. (1994). Optimisation of wastewater treatment plants by means of computer models. *Water Science and Technology*, **30**(4), 181–190.

EFOR Version 3.0 (1998). *User's Guide*. EFOR ApS, c/o Krüger A/S, Gladsaxevej 363, DK-2860 Søborg, Denmark.

Ekama, G. A., Barnard, J. L., Günthert, F. W., Krebs, P., McCorquodale, J. A., Parker, D. S., and Wahlberg, E. J. (1997). *Secondary settling tanks: Theory, modelling, design and operation*. IAWQ Scientific and Technical Report No. 6. IAWQ, London.

Entem, S., Lahoud, A., Yde, L., and Bendsen, B. (1998). Real time control of the sewer system of Boulogne Billancourt – a contribution to improving the water quality of the Seine. *Water Science and Technology*, **37**(1), 327–332.

Geiger, W. F. (1987). Flushing effects in combined sewer systems. In *Proc. Fourth Int. Conf. Urban Storm Drainage*, pp. 40–46, Lausanne.

Gelb, A. (1974). *Applied optimal estimation*. MIT Press, New York.

Grijspeerdt, K., Vanrolleghem, P., and Verstraete, W. (1995). Selection of one-dimensional sedimentation: Models for on-line use. *Water Science and Technology*, **31**(2), 193–204.

Grum, M. (1998). Incorporating concepts from physical theory into stochastic modelling of urban runoff pollution. *Water Science and Technology*, **37**(1), 179–185.

Gujer, W., Henze, M., Mino, T., and van Loosdrecht, M. (1999). Activated slugde model no. 3. *Water Science and Technology*, **39**(1), 183–193.

Gupta, K. and Saul, A. J. (1996). Specific relationships for the first flush load in combined sewer systems. *Water Research*, **30**(5), 1244–1252.

Härtel, L. and Pöpel, H. J. (1992). A dynamic secondary clarifier model including processes of sludge thickening. *Water Science and Technology*, **25**(6), 267–284.

Heip, L., Assel, J. V., and Swartenbroekx, P. (1997). Sewer flow quality modelling. *Water Science and Technology*, **36**(5), 177–184.

Henze, M., Grady, C. P. L., Gujer, W., v. R. Marais, G., and Matsuo, T. (1987). *Activated Sludge Model No. 1*. IAWPRC Scientific and Technical Report No. 1. IAWPRC, London.

Henze, M., Gujer, W., Mino, T., Matsuo, T., Wentzel, M. C., and v. R. Marais, G. (1995). *Activated Sludge Model No. 2*. IAWQ Scientific and Technical Report No. 3. IAWQ, London.

Henze, M., Gujer, W., Mino, T., Matsuo, T., Wentzel, M. C., v. R. Marais, G., and van Loosdrecht, M. C. M. (1999). Activated sludge model no.2D, ASM2D. *Water Science and Technology*, **39**(1), 165–182.

Hernebring, C., Ohlsson, L., Andreasson, M., and Gustafsson, L.-G. (1998). Interaction between the treatment plant and the sewer system in Halmstad:

Integrated upgrading based on real time control. *Water Science and Technology*, **37**(9), 127–134.

Jazwinski, A. H. (1970). *Stochastic processes and filtering theory*. Academic Press.

Kanaya, T., Fujita, I., Hayashi, H., Hiraoka, M., and Tsumura, K. (1985). Automatic measurement and analysis of process data in a combined wastewater treatment plant. In Drake, R., editor, *Instrumentation and control of water and wastewater treatment and transport systems*, Advances in Water Pollution Control, pp. 77–84. IAWPRC, Pergamon Press.

Kendall, M. G. and Stuart, A. (1979). *The Advanced Theory of Statistics*, volume 2. Griffin, London, 4th edition.

Kloeden, P. and Platen, E. (1995). *Numerical Solutions of Stochastic Differential Equations*. Springer, 2nd edition.

Koehne, M., Hoen, K., and Schuhen, M. (1995). Modelling and simulation of final clarifiers in wastewater treatment plants. *Mathematics and Computers in Simulation*, **39**, 609–616.

Lindberg, S., Nielsen, J. B., and Carr, R. (1989). An integrated PC-modelling system for hydraulic analysis of drainage systems. In *The first Australian Conference on technical computing in the Water Industry: WATERCOMP '89*, Melbourne, Australia.

Liong, S. Y. and Chan, W. T. (1993). Runoff volume estimates with neural networks. In Topping, B. H. V., editor, *Neural Networks and Combinatorial Optimization in Civil and Structural Engineering*, pp. 67–70. Civil-Comp Press.

Ljung, L. (1995). *System Identification Toolbox User's Guide*. The MathWorks, Inc. Third Printing.

Ljung, L. (1999). *System Identification, Theory for the User*. Prentice Hall, New Jersey, 2nd edition.

Madsen, H. (1995). *Time Series Analysis*. Department of Mathematical Modelling, Technical University of Denmark. (In Danish: Tidsrækkeanalyse).

Madsen, H. and Holst, J. (1996). *Modelling Non-Linear and Non-Stationary Time Series*. Department of Mathematical Modelling, Department of Mathematical Modelling.

Madsen, H. and Melgaard, H. (1991). The mathematical and numerical methods used in CTLSM – a program for ML-estimation in stochastic, continuous time dynamical models. Technical Report no. 7/1991, Institute of Mathematical Statistics and Operations Research, Technical University of Denmark, Lyngby, Denmark.

Madsen, H., Nielsen, J. N., and Baadsgaard, M. (1998). *Statistics in Finance*. Department of Mathematical Modelling, Technical University of Denmark.

Mark, O., Appelgren, C., and Larsen, T. (1995). Principles and approaches for numerical modelling of sediment transport in sewers. *Water Science and Technology*, **31**(7), 107–115.

Mark, O., Hernebring, C., and Magnusson, P. (1998a). Optimisation and control of the inflow to a wastewater treatment plant using integrated modelling tools. *Water Science and Technology*, **37**(1), 347–354.

Mark, O., Wennberg, C., van Kalken, T., Rabbi, F., and Albinsson, B. (1998b). Risk analyses for sewer systems based on numerical modelling and GIS. *Safety Science*, **30**(1998), 99–106.

Matsché, N. and Stumwöhrer, K. (1996). UV absorption as control-parameter for biological treatment plants. *Water Science and Technology*, **33**(12), 211–218.

Meinholz, T. L., Hansen, C. A., and Novotny, V. (1974). An application of the storm water management model. In Kao, D. T. Y., editor, *Proceedings of the National Symposion on Urban Rainfall and Runoff and Sediment Control*, pp. 109–113. University of Kentucky.

Melgaard, H. (1994). *Identification of Physical Models*. Ph.D. thesis, Institute of Mathematical Modelling, Technical University of Denmark. No. 1994–4.

Melgaard, H. and Madsen, H. (1991). CTLSM version 2.6 – a program for parameter estimation in stochastic differential equations. Technical Report no. 1/1993, Institute of Mathematical Statistics and Operations Research, Technical University of Denmark, Lyngby, Denmark.

Melgaard, H. and Madsen, H. (1993). CTLSM continuous time linear stochastic modelling. In Bloem, J., editor, *In: Workshop on Application of System Identification in Energy Savings in Buildings*, pp. 41–60. Institute for Systems Engineering and Informatics, Joint Research Centre, Ispra, Italy.

Mrkva, M. (1975). Automatic U.V.-control system for relative evaluation of organic water pollution. *Water Research*, **9**, 587–589.

Nielsen, M. and Önnerth, T. (1995). Improvement of a recirculating plant by introducing STAR control. *Water Science and Technology*, **31**(2), 171–180.

Nielsen, M. K., Bechmann, H., and Henze, M. (1999). Modelling and test of Aeration Tank Settling ATS. In *8th IAWQ Conference on Design, Operation and Economics of Large Wastewater Treatment plants*, pp. 199–206. International Association on Water Quality, IAWQ, Budapest University of Technology, Department of Sanitary and Environmental Engineering.

Nielsen, M. K., Carstensen, J., and Harremoës, P. (1996). Combined control of sewer and treatment plant during rainstorm. *Water Science and Technology*, **34**(3), 181–187.

Nouh, M. (1996). Simulation of water quality in sewer flows by neural networks. In Müller, editor, *Proceedings of the second int. conf. Hydroinformatics. Hydroinformatics '96*, volume 2, pp. 885–891, Balkema, Rotterdam.

Novotny, V., Jones, H., Feng, X., and Capodaglio, A. (1991). Time series analysis models of activated sludge plants. *Water Science and Technology*, **23**, 1107–1116.

Nowack, G. and Ueberbach, O. (1995). Die kontinuierliche SAK-Messung Aussagekraft, Statistik und Anwendungen. *Korresspondenz Abwasser*, **42**(11), 2020–2030.

Øksendal, B. (1995). *Stochastic Differential Equations*. Springer, 4th edition.

Olsson, G. (1992). Control of wastewater treatment systems. *ISA Transactions*, **31**(1), 87–96.

Olsson, G., Andersson, B., Hellström, B. G., Holmström, H., Reinius, L. G., and Vopatek, P. (1989). Measurements, data analysis and control methods in wastewater treatment plants – state of the art and future trends. *Water Science and Technology*, **21**, 1333–1345.

Önnerth, T. and Bechmann, H. (1995). Implementation of and results from advanced on-line computer control of a BNR recirculating plant. In *New and emerging environmental technologies and products conference for wastewater treatment and stormwater collection*, volume 11, pp. 51–72. Water Environment Federation.

Poulsen, N. K. (1995). *Stochastic Adaptive Control*. Department of Mathematical Modelling, Technical University of Denmark. (In Danish: Stokastisk adaptiv regulering).

Pu, H.-C. and Hung, Y.-T. (1995). Use of artificial neural networks: predicting trickling filter performance in a municipal wastewater treatment plant. *Environmental Management and Health*, **6**(2), 16–27.

Rangla, M. K., Burnham, K. J., and Stephens, R. I. (1998). Simulation of activated sludge process control strategies. In *International Conference on Simulation '98*, pp. 152–157. IEE. IEE Conf. Publ. No. 457.

Reynolds, D. M. and Ahmad, S. R. (1997). Rapid and direct determination of wastewater BOD values using a fluorescence technique. *Water Research*, **31**(8), 2012–2018.

Ruan, M. and Wiggers, J. B. M. (1997). Application of time-series analysis to urban storm drainage. *Water Science and Technology*, **36**(5), 125–131.

Ruban, G., Marchandise, P., and Scrivener, O. (1993). Pollution measurement accuracy using real time sensors and wastewater samples analysis. *Water Science and Technology*, **28**(11–12), 67–78.

Saget, A., Chebbo, G., and Bertrand-Krajewski, J.-L. (1996). The first flush in sewer systems. *Water Science and Technology*, **33**(9), 101–108.

Sjöberg, J., Zhang, Q., Ljung, L., Benveniste, A., Delyon, B., Glorennec, P.-Y., Hjalmarsson, H., and Juditsky, A. (1995). Nonlinear black-box modeling in system identification: a unified overview. *Automatica*, **31**(12), 1691–1724.

Takács, L., Patry, G. G., and Nolasco, D. (1991). A dynamic model of the thickening/clarification process. *Water Research*, **25**, 1263–1271.

van Luijtelaar, H. and Rebergen, E. W. (1997). Guidelines for hydrodynamic calculations on urban drainage in The Netherlands: Backgrounds and examples. *Water Science and Technology*, **36**(8–9), 253–258.

Vesilind, P. A. (1968). Design of prototype thickeners from batch settling tests. *Water & Sewage Works*, **115**, 302–307.

Vesilind, P. A. (1979). *Treatment and disposal of wastewater sludge*. Ann Arbor Science, 1st edition.

Ward, W., Vaccari, D. A., McMahon, D., Rivera, S., and Wojciechowski, E. (1996). A hybrid deterministic/nonlinear stochastic model of the activated sludge proces. In Zannetti, P. and Brebbia, C. A., editors, *Development and Application of Computer Techniques to Environmental Studies VI*, pp. 81–90. IEE, Comput. Mech. Publications.

Wass, P. D., Marks, S. D., Finch, J. W., Leeks, G. J. L., and Ingram, J. K. (1997). Monitoring and preliminary interpretation of in-river turbidity and remote sensed imagery for suspended sediment transport studies in the Humber catchment. *The Science of the Total Environment*, **194–195**, 263–283.

Wett, B., Gluderer, D., and Rauch, W. (1997). Denitrifikation beim Absetzvorgang. *GWF-Wasser/Abwasser*, **138**(7).

Young, P. and Wallis, S. (1985). Recursive estimation: A unified approach to the identification, estimation, and forecasting of hydrological systems. *Applied Mathematics and Computation*, **17**, 299–334.

Young, P. C., Jakeman, A. J., and Post, D. A. (1997). Recent advances in the data-based modelling and analysis of hydrological systems. *Water Science and Technology*, **36**(5), 99–116.

Zhao, H., Hao, O. J., and McAvoy, T. J. (1999). Approaches to modelling nutrient dynamics: ASM2, simplified model and neural nets. *Water Science and Technology*, **39**(1), 227–234.

Ph.D. theses from IMM

1. **Larsen, Rasmus.** (1994). *Estimation of visual motion in image sequences. xiv* + 143 pp.

2. **Rygard, Jens Moberg.** (1994). *Design and optimization of flexible manufacturing systems. xiii* + 232 pp.

3. **Lassen, Niels Christian Krieger.** (1994). *Automated determination of crystal orientations from electron backscattering patterns. xv* + 136 pp.

4. **Melgaard, Henrik.** (1994). *Identification of physical models. xvii* + 246 pp.

5. **Wang, Chunyan.** (1994). *Stochastic differential equations and a biological system. xxii* + 153 pp.

6. **Nielsen, Allan Aasbjerg.** (1994). *Analysis of regularly and irregularly sampled spatial, multivariate, and multi-temporal data. xxiv* + 213 pp.

7. **Ersbøll, Annette Kjær.** (1994). *On the spatial and temporal correlations in experimentation with agricultural applications. xviii* + 345 pp.

8. **Møller, Dorte.** (1994). *Methods for analysis and design of heterogeneous telecommunication networks.* Volume 1-2, *xxxviii* + 282 pp., 283-569 pp.

9. **Jensen, Jens Christian.** (1995). *Teoretiske og eksperimentelle dynamiske undersøgelser af jernbanekøretøjer. viii* + 174 pp.

10. **Kuhlmann, Lionel.** (1995). *On automatic visual inspection of reflective surfaces.* Volume 1, *xviii* + 220 pp., (Volume 2, *vi* + 54 pp., fortrolig).

11. **Lazarides, Nikolaos.** (1995). *Nonlinearity in superconductivity and Josephson Junctions. iv* + 154 pp.

12. **Rostgaard, Morten.** (1995). *Modelling, estimation and control of fast sampled dynamical systems. xiv* + 348 pp.

13. **Schultz, Nette.** (1995). *Segmentation and classification of biological objects. xiv* + 194 pp.

14. **Jørgensen, Michael Finn.** (1995). *Nonlinear Hamiltonian systems. xiv* + 120 pp.

15. **Balle, Susanne M.** (1995). *Distributed-memory matrix computations. iii* + 101 pp.

16. **Kohl, Niklas.** (1995). *Exact methods for time constrained routing and related scheduling problems. xviii* + 234 pp.

17. **Rogon, Thomas.** (1995). *Porous media: Analysis, reconstruction and percolation. xiv* + 165 pp.

18. **Andersen, Allan Theodor.** (1995). *Modelling of packet traffic with matrix analytic methods. xvi* + 242 pp.

19. **Hesthaven, Jan.** (1995). *Numerical studies of unsteady coherent structures and transport in two-dimensional flows.* Risø-R-835(EN) 203 pp.

20. **Slivsgaard, Eva Charlotte.** (l995). *On the interaction between wheels and rails in railway dynamics. viii* + 196 pp.

21. **Hartelius, Karsten.** (1996). *Analysis of irregularly distributed points. xvi* + 260 pp.

22. **Hansen, Anca Daniela.** (1996). *Predictive control and identification - Applications to steering dynamics. xviii* + 307 pp.

23. **Sadegh, Payman.** (1996). *Experiment design and optimization in complex systems. xiv* + 162 pp.

24. **Skands, Ulrik.** (1996). *Quantitative methods for the analysis of electron microscope images. xvi* + 198 pp.

25. **Bro-Nielsen, Morten.** (1996). *Medical image registration and surgery simulation. xxvii* + 274 pp.

26. **Bendtsen, Claus.** (1996). *Parallel numerical algorithms for the solution of systems of ordinary differential equations. viii* + 79 pp.

27. **Lauritsen, Morten Bach.** (1997). *Delta-domain predictive control and identification for control. xxii* + 292 pp.

28. **Bischoff, Svend.** (1997). *Modelling colliding-pulse mode-locked semiconductor lasers. xxii* + 217 pp.

29. **Arnbjerg-Nielsen, Karsten.** (1997). *Statistical analysis of urban hydrology with special emphasis on rainfall modelling.* Institut for Miljøteknik, DTU. *xiv* + 161 pp.

30. **Jacobsen, Judith L.** (1997). *Dynamic modelling of processes in rivers affected by precipitation runoff. xix* + 213 pp.

31. **Sommer, Helle Mølgaard.** (1997). *Variability in microbiological degradation experiments - Analysis and case study. xiv* + 211 pp.

32. **Ma, Xin.** (1997). *Adaptive extremum control and wind turbine control. xix* + 293 pp.

33. **Rasmussen, Kim Ørskov.** (1997). *Nonlinear and stochastic dynamics of coherent structures. x* + 215 pp.

34. **Hansen, Lars Henrik.** (1997). *Stochastic modelling of central heating systems. xxii* + 301 pp.

35. **Jørgensen, Claus.** (1997). *Driftsoptimering på kraftvarmesystemer.* 290 pp.

36. **Stauning, Ole.** (1997). *Automatic validation of numerical solutions. viii* + 116 pp.

37. **Pedersen, Morten With.** (1997). *Optimization of recurrent neural networks for time series modeling. x* + 322 pp.

38. **Thorsen, Rune.** (1997). *Restoration of hand function in tetraplegics using myoelectrically controlled functional electrical stimulation of the controlling muscle. x* + 154 pp. + Appendix.

39. **Rosholm, Anders.** (1997). *Statistical methods for segmentation and classification of images. xvi* + 183 pp.

40. **Petersen, Kim Tilgaard.** (1997). *Estimation of speech quality in telecommunication systems.* *x* + 259 pp.

41. **Jensen, Carsten Nordstrøm.** (1997). *Nonlinear systems with discrete and continuous elements.* 195 pp.

42. **Hansen, Peter S.K.** (1997). *Signal subspace methods for speech enhancement.* *x* + 226 pp.

43. **Nielsen, Ole Møller.** (1998). *Wavelets in scientific computing.* *xiv* + 232 pp.

44. **Kjems, Ulrik.** (1998). *Bayesian signal processing and interpretation of brain scans.* *iv* + 129 pp.

45. **Hansen, Michael Pilegaard.** (1998). *Metaheuristics for multiple objective combinatorial optimization.* *x* + 163 pp.

46. **Riis, Søren Kamaric.** (1998). *Hidden markov models and neural networks for speech recognition.* *x* + 223 pp.

47. **Mørch, Niels Jacob Sand.** (1998). *A multivariate approach to functional neuro modeling.* *xvi* + 147 pp.

48. **Frydendal, Ib.** (1998.) *Quality inspection of sugar beets using vision.* *iv* + 97 pp. + app.

49. **Lundin, Lars Kristian.** (1998). *Parallel computation of rotating flows.* *viii* + 106 pp.

50. **Borges, Pedro.** (1998). *Multicriteria planning and optimization. - Heuristic approaches.* *xiv* + 219 pp.

51. **Nielsen, Jakob Birkedal.** (1998). *New developments in the theory of wheel/rail contact mechanics.* *xviii* + 223 pp.

52. **Fog, Torben.** (1998). *Condition monitoring and fault diagnosis in marine diesel engines.* *xii* + 178 pp.

53. **Knudsen, Ole.** (1998). *Industrial vision.* *xii* + 129 pp.

54. **Andersen, Jens Strodl.** (1998). *Statistical analysis of biotests. - Applied to complex polluted samples.* *xx* + 207 pp.

55. **Philipsen, Peter Alshede.** (1998). *Reconstruction and restoration of PET images.* *vi* + 132 pp.

56. **Thygesen, Uffe Høgsbro.** (1998). *Robust performance and dissipation of stochastic control systems.* 185 pp.

57. **Hintz-Madsen, Mads.** (1998). *A probabilistic framework for classification of dermatoscopic images.* *xi* + 153 pp.

58. **Schramm-Nielsen, Karina.** (1998). *Environmental reference materials methods and case studies.* *xxvi* + 261 pp.

59. **Skyggebjerg, Ole.** (1999). *Acquisition and analysis of complex dynamic intra- and intercellular signaling events.* 83 pp.

60. **Jensen, Kåre Jean.** (1999). *Signal processing for distribution network monitoring.* *x* + 140 pp.

61. **Folm-Hansen, Jørgen.** (1999). *On chromatic and geometrical calibration.* *xiv* + 241 pp.

62. **Larsen, Jesper.** (1999). *Parallelization of the vehicle routing problem with time windows.xx* + 266 pp.

63. **Clausen, Carl Balslev.** (1999). *Spatial solitons in quasi-phase matched struktures.* *vi* + (flere pag.)

64. **Kvist, Trine.** (1999). *Statistical modelling of fish stocks.* *xiv* + 173 pp.

65. **Andresen, Per Rønsholt.** (1999). *Surface-bounded growth modeling applied to human mandibles.* *xxii* + 116 pp.

66. **Sørensen, Per Settergren.** (1999). *Spatial distribution maps for benthic communities.*

67. **Andersen, Helle.** (1999). *Statistical models for standardized preclinical studies.* *viii* + (flere pag.)

68. **Andersen, Lars Nonboe.** (1999). *Signal processing in the dolphin sonar system.* *xii* + 214 pp.

69. **Bechmann, Henrik.** (1999). *Modelling of wastewater systems.* *xviii* + 161 pp.